Title

Genome-Wide Association Study Identifies CXCR3 as a Partial Mediator of LPS-induced Periodontitis

Author

Hiyari, Sarah

Publication Date

2017

Peer reviewed|Thesis/dissertation

UNIVERSITY OF CALIFORNIA

Los Angeles

Genome-Wide Association Study Identifies CXCR3 as a Partial Mediator of LPS-induced Periodontitis

A dissertation submitted in partial satisfaction of the requirements for the degree Doctor of Philosophy in Oral Biology

by

Sarah Hiyari

2017

ABSTRACT OF THE DISSERTATION

Genome-Wide Association Study Identifies CXCR3 as a Partial Mediator of LPS-induced Periodontitis

by

Sarah Hiyari

Doctor of Philosophy in Oral Biology

University of California, Los Angeles, 2017

Professor Flavia Queiroz de mo Pirih, Co-Chair

Professor Sotirios Tetradis, Co-Chair

Periodontitis (PD) is characterized by bacterial infection and inflammation of supporting tissues of the teeth. If left untreated, PD can lead to tooth loss. PD affects ~47% of the U.S. population over 30 and, interestingly, twin studies have shown PD to be 50% heritable. While the host immunoinflammatory response and genetic background play a role in PD, few studies have mechanistically interrogated genetic targets to validate candidate genes associated with PD.

Objective: Identify genes that mediate Lipopolysaccharide (LPS)-induced periodontitis.

Methods: P. gingivalis (P.g.)-LPS was injected between maxillary molars in 104 strains of the Hybrid Mouse Diversity Panel (HMDP) 2x/week for 6 weeks. Following sacrifice, maxillae were scanned (microCT) and bone loss was quantitated. FaST-LMM was used to identify genetic loci associated to bone loss. Gene expression (microarray) and protein (histology) were further

assessed in A/J and C57BL/6J. CX-C motif chemokine receptor 3 (CXCR3) knockout (KO) and wild-type (WT) mice were analyzed radiographically and histologically after LPS-injections. AMG-487, an *in vivo* CXCR3 inhibitor, was injected systemically and locally and maxillae were analyzed radiographically and histologically after LPS-injections to investigate the therapeutic potential of CXCR3 inhibition.

Results: 50% heritability and a strain-dependent 6-fold difference in LPS-induced bone loss were observed across the HMDP. Our FaST-LMM and RNA expression data identified Cxcl family members (inflammatory immune cell chemoattractants essential in immune responses) as associated with PD. Additionally, Cxcl10 protein, as well as, an increase in immune cells and pro-inflammatory cytokines were observed in C57BL/6J (high bone loss) and not in A/J (low bone loss) after LPS-injections. Most interestingly, deleting CXCR3 (Cxcl10 receptor), demonstrated ~50% reduction in bone loss and a decrease in osteoclasts after LPS-injections compared to WT mice. Furthermore, mice treated with AMG-487 systemically and locally resulted in ~50% reduction in bone loss and decreased osteoclasts after LPS-injections.

Conclusions: Using a genome-wide association approach, we have identified CXCR3 as a possible target for modulating the host response in PD susceptibility. Our future work will characterize the CXCR3 pathway and validate other candidate genes associated with LPS-induced bone loss with the ultimate goal to identify patients at high risk to PD.

The dissertation of Sarah M Al-Hiyari is approved.

Aldons J. Lusis

Renate Lux

Sotirios Tetradis, Committee Co-Chair

Flavia Queiroz de mo Pirih, Committee Co-Chair

University of California, Los Angeles

2017

Table of Contents

ACKNOWLEDGEMENTS

Portions of this dissertation are already in print, therefore, I would like to thank RightsLink® and John Wiley & Sons A/S Publishing for permission to reproduce copyrighted material (Chapter 1).

In my time at UCLA working on my Ph.D., I was lucky to receive support and mentorship from many truly great people.

First, I would like to thank Dr. Aldons J. Lusis. Dr. Lusis is brilliant and he has the rare gift of making you feel brilliant just by association. Dr. Lusis is kind, generous, and genuinely cares about science, mentorship, and facilitating great work. Without him, several critical aspects of this dissertation would not have evolved into the data presented herein. I am grateful for his time and insight into this project.

Second, I would like to thank Dr. Renate Lux. Dr. Lux is one of the first people I met upon the start of my Ph.D. at UCLA. I rotated in Dr. Lux's lab my first summer in Los Angeles so I have know her my whole tenure as a Ph.D. student. Incidentally, Dr. Lux is the reason I completed my Ph.D. with my current Committee Co-Chairs. After my summer lab rotation was over, Dr. Lux suggested I contact Dr. Sotirios Tetradis as she thought I would be a good fit working with his group. Dr. Lux is not only and expert in her field, Microbiology, she has served as a faculty that I always feel comfortable speaking with and asking for advice.

Third, I would like to thank Dr. Sotirios Tetradis. Dr. Tetradis has served as my Committee Co-chair and throughout his mentorship, he has always provided experimental insight and has aided in better refining scientific strategy and execution. His expertise in bone biology has

greatly strengthened the data presented herein and I'm thankful for his involvement in the project.

Finally, in regard to my research committee, I would like to thank Dr. Flavia Pirih, my Committee Co-Chair. Out of all my committee members, Flavia is the faculty that I worked most closely with. While I could write an entirely separate dissertation on how much Flavia has supported me throughout my time as a Ph.D. student, I will keep it brief. In summary, Flavia has been my Ph.D. mentor, my dental clinician, but most importantly, she has been my friend. Under Flavia's mentorship, I have grown as a scientist and as a person and I'm grateful to Flavia and incredibly lucky for this experience.

I would also like to thank my family and friends for their continued support throughout this educational experience. Without them, this journey would've been far less enjoyable and I'm fortunate I was able to share it with so many people.

SARAH M AL-HIYARI

CURRICULUM VITAE

EDUCATION:

2017-2020	MBA - UCLA Anderson School of Management
2009-2010	MS, Molecular Pathology - TTU Health Sciences Center
2005-2009	BS, Microbiology - Texas Tech University

AWARDS:

2017	UCLA Anderson School of Management, Forte' Fellow $10,000
2016	UCLA: Dissertation Research Travel grant, $1,000
2016-2017	UCLA: Dissertation Year Fellowship, $20,000
2014-2015	American Academy of Implant Dentistry Student Research grant
	$2,500: "Genetic Influence of Healing in Extraction Sockets"
2014-2015	American Association for Dental Research: Government Affairs Fellow
2012-2016 Summer	NIH/NIDCR T90 Trainee: 5T90DE022734-03
2011-2016	UCLA Graduate Division Fellowship

TEACHING ACTIVITIES:

Spring 2017	UCLA Molecular Biology Teaching Assistant
Winter 2017	UCLA Microbial Genetics Teaching Assistant
Fall 2012-2015	UCLA Graduate Writing Center Consultant
Fall 2012	UCLA Introductory Microbiology Teaching Assistant

POSITIONS:

2014-2015	American Association for Dental Research (AADR) Gert Quigley Fellow
	AADR Government Affairs intern May-June 2014, Washington, DC.
2014-2015	AADR, National Student Research Group voting board member

CERTIFICATIONS AND LICENSES:

2010-Current Certified Molecular Biologist, American Society for Clinical Pathology

PUBLICATIONS:

1. **S. Hiyari** and K. Bennett. "Dental Diagnostics: molecular analysis of oral biofilms," Journal of Dental Hygiene, 2011.
2. Pirih, FQ; **Hiyari, S**; Leung, HY; Barroso, ADV; Jorge, ACA; Perussolo, J; Atti, E; Lin, Y-I; Tetradis, S; Camargo, PM. "A Murine Model of Lypopolysaccharide-Induced Peri-Implant Mucositis and Peri-Implantitis." Journal of Oral Implantology, 2014
3. Pirih, FQ; **Hiyari, S**; Barroso, ADV; Jorge, ACA; Perussolo, J; Atti, E; Tetradis,S; Camargo, PM. "Ligature-Induced Peri-Implantitis In Mice." Journal of Periodontal Research, 2014
4. **Hiyari, S**; Atti, E; Camargo, PM, Eleazar,E; Lusis AJ, Tetradis, S; Pirih, FQ. "Heritability of Periodontal Bone Loss." Journal of Periodontal Research, 2014
5. **Hiyari, S**; Naghibi, A; Wong, R, Sadreshkevary, R; Yi-Ling, L; Tetradis, S; Camargo, PM.; Pirih, FQ. "Susceptibility of Different Mouse Strains to Peri-Implantitis;" Journal of Periodontal Research, 2017
6. Araújo, A; Pereira, A; Addison, C; de Medeiros, C; Brito, G; Leitão, R; Araújo, L; Guedes, P; **Hiyari, S**; Pirih, FQ; de Araújo Júnior, R; "Effects of metformin on inflammation, oxidative stress, and bone loss in a rat model of periodontitis;" PLOS One, 2017

INTRODUCTION TO THE THESIS

The body of this dissertation is organized into three distinct Chapters (Chapter One, Chapter Two, and Chapter Three), two of which serve as independent publications either already in print, submitted and under peer review, or in final preparation for submission (Chapter One and Chapter Two). Chapter One and Chapter Two each contain their own: Introduction, Materials and Methods, Results, Conclusions, and Figures. Chapter Three discusses Future Directions covering new avenues of research related to Chapters One and Two.

Publications completed while a Ph.D. student and not included in this dissertation are as follows:

Pirih, FQ; **Hiyari, S**; Leung, HY; Barroso, ADV; Jorge, ACA; Perussolo, J; Atti, E; Lin, Y-I; Tetradis, S; Camargo, PM. "A Murine Model of Lypopolysaccharide-Induced Peri-Implant Mucositis and Peri-Implantitis." Journal of Oral Implantology, 2014

Pirih, FQ; **Hiyari, S**; Barroso, ADV; Jorge, ACA; Perussolo, J; Atti, E; Tetradis,S; Camargo, PM. "Ligature-Induced Peri-Implantitis In Mice." Journal of Periodontal Research, 2014

Hiyari, S; Naghibi, A; Wong, R, Sadreshkevary, R; Yi-Ling, L; Tetradis, S; Camargo, PM.; Pirih, FQ. "Susceptibility of Different Mouse Strains to Peri-Implantitis;" Journal of Periodontal Research, 2017

Araújo, A; Pereira, A; Addison, C; de Medeiros, C; Brito, G; Leitão, R; Araújo, L; Guedes, P; **Hiyari, S**; Pirih, FQ; de Araújo Júnior, R; “Effects of metformin on inflammation, oxidative stress, and bone loss in a rat model of periodontitis;” PLOS One, 2017

CHAPTER ONE

Heritability of Periodontal Bone Loss in Mice

Abstract

Periodontitis (PD) is an inflammatory disease of the periodontal tissues that compromises tooth support and can lead to tooth loss. Although bacterial biofilm is central in disease pathogenesis, host response plays an important role in the progression and severity of PD. Indeed, clinical genetic studies indicate that PD is 50% heritable. In this study, we hypothesized that the LPS injections lead to a strain-dependent periodontal bone loss pattern. We utilized five inbred mouse strains that derive the recombinant strains of the hybrid mouse diversity panel (HMDP). Mice received *P. gingivalis*-LPS injections for six weeks. Micro-CT analysis demonstrated a statistically significant strain-dependent bone loss. The most susceptible strain, C57BL/6J, had a 5-fold higher LPS-induced bone loss compared to the most resistant strain, A/J. More importantly, periodontal bone loss revealed 49% heritability, which closely mimics PD heritability for patients. To further evaluate functional differences that underlie periodontal bone loss, osteoclast numbers of C57BL/6J and A/J mice were measured *in vivo* and *in vitro*. *In vitro* analysis of osteoclastogenic potential showed higher number of osteoclasts in C57BL/6J compared to A/J mice. *In vivo* LPS-injections statistically significantly increased osteoclasts numbers in both groups. Importantly, the number of osteoclasts was higher in C57BL/6J vs. A/J mice. These data support a significant role of the genetic framework in LPS-induced periodontal bone loss and the feasibility of utilizing the HMDP to determine the genetic factors that affect periodontal bone loss. Expanding these studies will contribute in predicting patients genetically predisposed to PD and in identifying the biological basis of disease susceptibility.

Introduction

Periodontitis (PD) is “an inflammatory disease of the supporting tissues of the teeth caused by specific microorganisms or groups of specific microorganisms, resulting in progressive destruction of the periodontal ligament and alveolar bone with pocket formation, recession, or both” (1). According to the WHO, PD is a major cause of tooth loss in adults over the age of 40 (2).

Although bacterial biofilm is central in disease pathogenesis, strong evidence supports that the patient’s genetic framework significantly modifies the response of periodontal tissues,(3). Polymorphisms in cytokine-, surface receptor-, metabolism-, antigen recognition- and immunity receptor- related genes are associated with PD (3, 4). Moreover, twin studies have provided valuable support of the genetic influence in periodontal disease (5-8), estimating that PD is 50% heritable (6).

The complexity of PD, the heterogeneous genetic composition of patients, and the difficulty to control environmental parameters pose challenges to clinical genetic studies (4, 9), making animal models an attractive complement to human studies. Indeed, mouse studies on experimental periodontitis induced by *Porphyromonas gingivalis (P. gingivalis)* colonization reveal a strong genetic component in periodontal disease resistance and susceptibility and demonstrate that genetic determinants affect bacterial colonization, as well as periodontal bone levels (10, 11).

These studies provide valuable insight in the heritable aspects of periodontitis as a whole. However, PD is a multifactorial process that involves among others, bacterial colonization, biofilm organization and establishment, inflammatory host response, periodontal bone loss, and decreased tooth support (1). In order to begin dissecting the genetic influence in these pathogenetic disease processes individually, we explored the heritable nature of periodontal bone loss in response to a controlled inflammatory impact, by utilizing the five parental inbred strains of the Hybrid Mouse Diversity Panel (HMDP) (12, 13) and a well-characterized animal model that employs localized LPS delivery to the periodontal tissues (14-17).

Materials and Methods

Mice

Six-week-old male mice (A/J, DBA/2J, C3H/HeJ, BALBc/J, C57BL/6J) were obtained from the Jackson Laboratories (Bar Harbor, ME). In brief, mice were maintained in a temperature and light-controlled environment at UCLA. They were fed a standard chow. All mice were handled according to protocols approved by the Office for Protection of Research Subjects at UCLA and conforms to the ARRIVE guidelines (18).

Inflammatory Bone Loss Model

Mice were anesthetized with 3% isoflurane administered through a nose cone. Under the microscope (Leica Microsystems, Buffalo Grove, IL.), mice received 2 µl (20 µg) of *P. gingivalis*-LPS (InvivoGen, San Diego, CA) injections in between the 1^{st} and 2^{nd} maxillary molars on both sides of the maxilla, 2 times a week for 6 weeks (Figure 1-1A). We utilized a 10 µl Hamilton syringe with a 0.33 gauge needle (Hamilton Company USA, Reno, NV). Control animals were injected with 2 µl of vehicle (endotoxin-free water) or did not receive injections. This regimen was similar to previously published studies (16). No overt signs of tissue inflammation or soft tissue damage were observed during the course of injections (data not shown). Animals were sacrificed 6 weeks after the first injection. Maxillae were dissected and immersed in 10% buffered formalin for 48 hours.

Micro-CT Analysis

Maxillae were scanned using a μCT scanner (Skyscan 1172, Aartselaar, Belgium) with a voxel size of 10 μm (isotropic voxel) and anx-ray energy of 55 KVp and 181 μA. Each scan was conducted over a period of 21 minutes, with steps of 0.4°. Ten frames were averaged and a 0.5 mm aluminum filter was utilized. Virtual image slices were reconstructed using the cone-beam reconstruction software version 1.5 based on the Feldkamp algorithm.

Volumetric data were converted to DICOM format and were imported into Dolphin® software (Dolphin Imaging, Chatsworth, CA) for further analysis. To quantify the amount of bone loss, the imaged volume was oriented in the coronal (green) and transverse (blue) planes such that the sagittal plane (red) was parallel to the maxillary midline, identified by the intermaxillary suture and the coronal plane intersected the proximal area between the first and second maxillary molars (Figure 1-1B). Then, at the sagittal plane crossing the interproximal contact point of the 1st and 2nd molar crowns, the distance between the CEJ and the alveolar crest were measured for the distal surface of the 1st molar and the mesial and distal surface of the 2nd molar just below the contact point and 0.2 mm palatal to the contact point (Figure 1-1C).

To quantify the amount of bone loss in the 5 parental strains, the bone level was measured as described above for the right and left sides. Subsequently, the average distance in the control sites was subtracted from the distances on the LPS-injected sites and the remainder represented the net bone loss at the LPS-injected site.

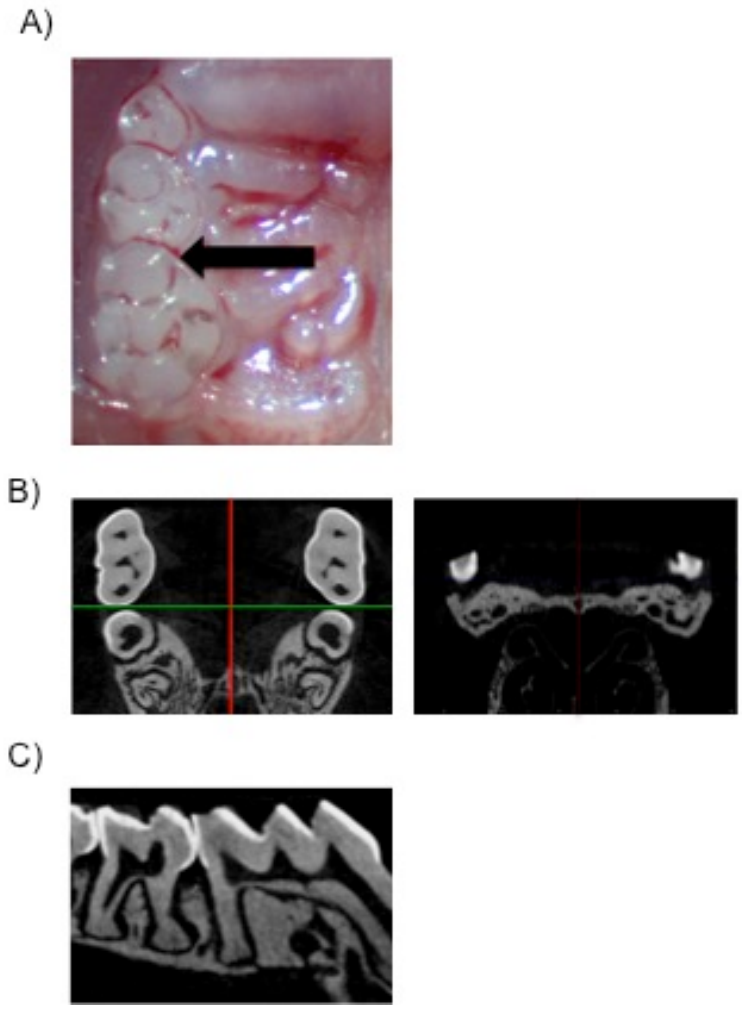

Figure 1-1: Injections and micro-computed tomography image/sample orientation. (A) Clinical image with the location of lipopolysaccharide injection. (B) Micro-computed tomography data were oriented in the orthogonal planes such that the red line denotes (sagittal plane), green line (coronal), blue line (transverse plane). The axial slices are parallel to the occlusal plane. The intermaxillary suture is parallel to the sagittal plane. (C) The distance from the cement-enamel junction to the alveolar crest was measured at the sagittal plane intersecting the interproximal molars. Yellow lines depict the measurement that was taken for distal of first molar and mesial of second molar.

Histology

Maxillae were decalcified in 15% EDTA for 4 weeks. Following decalcification, 5μM-thick sections were cut in the coronal plane using a microtome (McBain Instruments, Chatsworth, CA). Sections were stained with hematoxylin and eosin (H&E) using standard protocols (19). Slices were digitally imaged using Aperio ImageScope model V11.1.2.752 (Vista, CA.)

For osteoclast analysis, cells that presented with ≥2 nuclei, in contact with the bone surface, were classified as osteoclasts (20). Osteoclasts numbers were averaged for the right and left side for each mouse. Groups were compared using a Student's t-test.

Bone Marrow Cell Isolation and *in vitro* Osteoclast Differentiation

Total bone marrow cells were harvested from femurs and tibias of 4-week-old A/J and C57BL/6J male mice according to Pirih et al (21). In brief, cells were filtered through nylon mesh screens (70 μm BD Falcon, Franklin Lakes, NJ, USA). At day 8, non-adherent cells were enumerated using a hemocytometer with trypan blue, to determine cell viability. Then, non-adherent cells were re-plated at $1.8x10^5$ cells/well in a 24-well plate in osteoclastogenic medium (a-MEM + 10% FBS, 50 ng/mL M-CSF, 80 ng/mL sRANKL), which was replaced at day 3. At day 6, cells were fixed and tartrate resistant acid phosphatase (TRAP) staining was performed using a leukocyte acid phosphatase system (Sigma-Aldrich) according to manufacturers protocol (21). TRAP+ multinucleated cells (osteoclasts) were counted in three different areas of the well, under light microscope and each well was averaged, then 3 wells were averaged. Groups were compared using a Student's t-test.

Heritability

Heritability of the trait was estimated by fitting the data to the mixed model y=\mu + u + e, where y is a vector of phenotypes, \mu is the mean of the phenotypes, u is a random vector corresponding to the genetic component of the trait and e is a random vector corresponding to the environmental factor. The random vector u is assumed to be normally distributed with mean 0 and covariance matrix \sigma^2_g K where K is a kinship matrix encoding the genetic relationships and the random vector e is assumed to be normally distributed with mean 0 and

covariance matrix\sigma^2_e I. If K is the realized relationship matrix (22) then the ratio \sigma^2_g /(\sigma^2_g + \sigma^2_e) is an estimate for the heritability of the trait.

Statistical Analysis

At least 12 animals were utilized per strain (n≥6 animals/group) (n≥24 sites/group). Data among groups were compared by One-Way ANOVA and between groups by Student's t-test. P values <0.05 were considered significant.

Results

P. gingivalis-LPS Injection Induces Bone Loss in C57BL/6J Mice

To evaluate PD-bone loss in response to LPS injection, we utilized a well-characterized model of periodontal bone loss through the localized LPS delivery to the interdental papillae of maxillary molars in C57BL/6J mice (14-17) (Figure 1-1A). Three different treatments were performed a) LPS-injections (between the 1^{st} and second molars on both sides of the maxilla), b) vehicle injections (between the 1^{st} and second molars on both sides of the maxilla), or c) no injections. The micro-CT analysis revealed statistical significant alveolar bone loss at the interproximal space between the 1^{st}-2^{nd} maxillary molars at the LPS-injected sites compared to non-injected or veh-injected sites. No statistical difference was observed between the vehicle injected and non-injected animals (Figure 1-2). Since there was no statistical difference in the amount of bone loss comparing the non-injected and the vehicle injected sites (Figure 1-2), subsequent experiments were carried out utilizing non-injected sites as controls.

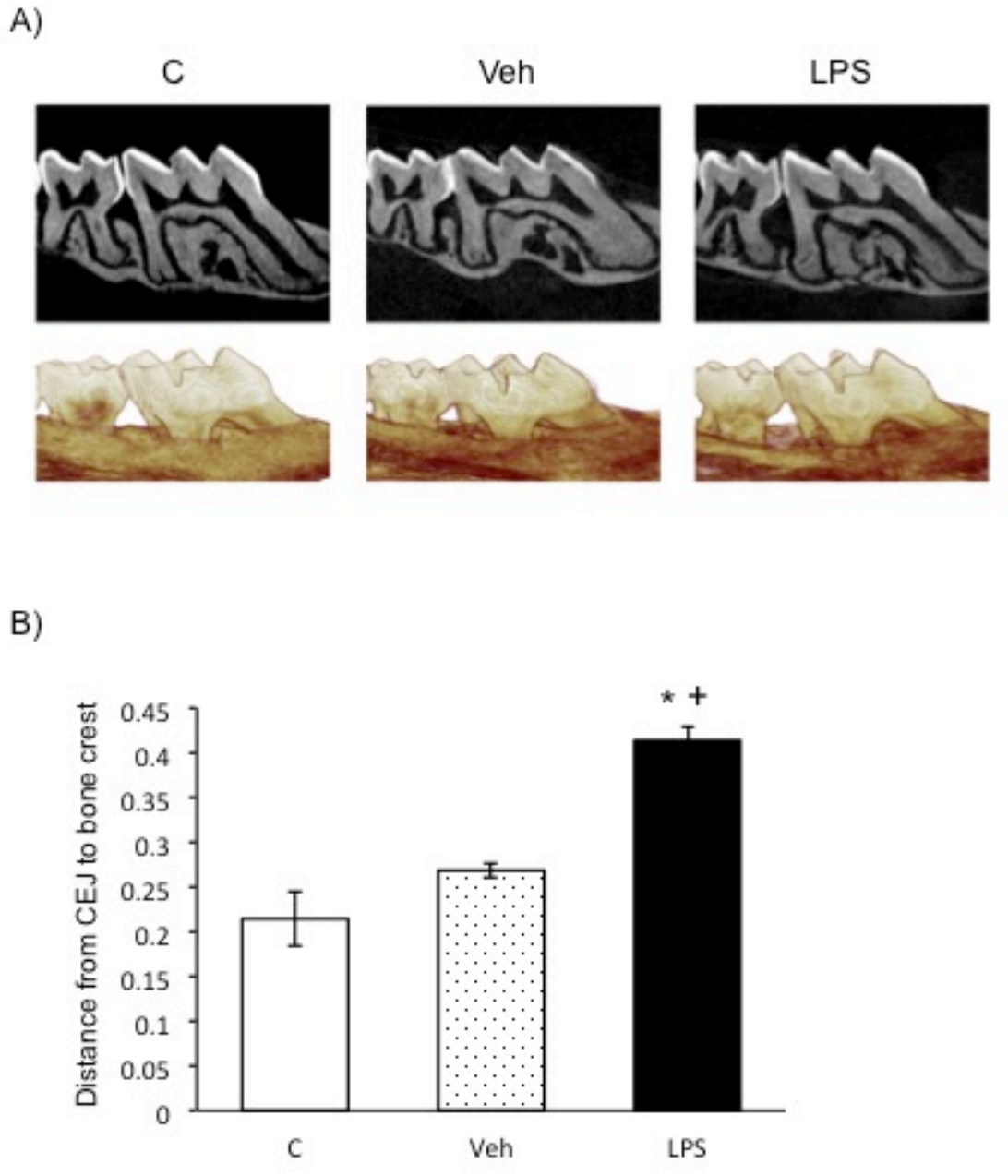

Figure 1-2: *P. gingivalis*-LPS induces periodontal bone loss. (A) Corrected sagittal and three-dimensional reformatted representative images of non-injected (C), vehicle- or LPS-injected mice. (B) Graph of the distance between the CEJ to the alveolar bone level (mm) in non-injected, vehicle- or LPS-injected sites (average ± SEM) at the distal of the first molar and mesial of the second molar. Statistical analysis was performed by the Student's *t*-test (n≥24 sites/group). *p≤0.001 compared to control and +p<0.0001 compared to vehicle. CEJ, cement-enamel junction; LPS, lipopolysaccharide; Veh, vehicle.

Bone Loss is Strain-Dependent

We utilized the *P.g.* LPS-injection induced inflammatory bone loss model described above to 5 classical inbred strains (BALB/cJ, C3H/HeJ, DBA/2J, A/J, and C57BL/6J), that derived the recombinant inbred strains of the HMDP, to explore genetic contribution of LPS-injection induced bone loss (Figure 1-3). Each mouse strain was divided in 2 groups: a) LPS-injected or b) non-injected control. For each strain, bone loss was calculated by subtracting the average CEJ to bone crest distance in the non-injected animals from each LPS-injected site. C57BL/6J was the most susceptible strain to LPS-induced bone loss and presented a 5-fold higher bone loss compared to the most resistant A/J strain (Figure 1-3B).

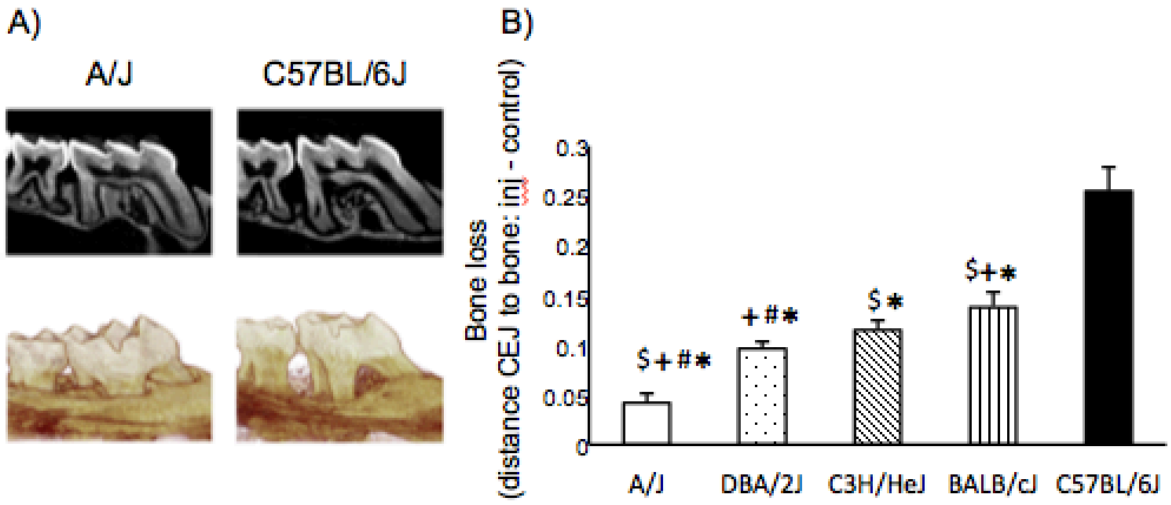

Figure 1-3: *P. gingivalis*-lipopolysaccharide induces strain-dependent bone loss. (A) Corrected sagittal and three-dimensional reformatted representative images of A/J and C57BL/6J lipopolysaccharide-injected mice. (B) Graph of periodontal bone loss (mm) of lipopolysaccharide-injected sites subtracted by the respective controls (average ± SEM) at the distal of the first molar and mesial of the second molar. Statistical analysis between groups was performed by the Students *t*-test (n≥24 sites/group). P<0.001, * statistically significant compared to C57BL/6J, $ statistically significant compared to DBA/2J, + compared to C3H/HeJ, # compared to BALB/cJ. Significance between BALB/cJ compared to C3H/HeJ is $p < 0.05$. CEJ, cemento-enamel junction.

LPS-Injection-Induced Bone Loss is 49% Heritable

Based on the data presented above, (Figure 1-3), heritability was calculated for LPS-induced bone loss in these 5 mouse strains. The heritability estimate for periodontal bone loss in the 5 parental strains of the HMDP was 49%, a value that closely resembles heritability measurements of 50% for PD in patients (6, 23).

C57BL/6J Mice Have Increased Osteoclastogenic Potential Compared to A/J *in vitro*

To assess whether the differences in bone loss between the two strains were in part due to inherent differences in osteoclastogenic potential, we evaluated osteoclast differentiation of C57BL/6J and A/J derived bone marrow by performing TRAP staining *in vitro.* A statistically significant increase in $TRAP^{+}$ multinucleated cells was observed in the C57BL/6J compared to the A/J cells (Figure 1-4).

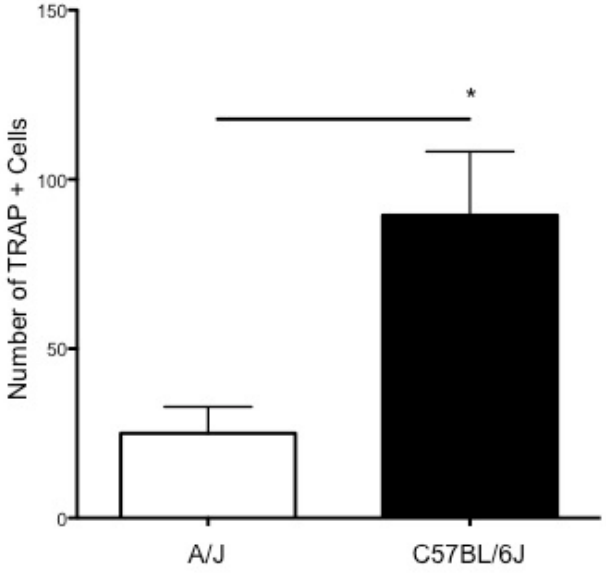

Figure 1-4: C57BL/6J mice have increased osteoclastogenic potential as compared to A/J in vitro. Graph of number of TRAP+ cells. Statistical analysis was performed using the Student's *t*-test. * Statistically significant compared to A/J ($p < 0.05$). TRAP, tartrate resistant acid phosphatase.

Osteoclast Numbers Were Higher in C57BL/6J Compared to A/J Mice Following LPS-Injections *in Vivo*

To identify cellular differences that accompany periodontal bone loss, we evaluated osteoclast numbers of C57BL/6J vs. A/J mice after 5 LPS injections *in vivo*. LPS injections induced a statistically significant increase in osteoclast numbers in both strains. Importantly, a significantly higher osteoclast number increase was observed in the C57BL/6J compared to A/J mice (Figure 1-5).

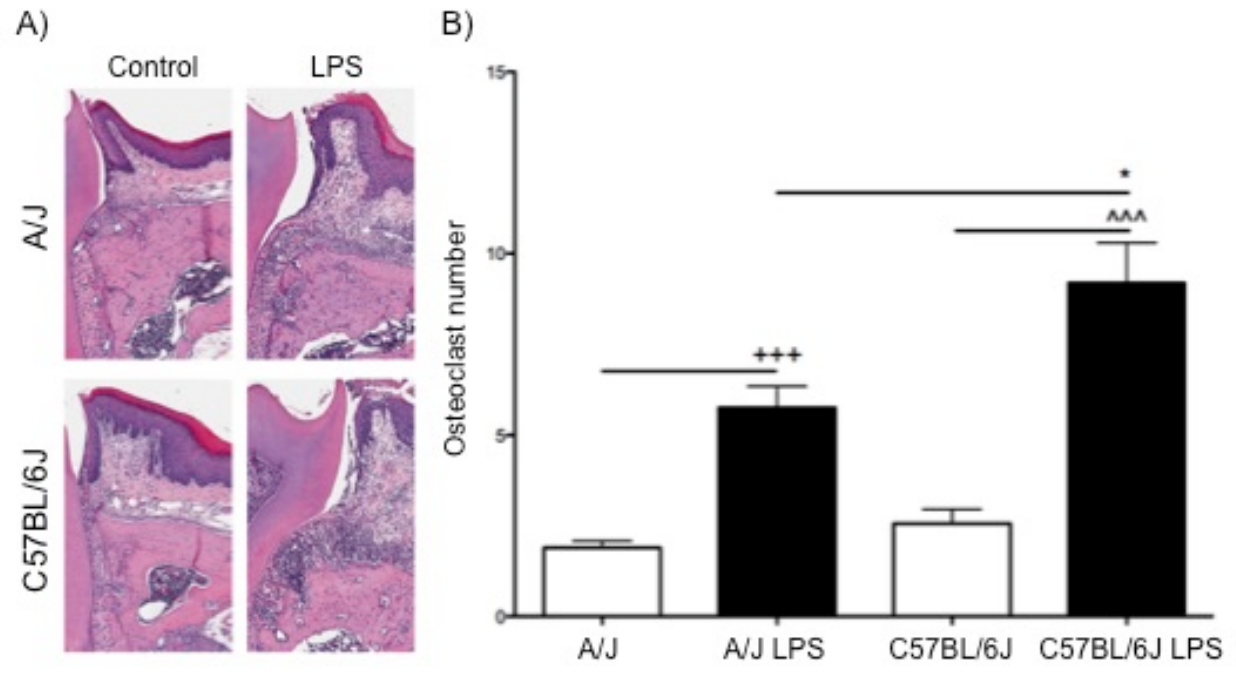

Figure 1-5: *P. gingivalis*-LPS injections increases osteoclasts in C57BL/6J as compared to A/J mice. (A) Representative hematoxylin and eosin images of A/J control A/J LPS injections, C57BL/6J control and C57BL/6J LPS injections. (B) Graph of number of osteoclasts in A/J control, A/J LPS-injected, C57BL/6J control C57BL/6J LPS-injected (n ≥ 6 mice/group). Statistical analysis between groups was performed using the Students *t*-test, *p < 0.05, ***P < 0.001. LPS, lipopolysaccharide.

Discussion

PD is a polymicrobial infection-driven inflammatory disease that involves complex processes, such as biofilm formation by diverse microbial species, inflammatory response to a multifaceted microbial invasion, and activation of multiple signaling pathways that lead to bone resorption and attachment loss (24). Even though PD is a multifactorial disease, the genetic component is highly significant and estimated to explain 50% of disease burden (8). Moreover, PD heritability involves a large number of genes, each accounting for a small fraction of the disease (25), making GWAS studies an ideal tool to identify genes involved in this trait.

GWAS can be accomplished by human or animal studies, each complementing one other. To date only a few groups have performed GWAS for PD in humans (26, 27). These studies have identified genes that are likely to be important in periodontitis. However, the main disadvantage of human GWAS is the requirement of large sample size. Therefore, frequently the power is insufficient to detect genes with a small contribution. Mice share structural, functional and genetic traits with humans. Moreover, powerful molecular and genetic tools developed in the past two decades make mice an ideal animal model for the study of complex traits. Mouse GWAS explored diverse conditions such as cardiovascular disease, atherosclerosis, diabetes, inflammatory diseases, hearing, and even behavior (28-33).

Studies performed in inbred mouse strains demonstrated variable bone loss in bacteria-induced periodontitis. In addition, a large variability in bacterial counts recovered among different strains was detected, pointing to a possible role of genetics in bacterial colonization (11). To study the genetic component of periodontal bone response in mice we elected to utilize an inflammatory model, analyzing the host response to a constant bacterial insult, bypassing the genetic influence in microbial colonization. We employed the well-characterized model of periodontal

bone loss through the localized LPS delivery in mice to focus on the host response by analyzing bone loss as the outcome measurement (14-17). Moreover, we utilized *P. gingivalis*-derived LPS for multiple reasons. *P. gingivalis,* a gram-negative anaerobic rod and member of the "red complex", is widely recognized as a predominant contributor to chronic PD in humans (24, 34). Additionally, diverse cytokine and chemokine responses of gingival fibroblasts and macrophages have been reported utilizing *P. gingivalis* vs. *E. coli* LPS (35). Finally, *P. gingivalis* infection in mice produces inflammation of the periodontal tissues and associated periodontal bone loss (10, 11).

Herein, utilizing a model of *P. gingivalis* LPS-induced periodontal bone loss and high-resolution micro-CT, we demonstrated differences in bone loss pattern among 5 classic mouse inbred strains. These differences were expected since the utilization of animal models for evaluating genetic determinants of PD have been proposed (36-38). More recently, oral infection of various inbred mouse strains with human strains of *P. gingivalis* demonstrates that susceptibility to alveolar bone loss is a genetically modified trait. Some mouse strains were highly susceptible, while others were resistant to alveolar bone loss. Importantly, F1 offsprings of susceptible and resistant strains demonstrated various patterns of heritability, suggesting the existence of recessive and dominant resistance alleles. The importance of exploiting the mouse model to investigate loci associated with susceptibility or resistance to inflammation-induced alveolar bone loss was concluded (10, 11).

More importantly, we detected 49% heritability in bone loss similar to the heritability observed in humans (6). In addition, our data is in agreement with published data in mouse models where alveolar bone loss is a genetically modified trait. (39, 40).

The pathogenesis of periodontitis is complex, involving many different cell types (41-43). The

LPS-injection model, as mentioned earlier, bypasses the bacterial colonization process and allows for a more simplified method of studying the inflammatory mediators of this disease. To begin dissecting the mechanisms by which the observed interstrain differences on periodontal bone loss occur, we evaluated the osteoclastogenic potential of A/J and C57BL/6J *in vitro*. We observed, under supra-physiologic conditions, that C57BL/6J bone marrow cells have a stronger osteoclastogenic potential. To further explore the differences that might mediate periodontal bone loss and how it correlates with our micro-CT findings, we evaluated the number of multinucleated osteoclasts *in vivo*. Indeed, *in vivo,* C57BL/6J mice demonstrated a more pronounced inflammatory response with a higher number of osteoclasts after LPS injections when compared to A/J mice. Our results corroborate with studies that demonstrate a hyper-responsiveness to LPS in C57BL/6J mice as compared to A/J mice. The hyper-responsiveness in C57BL/6J mice includes an increase: in vasculitis, in neutrophil numbers, in polymorphonuclear cells and splenocytes followed by LPS treatment (44-46). Moreover, there is an increased production of interleukin-1 by C57BL6/J mice after LPS-injections as compared to A/J mice (44). Additionally, C57BL/6J mice have a lower bone mineral density phenotype compared to A/J (47) further supporting our findings. Clearly the observed differences in osteoclast differentiation and numbers are only part of the pathophysiologic mechanism underlying periodontal bone loss. Immune cell activation, osteoblastic function, cytokine release, extracellular matrix remodeling are all processes that would contribute to the observed interstrain differences. We plan future studies to address variations among the HMDP strains that will shed light to genetic determinants of the periodontal bone loss response.

The HMDP panel consists of 100 commercially available inbred mouse strains selected for systematic genetic analyses of complex traits. These strains were selected with the intent to increase resolution of genetic mapping, offer a renewable resource of inbred mice, and provide for a shared repository for data accumulation that would allow the integration of data across

multiple scales including transcriptomic, metabolomic, proteomic, and clinical phenotypes (12). The 100 strains consist of 29 classic inbred strains used for initial association mapping (48, 49) and 71 recombinant inbred (RI) strains (12). The HMDP offers a powerful genetic approach for the study of complex genetic traits. Moreover, the HMDP is currently used to investigate a variety of clinical traits including diet-induced obesity, hearing loss, heart failure, atherosclerosis, bone mineral density and diabetes (12, 50-52). Therefore, determining periodonto-pathogenic LPS-induced bone loss in a mouse model will allow us to expand our studies to perform genome wide association studies (GWAS) utilizing the HMDP. Expanding these studies will contribute in identifying pathways important in disease initiation development; moreover, it will assist in predicting in patients genetically predisposed to PD and in identifying the biological basis of disease susceptibility. The HMDP offers a powerful genetic approach for the study of complex genetic traits. The HMDP is currently used to investigate a variety of clinical traits including diet-induced obesity, hearing loss, heart failure, atherosclerosis, bone mineral density and diabetes (12, 50-52). We will exploit on these powerful mouse genetics approach to begin unraveling murine genetics affecting periodontal bone loss with an eye towards future translational studies on genetic and environmental regulators of human PD.

Our data supports a significant role of the genetic framework in LPS-induced periodontal bone loss and the feasibility of utilizing the HMDP to explore these genetic factors. Moreover, it corroborates with data in the literature. Expanding these studies will contribute in identifying the biological basis of disease susceptibility. Such understanding would help recognize patients with high-risk or resistance for development of periodontitis and would inform targeted treatment interventions for patients with the disease as we move towards a personalized diagnostic and interventional approach of periodontitis.

Acknowledgements

This work was supported by the NIH/NIDCR DE023901-01 minority supplement DE 019465- S1 and the UCLA School of Dentistry Seed Grant. SH was supported by the NIH/NIDCR T90 DE022734-01. The author(s) declare no potential conflicts of interest with respect to the authorship and/or publication of this article.

References:

1. Hinrichs, J.E., and Novak, M.J. 2012. Classification of Diseases and Conditions Affecting the Periodontium. In *Carranza's Clinical Periodontology*. M.G. Newman, H.H. Takei, P.R. Klokkevold, and F.A. Carranza, editors: Elsevier. 34-64.

2. Petersen, P.E. 2003. The World Oral Health Report 2003: continuous improvement of oral health in the 21st century--the approach of the WHO Global Oral Health Programme. *Community Dent Oral Epidemiol* 31 Suppl 1:3-23.

3. Kinane, D.F., Shiba, H., and Hart, T.C. 2005. The genetic basis of periodontitis. *Periodontol 2000* 39:91-117.

4. Vijayalakshmi, R., Geetha, A., Ramakrishnan, T., and Emmadi, P. 2010. Genetic polymorphisms in periodontal diseases: an overview. *Indian J Dent Res* 21:568-574.

5. Corey, L.A., Nance, W.E., Hofstede, P., and Schenkein, H.A. 1993. Self-reported periodontal disease in a Virginia twin population. *J Periodontol* 64:1205-1208.

6. Michalowicz, B.S., Diehl, S.R., Gunsolley, J.C., Sparks, B.S., Brooks, C.N., Koertge, T.E., Califano, J.V., Burmeister, J.A., and Schenkein, H.A. 2000. Evidence of a substantial genetic basis for risk of adult periodontitis. *J Periodontol* 71:1699-1707.

7. Michalowicz, B.S. 1994. Genetic and heritable risk factors in periodontal disease. *J Periodontol* 65:479-488.

8. Michalowicz, B.S., Aeppli, D., Virag, J.G., Klump, D.G., Hinrichs, J.E., Segal, N.L., Bouchard, T.J., Jr., and Pihlstrom, B.L. 1991. Periodontal findings in adult twins. *J Periodontol* 62:293-299.

9. Kinane, D.F., and Hart, T.C. 2003. Genes and gene polymorphisms associated with periodontal disease. *Crit Rev Oral Biol Med* 14:430-449.

10. Hart, G.T., Shaffer, D.J., Akilesh, S., Brown, A.C., Moran, L., Roopenian, D.C., and Baker, P.J. 2004. Quantitative gene expression profiling implicates genes for susceptibility and resistance to alveolar bone loss. *Infect Immun* 72:4471-4479.

11. Baker, P.J., Dixon, M., and Roopenian, D.C. 2000. Genetic control of susceptibility to Porphyromonas gingivalis-induced alveolar bone loss in mice. *Infect Immun* 68:5864-5868.

12. Bennett, B.J., Farber, C.R., Orozco, L., Kang, H.M., Ghazalpour, A., Siemers, N., Neubauer, M., Neuhaus, I., Yordanova, R., Guan, B., et al. 2010. A high-resolution association mapping panel for the dissection of complex traits in mice. *Genome Res* 20:281-290.

13. Ghazalpour, A., Rau, C.D., Farber, C.R., Bennett, B.J., Orozco, L.D., van Nas, A., Pan, C., Allayee, H., Beaven, S.W., Civelek, M., et al. 2012. Hybrid mouse diversity panel: a panel of inbred mouse strains suitable for analysis of complex genetic traits. *Mamm Genome* 23:680-692.

14. Li, Q., Valerio, M.S., and Kirkwood, K.L. 2012. MAPK usage in periodontal disease progression. *J Signal Transduct* 2012:308943.

15. Rogers, J.E., Li, F., Coatney, D.D., Rossa, C., Bronson, P., Krieder, J.M., Giannobile, W.V., and Kirkwood, K.L. 2007. Actinobacillus actinomycetemcomitans lipopolysaccharide-mediated experimental bone loss model for aggressive periodontitis. *J Periodontol* 78:550-558.

16. Sartori, R., Li, F., and Kirkwood, K.L. 2009. MAP kinase phosphatase-1 protects against inflammatory bone loss. *J Dent Res* 88:1125-1130.

17. Patil, C., Rossa, C., Jr., and Kirkwood, K.L. 2006. Actinobacillus actinomycetemcomitans lipopolysaccharide induces interleukin-6 expression through multiple mitogen-activated protein kinase pathways in periodontal ligament fibroblasts. *Oral Microbiol Immunol* 21:392-398.

18. Kilkenny, C., Browne, W.J., Cuthill, I.C., Emerson, M., and Altman, D.G. 2010. Improving bioscience research reporting: the ARRIVE guidelines for reporting animal research. *PLoS Biol* 8:e1000412.

19. Cowan, C.M., Shi, Y.Y., Aalami, O.O., Chou, Y.F., Mari, C., Thomas, R., Quarto, N., Contag, C.H., Wu, B., and Longaker, M.T. 2004. Adipose-derived adult stromal cells heal critical-size mouse calvarial defects. *Nat Biotechnol* 22:560-567.

20. Chaichanasakul, T., Kang, B., Bezouglaia, O., Aghaloo, T.L., and Tetradis, S. 2013. Diverse Osteoclastogenesis of Bone Marrow From Mandible versus Long Bone. *J Periodontol*.

21. Pirih, F.Q., Michalski, M.N., Cho, S.W., Koh, A.J., Berry, J.E., Ghaname, E., Kamarajan, P., Bonnelye, E., Ross, C.W., Kapila, Y.L., et al. Parathyroid hormone mediates hematopoietic cell expansion through interleukin-6. *PLoS ONE* 5:e13657.

22. Yang, J., Lee, S.H., Goddard, M.E., and Visscher, P.M. 2011. GCTA: a tool for genome-wide complex trait analysis. *Am J Hum Genet* 88:76-82.

23. Tenesa, A., and Haley, C.S. 2013. The heritability of human disease: estimation, uses and abuses. *Nat Rev Genet* 14:139-149.

24. Hajishengallis, G. 2009. Porphyromonas gingivalis-host interactions: open war or intelligent guerilla tactics? *Microbes Infect* 11:637-645.

25. Yoshie, H., Kobayashi, T., Tai, H., and Galicia, J.C. 2007. The role of genetic polymorphisms in periodontitis. *Periodontol 2000* 43:102-132.

26. Divaris, K., Monda, K.L., North, K.E., Olshan, A.F., Reynolds, L.M., Hsueh, W.C., Lange, E.M., Moss, K., Barros, S.P., Weyant, R.J., et al. 2013. Exploring the genetic basis of chronic periodontitis: a genome-wide association study. *Hum Mol Genet* 22:2312-2324.

27. Teumer, A., Holtfreter, B., Volker, U., Petersmann, A., Nauck, M., Biffar, R., Volzke, H., Kroemer, H.K., Meisel, P., Homuth, G., et al. 2013. Genome-wide association study of chronic periodontitis in a general German population. *J Clin Periodontol* 40:977-985.

28. Welch, C.L. 2012. Beyond genome-wide association studies: the usefulness of mouse genetics in understanding the complex etiology of atherosclerosis. *Arterioscler Thromb Vasc Biol* 32:207-215.

29. Sieberts, S.K., and Schadt, E.E. 2007. Moving toward a system genetics view of disease. *Mamm Genome* 18:389-401.

30. Breyer, M.D., Tchekneva, E., Qi, Z., Takahashi, T., Fogo, A.B., and Harris, R.C. 2007. Examining diabetic nephropathy through the lens of mouse genetics. *Curr Diab Rep* 7:459-466.

31. Flint, J., and Mott, R. 2008. Applying mouse complex-trait resources to behavioural genetics. *Nature* 456:724-727.

32. Khor, B., Gardet, A., and Xavier, R.J. 2011. Genetics and pathogenesis of inflammatory bowel disease. *Nature* 474:307-317.

33. White, C.H., Ohmen, J.D., Sheth, S., Zebboudj, A.F., McHugh, R.K., Hoffman, L.F., Lusis, A.J., Davis, R.C., and Friedman, R.A. 2009. Genome-wide screening for genetic loci associated with noise-induced hearing loss. *Mamm Genome* 20:207-213.

34. Socransky, S.S., Haffajee, A.D., Cugini, M.A., Smith, C., and Kent, R.L., Jr. 1998. Microbial complexes in subgingival plaque. *J Clin Periodontol* 25:134-144.

35. Jones, K.J., Ekhlassi, S., Montufar-Solis, D., Klein, J.R., and Schaefer, J.S. 2010. Differential cytokine patterns in mouse macrophages and gingival fibroblasts after stimulation with porphyromonas gingivalis or Escherichia coli lipopolysaccharide. *J Periodontol* 81:1850-1857.

36. Baer, P.N., Crittenden, L.B., Jay, G.E., Jr., and Lieberman, J.E. 1961. Studies on periodontal disease in the mouse. II. Genetic and meternal effects. *J Dent Res* 40:23-33.

37. Baer, P.N., and Lieberman, J.E. 1960. Periodontal disease in six strains of inbred mice. *J Dent Res* 39:215-225.

38. Baer, P.N., and Lieberman, J.E. 1959. Observation of some genetic characteristics of the periodontium in three strains of inbred mice. *Oral Surg Oral Med Oral Pathol* 12:820-829.

39. Shusterman, A., Salyma, Y., Nashef, A., Soller, M., Wilensky, A., Mott, R., Weiss, E.I., Houri-Haddad, Y., and Iraqi, F.A. 2013. Genotype is an important determinant factor of host susceptibility to periodontitis in the Collaborative Cross and inbred mouse populations. *BMC Genet* 14:68.

40. Shusterman, A., Durrant, C., Mott, R., Polak, D., Schaefer, A., Weiss, E.I., Iraqi, F.A., and Houri-Haddad, Y. 2013. Host susceptibility to periodontitis: mapping murine genomic regions. *J Dent Res* 92:438-443.

41. Page, R.C., and Kornman, K.S. 1997. The pathogenesis of human periodontitis: an introduction. *Periodontol 2000* 14:9-11.

42. Bartold, P.M., and Narayanan, A.S. 2006. Molecular and cell biology of healthy and diseased periodontal tissues. *Periodontol 2000* 40:29-49.

43. Ohlrich, E.J., Cullinan, M.P., and Seymour, G.J. 2009. The immunopathogenesis of periodontal disease. *Aust Dent J* 54 Suppl 1:S2-10.

44. Brandwein, S.R., and Maenz, L. 1992. Defective lipopolysaccharide-induced production of both interleukin 1 alpha and interleukin 1 beta by A/J mouse macrophages is posttranscriptionally regulated. *J Leukoc Biol* 51:570-578.

45. O'Malley, J., Matesic, L.E., Zink, M.C., Strandberg, J.D., Mooney, M.L., De Maio, A., and Reeves, R.H. 1998. Comparison of acute endotoxin-induced lesions in A/J and C57BL/6J mice. *J Hered* 89:525-530.

46. Silver, L.M. 1995. *Mouse genetics : concepts and applications*. New York: Oxford University Press. xiii, 362 p. pp.

47. Beamer, W.G., Donahue, L.R., Rosen, C.J., and Baylink, D.J. 1996. Genetic variability in adult bone density among inbred strains of mice. *Bone* 18:397-403.

48. Cervino, A.C., Darvasi, A., Fallahi, M., Mader, C.C., and Tsinoremas, N.F. 2007. An integrated in silico gene mapping strategy in inbred mice. *Genetics* 175:321-333.

49. Grupe, A., Germer, S., Usuka, J., Aud, D., Belknap, J.K., Klein, R.F., Ahluwalia, M.K., Higuchi, R., and Peltz, G. 2001. In silico mapping of complex disease-related traits in mice. *Science* 292:1915-1918.

50. Farber, C.R., Bennett, B.J., Orozco, L., Zou, W., Lira, A., Kostem, E., Kang, H.M., Furlotte, N., Berberyan, A., Ghazalpour, A., et al. 2011. Mouse genome-wide association and systems genetics identify Asxl2 as a regulator of bone mineral density and osteoclastogenesis. *PLoS Genet* 7:e1002038.

51. Ghazalpour, A., Bennett, B., Petyuk, V.A., Orozco, L., Hagopian, R., Mungrue, I.N., Farber, C.R., Sinsheimer, J., Kang, H.M., Furlotte, N., et al. 2011. Comparative analysis of proteome and transcriptome variation in mouse. *PLoS Genet* 7:e1001393.

52. Park, C.C., Gale, G.D., de Jong, S., Ghazalpour, A., Bennett, B.J., Farber, C.R., Langfelder, P., Lin, A., Khan, A.H., Eskin, E., et al. 2011. Gene networks associated with conditional fear in mice identified using a systems genetics approach. *BMC Syst Biol* 5:43.

CHAPTER TWO

Genome-Wide Association Study Identifies CXCR3 as a Partial Mediator of LPS-induced Periodontitis

Abstract:

Periodontitis (PD) is characterized by bacterial infection and inflammation of tooth supporting structures and can lead to tooth loss. PD affects ~47% of the U.S. population over 30 and is 50% heritable. While the host immunoinflammatory response and genetic background play a role, few studies have mechanistically validated candidate genes associated with PD. Using a Genome-wide Association Study (GWAS), we aimed to identify genes that mediate Lipopolysaccharide (LPS)-induced PD, as well as, mechanistically interrogate candidate genes. Through GWAS, we identified ~47% heritability and a strain-dependent 6-fold difference in LPS-induced bone loss across the Hybrid Mouse Diversity Panel (HMDP). Using FaST-LMM and RNA expression data, we identified Cxcl family members as associated with PD. Additionally, Cxcl10 protein and an increase in immune cells and pro-inflammatory cytokines were observed in C57BL/6J (high bone loss strain) and not in A/J (low bone loss strain) after LPS-injections. Most interestingly, deleting CXCR3 (Cxcl9 and10 receptor), demonstrated ~50% reduction in bone loss and decreased osteoclasts after LPS-injections compared. Furthermore, WT mice treated with AMG-487 (CXCR3 antagonist) resulted in ~45% reduction in bone loss and decreased osteoclasts after LPS-injections. Therefore, CXCR3 might serve as a possible target for modulating the host response in PD susceptibility.

Introduction:

Periodontitis (PD) is characterized by a bacterial infection and inflammation that destroys the tissues that surround and support the teeth. If left untreated, PD can result in tooth loss (1, 2). PD affects 47.2% and 70.1% of the population over the age of 30 and 65 respectively (1). Microorganisms are central to PD pathogenesis and *P. gingivalis (P.g.)* is a significant species involved in PD infection. Moreover, *P.g.* is classified as a keystone species in PD disease progression and is consistently found around teeth with PD (3). In addition to bacteria, environmental and genetic factors contribute to the risk of developing PD. A classic study on tea laborers, with no access to oral hygiene or dental care, highlighted that under similar environmental circumstances, there were wide variations of PD susceptibility, suggesting that PD has a significant genetic component (4). Moreover, twin studies, after adjustment for environmental and external factors, concluded that approximately 50% of the variance observed in PD is attributed to genetics (5, 6). These studies emphasize that there are inherent host response differences in PD susceptibility and progression (5, 6). When combining host response differences and environmental factors, PD presents as a complex (polygenic) disease (7, 8). Complex trait diseases involve many genetic and non-genetic factors, i.e. environmental factors, where each factor can play a small role in trait/disease presentation (9). While environmental factors play a role in complex trait diseases, genetic involvement is the predominant culprit considering the heritability of most complex traits (9). Unfortunately, the detailed genetic influence in the pathogenesis of PD is not fully understood.

Genome-wide association studies (GWAS) have emerged as a powerful tool to investigate the genetic architecture of complex trait diseases. GWAS allows for the unbiased interrogation of the entire genome in order to identify single nucleotide polymorphisms (SNPs) associated with disease. In order to compliment human GWAS, animal models can be used and they offer

several advantages. Mice specifically, share similar structural, functional, and genetic traits to humans (10). Moreover, there are powerful molecular and genetic tools, as well as repositories of mouse phenotypic, genotypic, metabolomic, and proteomic databases available in order to characterize disease pathogenesis (10). Additionally, a major advantage of mouse studies is the ability to dissect disease and signaling pathways through genetic manipulation including knock-in and knock-out mice. Several mouse panels, including the Hybrid Mouse Diversity Panel (HMDP) (11) and the Collaborative Cross (CC) (12) have been designed to capture the genetic variation present in populations, as well as, provide high statistical power and fine mapping of the genome. Specifically, the HMDP offers a powerful genetic approach to study complex genetic diseases (11). The HMDP is comprised of classic inbred and recombinant inbred mice densely genotyped for single nucleotide polymorphisms (SNPs), which provide fine genetic mapping resolution and statistical genotype to phenotype association (13).

Previously, our group analyzed susceptibility to *Porphyromonas gingivalis* (*P.g*) Lipopolysaccharide (LPS)-induced bone loss and identified A/J, highly resistant, and C57BL/6J, highly susceptible, mouse strains to PD (14). Furthermore, we observed strain-dependent bone loss in the five parental strains of the HMDP, as well as, ~50% heritability, which corroborates findings in patients (6, 14, 15). Expanding from this previous study, here, we employed a GWAS on classic and recombinant inbred strains of the HMDP to identify genetic mediators of LPS-induced periodontitis and its potential implications in disease development.

Results:

LPS-induced Strain-Dependent Bone Loss across the HMDP

In order to assess differences in response to *P.g.* LPS in the Hybrid Mouse Diversity Panel (HMDP), linear bone loss was quantitated at the injection site (between the first and second molars) after six weeks. Bone loss quantitation of 104 strains of the HMDP revealed a strain-dependent bone loss response to *P.g.* LPS (Figure 2-1A). BXH8/TyJ, a strain derived from a cross between C3H/HeJ and C57BL/6J presented with the least amount of bone loss after LPS injections (0.071 ± 0.010). In contrast, BXD84/RwwJ, a strain derived from a cross between DBA/2J and C57BL/6J presented with the highest amount of bone loss after LPS injections (0.468 ± 0.030) (Figure 1A and 1B). Radiographically, representative micro-CT images showed alveolar bone loss in between the first and second molars at the LPS injection site (Figure 2-1B).

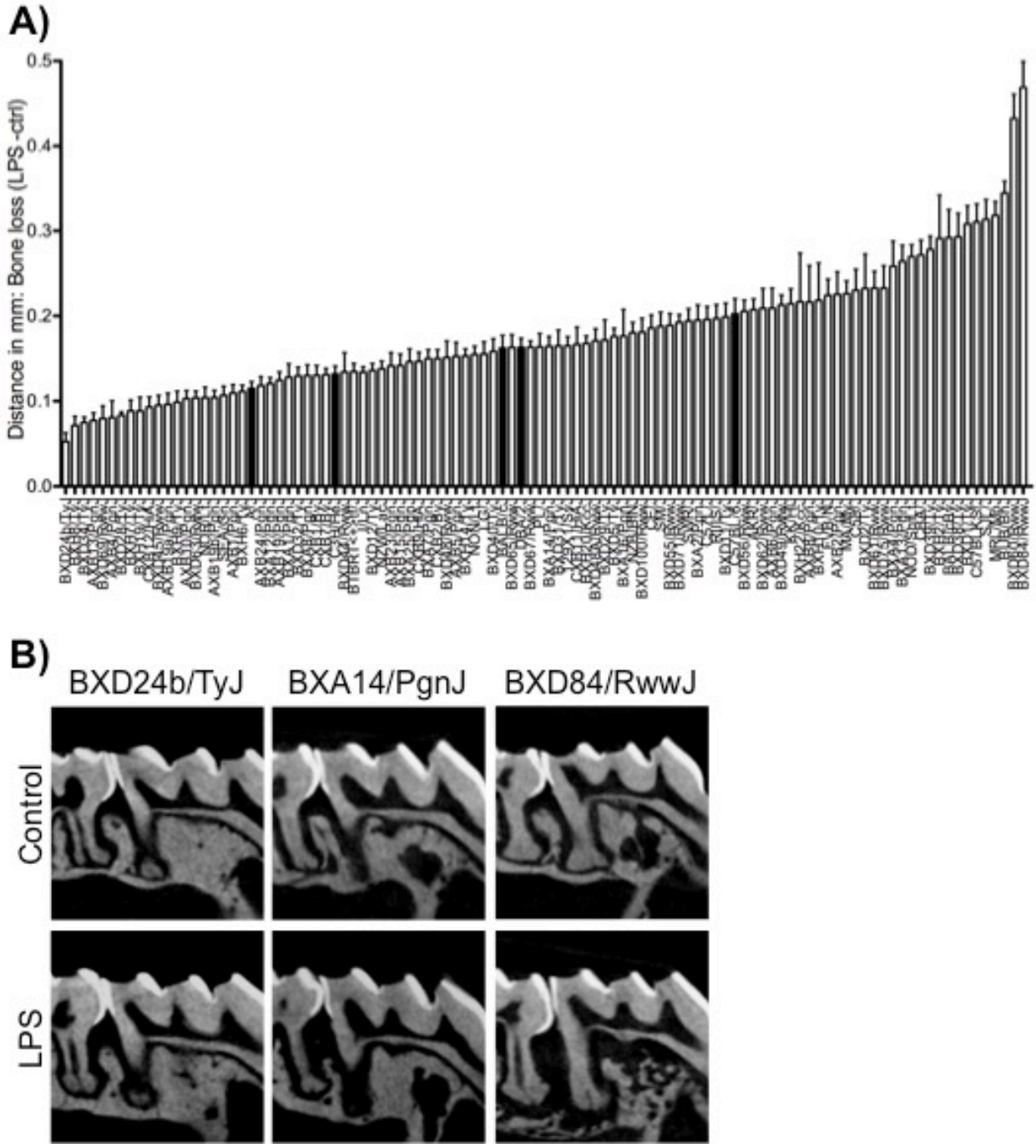

Figure 2-1: Radiographic evaluation after six weeks of P.g.-LPS injections (A) Graph representing bone loss in mm (LPS-ctrl) in 104 strains of the Hybrid Mouse Diversity Panel (HMDP) n≥6 mice/strain. Data is represented as mean ± standard error of the mean (SEM). The black bars represent the five parental strains of the HMDP. (B) Representative radiographic images of control and LPS treated strains of the HMDP. BXD24b/TyJ lost the least amount of bone while BXD84/RwwJ lost the most amount of bone.

Genome-Wide Association of SNPs to LPS-induced Bone Loss

To correlate the differences in bone loss phenotype to the differences in genotype across the HMDP, a genome-wide association study was performed using Factored-Spectrally Transformed-Linear Mixed Modeling (FaST-LMM). Using an initial significance threshold of 10^{-4}, the Manhattan plot showed statistically significant peaks across multiple chromosomes including chromosomes 1, 3, 4, 7, 5, 9, and 19 (Figure 2-2A). In total, we identified over 800 single nucleotide polymorphisms (SNPs) with a significance value of 10^{-4} or higher as associated with LPS-induced PD. Out of the ~800 SNPs, the majority presented with a significance value of 10^{-4} (~700 SNPs) which included genes, such as Toll-like receptor (*Tlr*) *Tlr4* (Chr4), *Tlr9* (Chr9), and tumor necrosis factor-alpha (*Tnf-A*) family members including *Tnfsf10* (Chr3), already known to be increased in PD (16-21), as well as new gene candidates not previously associated with PD (Chr1: *Il-19*, *Cdc73*, *Tgfb2*, *Brinp3*, *Pou2f1*, *Nuf2*; Chr19: *Pcsk5*, *Ostf1*, *Prune2*, *Gcnt1*, *Trpm6*, *Gna14*, *Foxb2*) (Figure 2-2A). While many SNPs fell under statistically significant peaks along these chromosomes, we prioritized rs33249065 located on Chr. 5 in a region enriched with chemokine (C-X-C motif) ligands (CXCL), specifically, *Cxcl9* and *Cxcl10* (Figure 2-2B). This region was prioritized based on gene and protein expression data described below.

Furthermore, we assessed heritability for LPS-induced bone loss across the HMDP using two approaches: “broad sense” and “narrow sense.” Broad sense heritability evaluates total heritability. In contrast, narrow sense heritability evaluates additive genetic variance (22). For LPS-induced bone loss, broad sense heritability was calculated at ~53% while narrow sense heritability was calculated at ~46%. For our trait, the broad sense heritability calculation was larger than narrow sense heritability suggesting that gene-by-gene interactions or non-additive factors are important in LPS-induced bone loss (22).

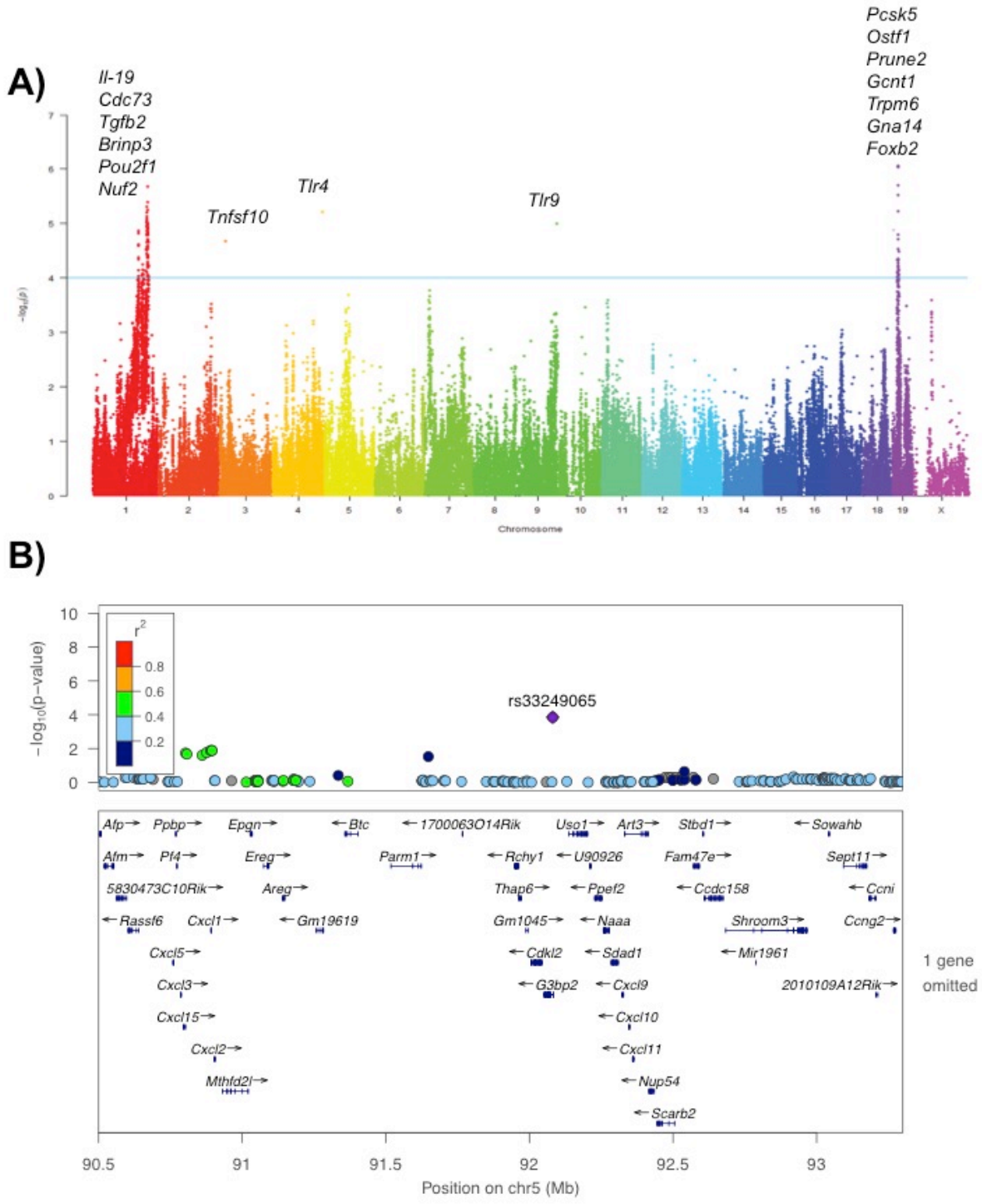

Figure 2-2: Genome-wide association for P.g.-LPS induced bone loss (A) Manhattan plot for *P.g.*-LPS induced bone loss. (B) High resolution regional plot generated through LocusZoom. Zoom up on Chr 5. The blue horizontal bars denote a gene's physical location. The linkage disequilibrium (LD) of the highlighted SNP at the locus is denoted by the color of the SNP. Highly correlated SNPs would be shown in red (in strong LD with each other), while weakly correlated SNPs are shown in navy (correlation represented by r^2 color scale, inset).

Correlation of Genome-Wide Macrophage Gene Expression to Candidate Genes in LPS-induced Bone Loss

It is well documented that macrophages are increased in patients with PD (23, 24) as part of the host immune response to periodontopathogens. Therefore, we aimed to correlate our bone loss FaST-LMM association mapping to a previous GWAS utilizing the HMDP assessing macrophage expression Quantitative Trait Loci (eQTL) in response to LPS treatment (25). Several genes classified as immune response genes including growth factor receptor bound protein 2-associated protein 3 (*Gab3*), involved in cytokine signaling pathways and macrophage differentiation, and mitogen-activated protein kinase 7 (*Map2k7*), which mediates responses to proinflammatory cytokines, were correlated to both macrophage response to LPS and LPS-induced bone loss. Interestingly, *Cxcl* family members *(Cxcl15 and Cxcl17*) were also correlated ($p<0.05$) to both macrophage response to LPS and LPS-induced bone loss (Table 2-1).

Interestingly, when assessing functional significance of genes correlated to macrophage response to LPS and LPS-induced bone loss through gene ontology (GO), many genes fell under the inflammatory response/cytokine pathway including *Ccr5* and *Ccr8* (chemokine receptors), and immune system processes including Gab3 as previously discussed. The full table of genes correlated to both macrophage response to LPS and LPS-induced bone loss is in Supplemental Table 2-2.

Gene	p Value
Gab3	0.000823418
Map5k7	0.000823418
Cxcl15	0.018472638
Cxcl17	0.010371218

Table 2-1: Genes correlated to macrophage response to LPS and LPS-induced bone loss

Cxcl Family Members Show Increased Gene Expression in a High Bone Loss Strain

To further, evaluate differences in mRNA expression levels, in strains with high and low amount of bone loss after LPS injection, we performed microarray analysis utilizing the parental strain with the lowest (A/J) and the highest (C57BL/6J) amount of bone loss (Figure 2-1A).

Significant differences in mRNA expression were observed between A/J and C57BL/6J four hours after LPS treatment (Table 2-2). *Cxcl* family members were among the statistically significant differentially expressed genes induced by LPS. The primary genes of interest were genes that were significantly induced in C57BL/6J LPS treated mice, but not induced in A/J LPS treated mice. For instance, *Cxcl9* induction was 38.87 fold difference), and *Cxcl10* (19.23 fold difference) (Table 2-2). Both *Cxcl* chemokines are involved in chemoattraction of immune cells including monocytes/macrophages, T-cells, natural killer cells, and dendritic cells (26-28). Additionally the chemokines *Ccl4* (5.77 fold difference) and *Ccl7* (3.55 fold difference), which are involved in macrophage inflammatory response and monocyte chemoattraction respectively, were induced in C57BL/6J LPS treated mice and not in A/J LPS treated mice highlighting that several host immune response pathways were significantly induced after LPS treatment in a our high bone loss strain.

Gene	Fold Change	p Value
Ccl4	5.77	0.001078
Ccl7	3.55	0.000648
Cxcl1	7.02	0.004294
Cxcl9	38.87	0.020823
Cxcl10	19.23	0.009514

Table 2-2: Differential gene expression induced by LPS only in C57BL/6J

Immune and Pro-inflammatory Markers Show Increased Expression in a High Bone Loss Strain

To further characterize differences between A/J, a low bone loss strain, and C57BL/6J, a high bone loss strain, tissues specimens were analyzed for immune and pro-inflammatory cellular markers through immunohistochemistry (IHC) staining. Neutrophil and T-cell protein expression was assessed in A/J and C57BL/6J mice after LPS treatment because neutrophils and T-cells are known to infiltrate into periodontal lesions in response to infection and inflammation (29, 30). When comparing controls groups, there was no difference in immunostaining between C57BL/6J control and A/J control groups for both neutrophils and T-cells. However, C57BL/6J LPS-treated groups presented with increased expression of neutrophils and T-cells (Figure 2-3A and 2-3B, black arrows) compared to A/J-LPS treated mice. Furthermore, when staining for CXCL10 protein (chemokine responsible for a wide array of immune response cascades), which was highly associated in our GWAS and up-regulated in our gene expression data (microarray), C57BL/6J LPS-treated specimens presented with increased protein expression of CXCL10 (Figure 2-3C, black arrows) compared to A/J LPS treated mice. Again, there was no basal difference in CXCL10 protein expression between C57BL/6J control and A/J control groups.

To evaluate pro-inflammatory mediators, protein levels of three pro-inflammatory markers including nuclear factor kappa-light-chain-enhance of activated B cells (NF-κB), cyclooxygenase-2 (COX-2), and tumor necrosis factor-alpha (TNF-A), which are known to have increased expression in patients with PD, were assessed (21, 31, 32). C57BL/6J LPS treated animals showed increased protein expression of all three pro-inflmamatory mediators as evident by the brown/red immunoreactivity/staining (Supplemental Figure 2-1A, 2-1B, 2-1C, black arrows) compared to A/J LPS treated mice. For all three pro-inflammatory markers, there was no qualitative difference between C57BL/6J control mice and A/J control mice.

Degradation of the extracellular matrix, caused by the action of matrix metalloproteinase (MMP) enzymes, is a host-mediated response in periodontitis (33). Therefore, staining for MMP-8 and MMP-13, which are associated with periodontitis in patients (34, 35), was assessed in A/J and C57BL/6J mice. After LPS treatment, C57BL/6J mice presented with increased immunoreactivity and protein expression of both MMP-8 and MMP-13 shown by the brown/red stain (Supplemental Figure 2-2A and 2-2B, black arrows). When comparing C57BL/6J control groups to A/J control groups, there was no qualitative difference in MMP-8 or MMP-13 protein expression.

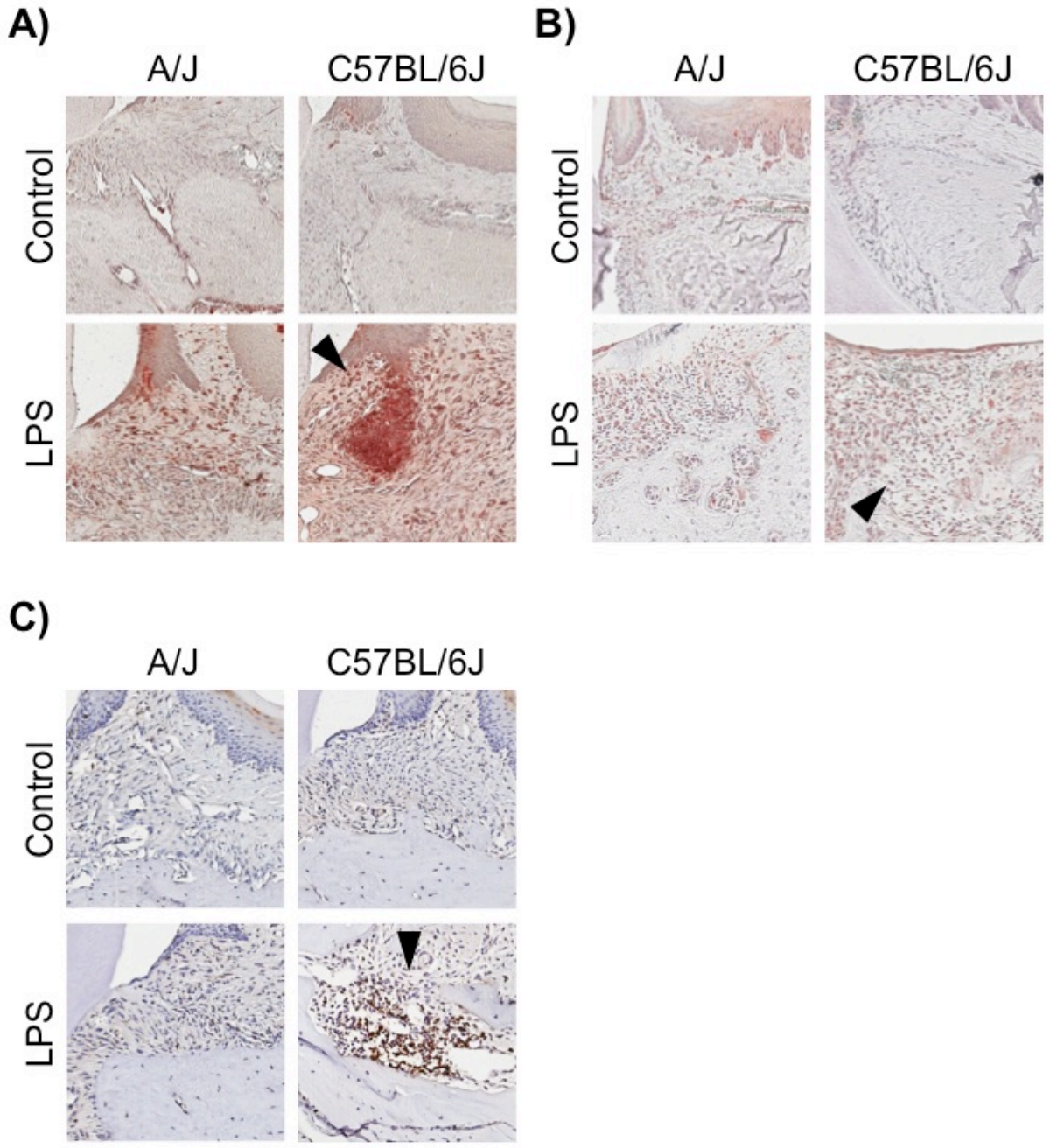

Figure 2-3: Histological assessment of immune cells and cytokine protein expression (A) Neutrophil immunostaining in A/J control, A/J LPS, C57BL6/J control, and C57BL6/J LPS treated mice. Noted the increased staining in C57BL6/J LPS compared to A/J LPS (black arrow). (B) CD3+ T-cell immunostaining in A/J control, A/J LPS, C57BL6/J control, and C57BL6/J LPS treated mice. Noted the increased staining in C57BL6/J LPS compared to A/J LPS (black arrow). (C) CXCL10 immunostaining in A/J control, A/J LPS, C57BL6/J control, and C57BL6/J LPS treated mice. Noted the increased staining in C57BL6/J LPS compared to A/J LPS (black arrow). All images are at 20X.

Cxcr3 Knock-out Mice Present with Reduced Bone Loss After LPS Treatment

Based on the GWAS, gene expression, and IHC data, the *Cxcl9* and *Cxcl10* pathway was further investigated to better understand their involvement in LPS-induced periodontal bone loss. As stated previously, *Cxcl9* and *Cxcl10*, are involved in an array of immune responses including recruitment of monocytes/macrophages, T-cells, natural killer cells, and dendritic cells (26-28). Furthermore, all three chemokines propagate their responses through the C-X-C motif chemokine receptor 3 (CXCR3). Therefore, in order to inhibit the function of all three chemokines, we employed a *Cxcr3* knockout (KO) mouse and our *P.g.* LPS injection model.

After 12 LPS injections, *Cxcr3* KO mice presented with statistically significant less bone loss compared to WT (Figure 2-4). Radiographically, WT LPS treated mice showed a clear reduction in alveolar bone in between the first and second molars compared to *Cxcr3* KO mice (Figure 2-4A and 2-4B).

In order to confirm that the differences observed were in fact due to LPS treatment and not due to inherent bone quality differences between *Cxcr3* KO and WT mice, we assessed initial bone volume/tissue volume (BV/TV) in *Cxcr3* KO and WT control animals. For both the maxillae and mesial trabecular bone distal from the growth plate in the femur, there was no statistical difference between BV/TV between *Cxcr3* KO and WT mice (Supplemental Figure 2-3).

Following radiographic assessment of bone loss, *Cxcr3* KO and WT mice were further analyzed for histological changes. Through hematoxylin and eosin (H&E) staining, there was an increase in cellular infiltrates observed in the WT LPS treated group compared to the *Cxcr3* KO group (Figure 2-4C, yellow arrow). Comparing WT control mice to *Cxcr3* KO control mice there was no difference in cellular infiltrates (purple cells in the epithelial tissue). Further assessment of

protein expression of pro-inflammatory marker, COX-2, showed increased staining in WT LPS treated groups compared to *Cxcr3* KO LPS treated animals. Again, when comparing WT control mice to *Cxcr3* KO control mice, there was no overt difference in COX-2 expression.

In addition to pro-inflammatory markers, osteoclast numbers were evaluated through tartrate resistant acid phosphatase (TRAP) staining after LPS injections between WT and *Cxcr3* KO mice (Figure 2-5). When comparing WT LPS treated to *Cxcr3* KO LPS treated, WT mice presented with statistically significantly more TRAP+ cells compared to *Cxcr3* KO mice (Figure 2-5B). Focusing on control groups, WT control mice presented with significantly more osteoclasts compared to *Cxcr3* KO control mice. Furthermore, when normalizing osteoclast numbers to alveolar bone length and surface area considered in analysis, WT LPS treated mice presented with statistically significantly more osteoclasts per bone length and bone surface area compared to *Cxcr3* KO LPS treated mice (Figure 2-5C and 2-5D).

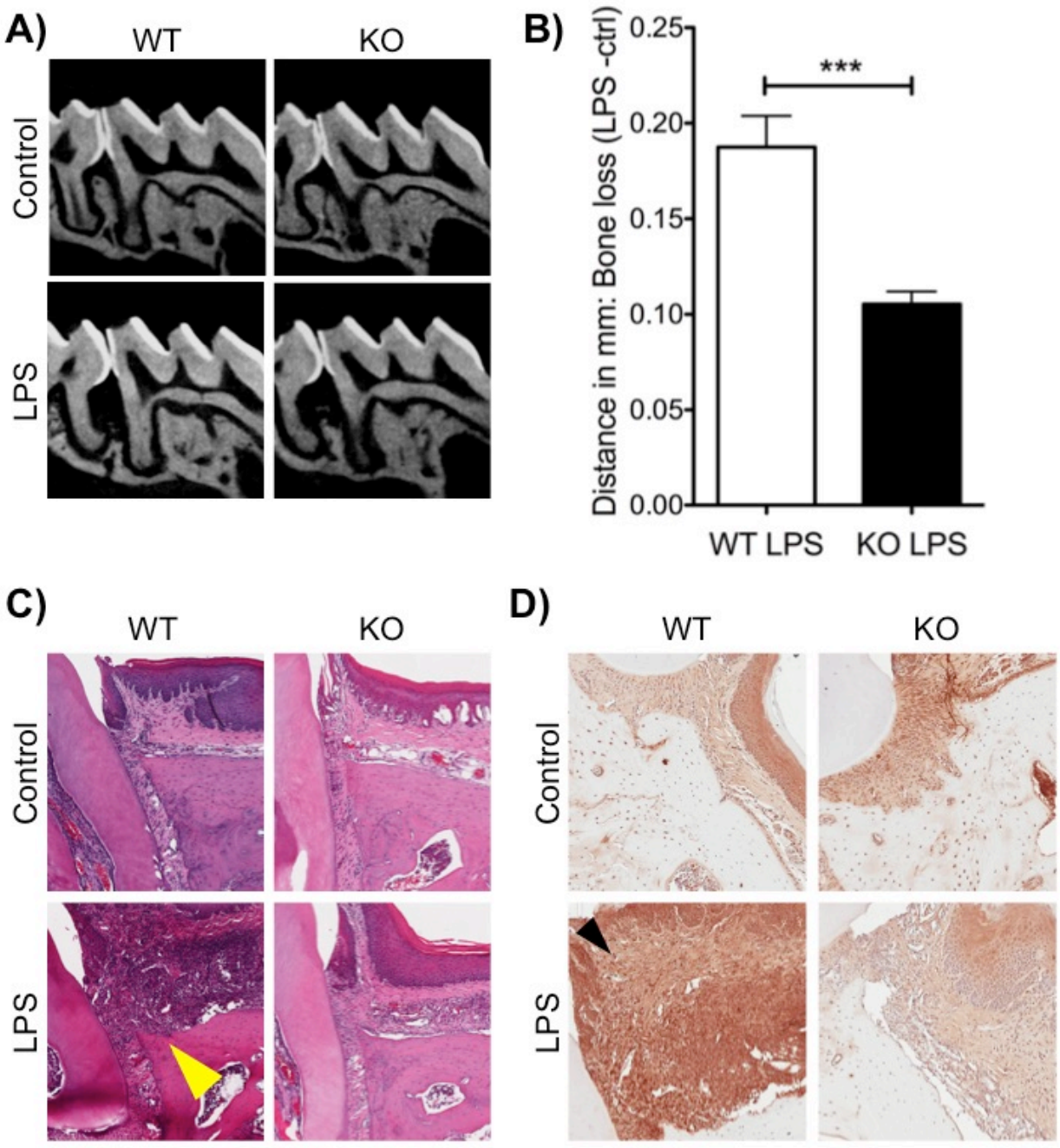

Figure 2-4: Deletion of Cxcr3 in vivo causes a reduction in bone loss (A) Representative radiographic images of wild-type (WT) and *Cxcr3* knock-out (KO) control and LPS treated mice. Note the increased bone loss in the WT LPS group compared the KO LPS group. (B) Graph representing the bone loss (ctrl-LPS) of WT and KO mice. Significance was compared using a Student's *t* test. n=3 mice/group, p≤0.05*, p≤0.01**, p≤0.001***. Data represented as mean ± standard error of the mean (SEM). (C) Hematoxylin and eosin stained tissue sections of WT and KO control and LPS treated groups. Increased inflammatory infiltrates in the WT LPS group is denoted by the yellow arrow. (D) COX-2 immunostaining in WT and KO control and LPS groups. Increased COX-2 expression (brown stain) is denoted by the black arrow in the WT LPS.

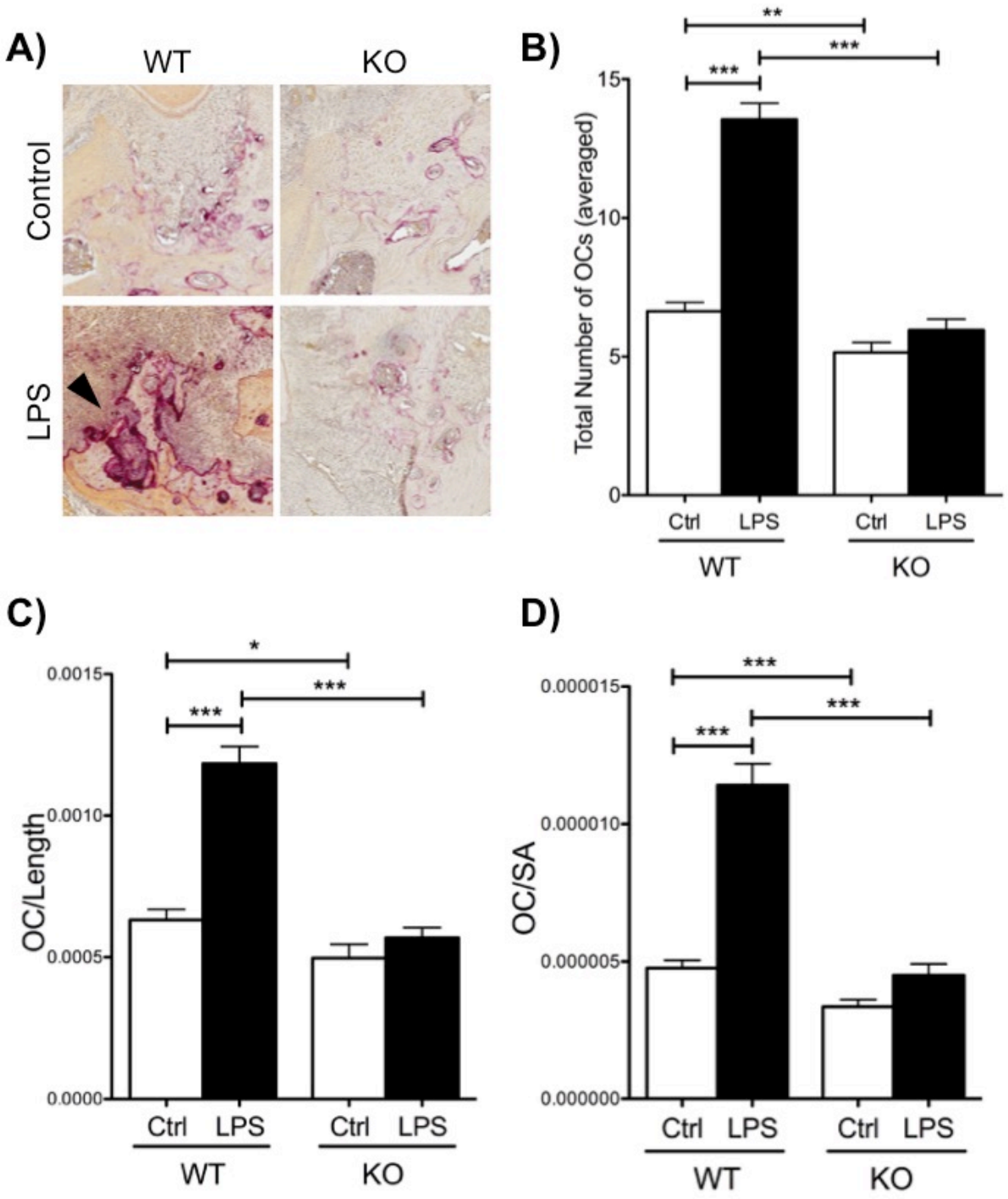

Figure 2-5: Histological assessment of osteoclast numbers in WT and Cxcr3 KO mice (A) Tartrate Resistant Acid Phosphatase (TRAP+) staining for osteoclasts. Note the increase in TRAP+ cells in WT LPS treated mice (black arrow) compared to KO LPS treated mice. 20X magnification. (B) Graph representing total number of averaged osteoclasts in WT and *Cxcr3* KO control and LPS groups. (C) Graph representing osteoclast numbers divided by the length of alveolar bone measured. (D) Graph representing osteoclast numbers divided by the surface area (SA) of the alveolar bone considered in analysis. For all graphs (B, C, and D): Significance was compared using a Student's *t* test. n=3 mice/group, p≤0.05*, p≤0.01**, p≤0.001***. Data represented as mean ± standard error of the mean (SEM).

CXCR3 Antagonist Reduces Bone Loss *in vivo*

After LPS injections, *Cxcr3* KO mice exhibited a reduction in bone loss and osteoclast numbers compared to WT mice. Therefore, we choose to investigate if inhibition of CXCR3 *in vivo* through a CXCR3 antagonist would produce similar results we utilized AMG-487. AMG-487 is a commercially available CXCR3 antagonist that inhibits CXCR3-cell migration mediated by the chemokines CXCL9 and CXCL10.

After 12 LPS injections, LPS injected mice treated with AMG-487 showed a significant reduction in bone loss compared to LPS treated veh-injected mice (Figure 2-6A and 2-6B). Normalizing bone loss to control, LPS injected mice treated with AMG-487 showed ~45% reduction in bone loss compared to LPS injected veh treated mice (Figure 2-6C). Histologically, after LPS treatment, AMG-487 presented with a qualitative reduction in cellular infiltrates as compared to LPS vehicle treated animals (Figure 2-6D). Further assessment of osteoclast numbers showed that after LPS treatment, AMG-487 statistically significantly reduced the total number of TRAP+ cells compared to LPS vehicle treated mice (Figure 2-7A and 2-7B). Normalizing osteoclast numbers to bone length, showed similar results (Figure 2-7C).

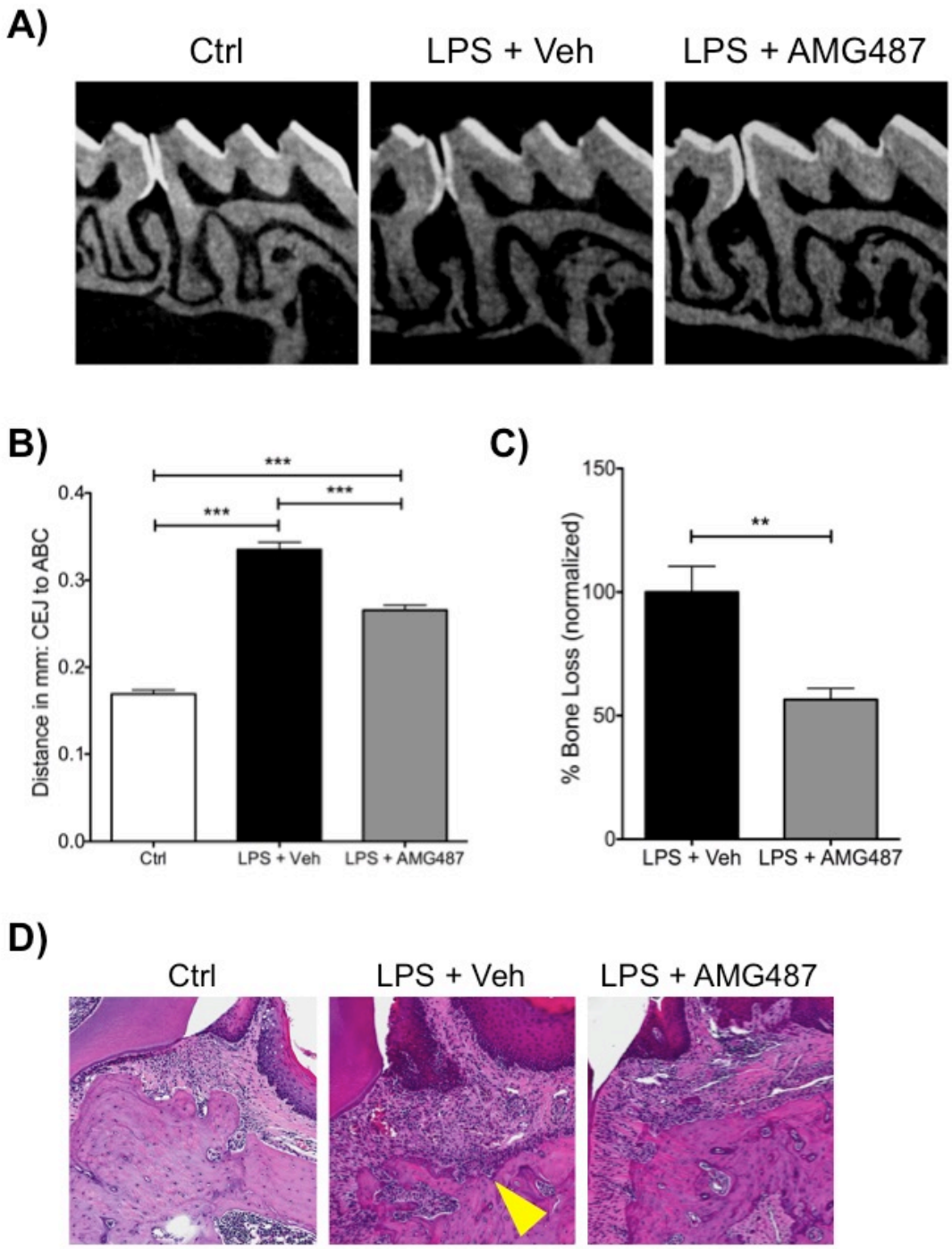

Figure 2-6: Systemic delivery of CXCR3 antagonist (AMG-487) reduces bone loss *in vivo* (A) Representative radiographic images of control (ctrl), *P.g.*-LPS + veh injections, and *P.g.*-LPS + AMG-487. Note the reduction in alveolar bone (in between the first and second molars) in the *P.g.*-LPS + veh group. (B) Graph representing the averaged bone levels in control (Ctrl), *P.g.*-LPS + veh injections, and *P.g.*-LPS + AMG-487 groups. (C) Graph representing normalized bone loss (control group subtracted) in *P.g.*-LPS + veh injections and *P.g.*-LPS + AMG-487 groups. For both graphs (B and C): Significance was compared using a Student's *t* test. n≥5 mice/group, p≤0.05*, p≤0.01**, p≤0.001***. Data represented as mean ± standard error of the mean (SEM). (D) Hematoxylin and eosin (H&E) stained slides of control (Ctrl), *P.g.*-LPS + veh injections, and *P.g.*-LPS + AMG-487 groups. Note the increased cellular infiltrates in the *P.g.*-LPS + veh injection group (yellow arrow). 20X magnification.

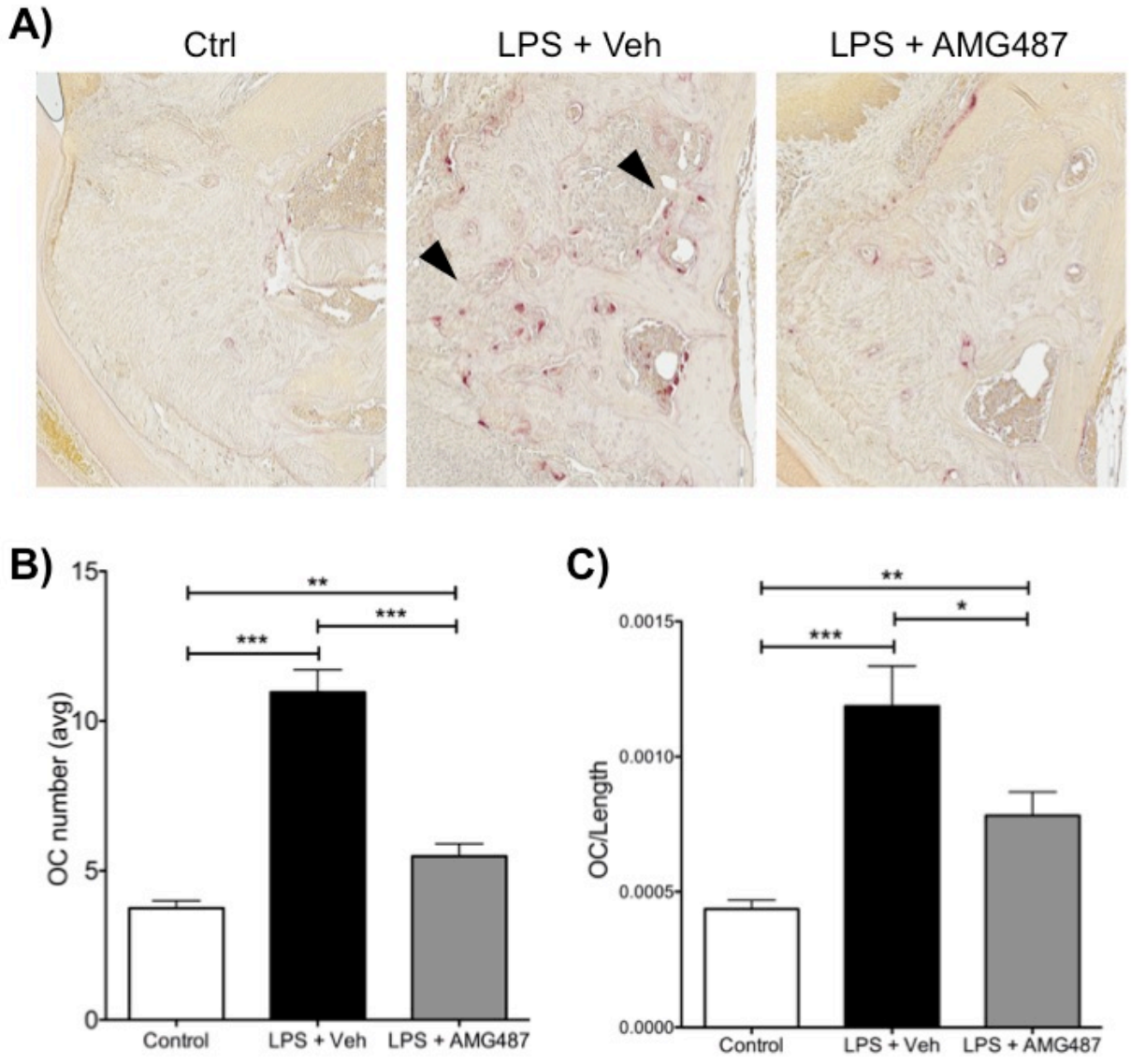

Figure 2-7: Histological assessment of osteoclast numbers after AMG-487 treatment (A) Tartrate Resistant Acid Phosphatase (TRAP) staining of control (Ctrl), *P.g.*-LPS + veh injections, and *P.g.*-LPS + AMG-487 groups. Note the increase in TRAP+ cells in the *P.g.*-LPS + veh injection group (black arrows). 20X magnification. (B) Graph representing the averaged total number of osteoclasts in control (Ctrl), *P.g.*-LPS + veh injections, and *P.g.*-LPS + AMG-487 groups. (C) Graph representing the averaged osteoclast number divided by the alveolar bone length considered in analysis in control (Ctrl), *P.g.*-LPS + veh injections, and *P.g.*-LPS + AMG-487 groups. For both graphs (B and C): Significance was compared using a Student's *t* test. n≥5 mice/group, p≤0.05*, p≤0.01**, p≤0.001***. Data represented as mean ± standard error of the mean (SEM).

Discussion:

Periodontitis (PD), as mentioned previously, is a complex disease with genetic and environmental influences, which can be a challenge to dissect in a clinical setting. Through novel resources and technologies, the mouse has become an invaluable tool to interrogate complex trait diseases, including PD, and here we utilized a GWAS approach to identify genetic mediators of PD. Herein, we demonstrated that over 800 single nucleotide polymorphisms (SNPs) were identified as associated to PD, and one gene family, including the genes *Cxcl9 and Cxcl10,* were selected for validation by deleting the CXCR3 receptor. Furthermore, utilizing *Cxcr3* knockout mice and competitive inhibition with a CXCR3 antagonist, we demonstrated that approximately 50% of the PD phenotype could be rescued *in vivo*. Most importantly, this finding paves the way for blocking CXCR3 as a potential therapeutic modality for patients presenting with PD and the GWAS approach allows for further mechanistic dissection of candidate genes associated to PD.

In an effort to better characterize and understand the genetic underpinning of PD pathogenesis, several groups have utilized a GWAS approach using patient cohorts (36-42). These studies have highlighted that there is indeed a significant genetic component in PD; however, patient study designs have inherent challenges including: controlling for environmental factors, i.e. oral hygiene habits, smoking status, and the presence of other systemic conditions including diabetes and heart disease, which can all have an effect on clinical and research outcomes. Additionally, identifying time of disease onset and standard disease classifications is hard to achieve in patient studies. Even so, patient studies have allowed us to begin to better understand PD pathogenesis.

Multiple studies have used GWAS in clinical cohorts of PD, including chronic PD (characterized by slow progression and most prevalent in adults) (43) and aggressive PD (characterized by

rapid destruction, familial aggregation, and patients often present with a reduced microbial load relative to the amount of tissue destruction) (44). Clinical cohorts of German/Dutch (37, 40, 44), European Americans as part of the atherosclerosis risk community (42, 45), Hispanics/Latinos (41), Koreans (46), Libyans (47), and Japanese (48) populations have all been examined through a case-control study design. GWAS in humans have begun to lay the foundation for identifying genetic targets associated with disease and have been very effective. Several genes have been associated to chronic and aggressive PD including *IL-1A* and *IL-1B* (49-52), which have been found to be associated in different ethnic cohorts including Caucasians, Asians, Indians, and Brazilian populations. Interestingly, different SNPs within *IL-1A* and *IL-1B* were reported in each ethnic population. Furthermore, several groups have also identified SNPs in *Tnf-A*, *Tlr2*, and *Tlr4* with specific polymorphisms associated with each ethnic group including Caucasians, Asians, Chinese, Brazilians, Turkish, Indians and Africans (53-57). Importantly, we observed *Tnf* and *Tlr* gene family members as associated with LPS-induced bone loss in our mouse model of PD, which suggests that animal studies can be designed with clinical translation in mind. When assessing human data, it is important to consider that most human GWAS conclude after gene discovery/gene association and it is difficult to confidently define how a gene affects the overall trait. Therefore, animal models, in which molecular tools can be employed, including genetic manipulation through knock-in or knock-out mice and evaluating gene-by-gene influence, can greatly compliment findings in human populations.

Two mouse panels are at the forefront of mouse GWAS studies: the Collaborative Cross (CC) and the Hybrid Mouse Diversity Panel (HMDP) (13). The CC is comprised of recombinant inbred strains from eight genetically diverse founder strains (12). Additionally, the CC includes wild-derived strains in order to capture more genetic variation that is present in a population, however, this impacts study reproducibility. In contrast, the HMDP includes classic inbred strains included to capture genetic variety and recombinant inbred strains included to provide

fine mapping resolution, which were all selected to account for differences in population structure (13, 58). Additionally, because all of the strains in the HMDP are commercially available and densely genotyped, experiments can easily be reproduced and tested on a variety of parameters. While there are differences in both the CC and the HMDP, both panels perform well for GWAS approaches. Indeed several groups, including our own have employed either the CC or the HMDP to further investigate the genetic contribution to PD. Using the CC and an oral infection model of PD, Shusterman et al, showed that BALB/cJ mice were highly susceptible and DBA/2J, C57BL/6J, and A/J mice were highly resistant to bacterial-induced PD (59). Expanding on the CC and their previous study, Shusterman et al utilized F_2-crosses from A/J (resistant to oral infection-induced PD) and BALB/cJ (susceptible to oral infection-induced PD) to analyze gene expression changes, as well as, correlate data with patient GWAS. Interestingly, they observed that the *Cxcl4/Cxcl7/Cxcl5* gene cluster was associated with aggressive PD in German and European American populations (60).

In contrast, our group focused our preliminary work and the present study utilizing the HMDP. Our initial studies employed the five parental strains of the HMDP: A/J, DBA/2J, BALB/cJ, C3H/HeJ, and C57BL/6J (14). To finely isolate the host response and bypass any genetic influences in host bacterial colonization, we choose to induce PD using *P. gingivalis* (*P.g.*) lipopolysaccharide (LPS) (14). Through this, we observed strain-dependent alveolar bone loss after LPS injections and A/J presented with the least amount of bone loss, while C57BL/6J presented with the most amount of bone loss and statistically more osteoclasts compared to A/J. Additionally, heritability for *P.g.*-LPS induced bone loss was ~50%, which is consistent with reports in patients. Expanding from this initial work, in the present study, we chose to employ the same methodologies using the HMDP to perform a GWAS on LPS-induce PD. Through this, we identified over 800 SNPs with a significance value of 10^{-4} or higher as associated with our trait. While the majority of the significant SNPs were at a values of 10^{-4} (~700 SNPs), ~70

SNPs showed a significance value of 10^{-5}, ~20 SNPs showed a significance value of 10^{-6}, ~10 SNPs presented with values of 10^{-7}, and ~10 SNPs presented with values of 10^{-8}. This big data approach allows for many additional avenues for further investigation of how these SNPs mechanistically affect PD susceptibility and severity.

In our pool of significantly associated SNPs, several previously identified genes or gene families emerged, which again emphasizes the translational potential of mouse data to human studies. Specifically, Toll-like receptor 9 (*Tlr9*), Toll-like receptor 4 (*Tlr4*), and several members of the Tumor Necrosis Factor (*Tnf*) gene family (*Tnfsf14*, *Tnfsf14*, and *Tnfsf8*) were identified under highly significant regions on the Manhattan plot in our data. *Tlr*'s are a class of proteins that play a role in the innate immune response and many *Tlr*'s have been implicated in animal models and patient cohorts in studies of PD. Kim et al, using a *Tlr9* homozygous KO mouse, showed that *Tlr9* KO mice were resistant to *P.g.*-infection induced bone loss compared to WT controls (17). Furthermore, *Tlr9* KO mice presented with reduced expression of pro-inflammatory mediators interleukin-6 (IL-6), TNF, and receptor-activator of nuclear factor kappa B ligand (RANKL) compared to WT mice (17). Analyzing patient gingival specimens, Chen et al found that patients with PD presented with increased expression of TLR9 compared to patients with gingivitis (18). Similar data has been observed with respect to *Tlr4*. In a meta-analysis for polymorphisms of *Tlr4* in patient cohorts, Chrzeszczyk et al found that the *Tlr4* Asp299Gly allele caused patients to have an increase risk of chronic PD (16). The TNF superfamily, which are a group of cytokines involved in systemic inflammation, have also been associated with PD in patient studies, the most common TNF-A being associated with PD (20, 21). Specifically, in an effort to prioritize candidate genes involved in PD, Zhan et al, found *Tnfsf14* to be an interested candidate associated with PD and one, which needs further mechanistic validation (19).

Out of all the genes up-regulated in our GWAS, we elected to validate the *Cxcl* family because in addition to the significant association in the GWAS, we observed increased gene expression (through microarray) and protein expression (through IHC) in C57BL/6J (high bone loss strain), compared to A/J (low bone loss strain). Interestingly, we were also able to correlate our GWAS findings with a previously performed GWAS assessing macrophage gene expression changes in response to LPS in the HMDP. Through this, we identified several *Cxcl* family members as associated with both LPS-induced bone loss and macrophage response to LPS suggesting common pathways involved in the host immunoinflammatory response to bacteria. Most importantly, we were able to start dissecting the *Cxcl* pathway to identify a common receptor, CXCR3, and mechanistically interrogate how absence of *Cxcr3* affects LPS-induced PD. *Cxcl9* and *Cxcl10* are involved in the development, function and homeostasis of the immune system. Chemokines, as a class, are proteins involved in immune cell recruitment, inflammation, and immune surveillance (61, 62). The CC and the C-X-C subfamilies constitute the majority of chemokines (63). Specifically, *Cxcl10*, acts as a chemoattractant for monocytes/macrophages, T-cells, NK cells, and dendritic cells, and promotes T-cell adhesion to endothelial cells (26, 27). Monocytes, endothelial cells, and fibroblasts secrete *Cxcl10* (28) and its receptor, CXCR3, have been associated with immunoinflammatory diseases including: liver disease, cardiovascular disease; autoimmune diseases including: type 1 diabetes, autoimmune thyroiditis, Graves' disease, and ophthalmopathy; and systemic diseases including: rheumatoid arthritis, psoriatic arthritis, systemic lupus erythematosus, mixed cryoglobulinemia, Sjögren syndrome, and systemic sclerosis (28, 62, 64-72). To date, *Cxcl10*'s role in PD pathogenesis has not been fully investigated.

A few groups have begun to unravel cytokine and chemokine gene expression patterns utilizing patient samples of PD. In human gingival tissues with PD, CXCL8 levels were increased compared to healthy controls (73). Furthermore, specific polymorphisms in *Cxcl8* have been

shown to be more highly associated with apical PD, which suggests that specific cytokines could play a large role in PD susceptibility and development (74). Indeed, expression of several CXCL family members including CXCL3 (75), CXCL8, CXCL12 (76), and CXCL16 (77) are increased in patients with PD. In addition to an increase in chemokine ligands, expression of several of the CXCL receptors has been reported as increased in patients with PD including CXCR1, CXCR2, and CXCR4 (78). Taken together, this highlights the need for further investigation into the intricate pathways involved in the host immunoinflammatory response and chemokine expression in PD.

The role of CXCR3 and its ligands, CXCL9 and CXCL10, in other systemic diseases in both humans and animals including diabetes (79-82) and cardiovascular disease (83-86) have been investigated. Specifically, CXCL10 chemokine levels were increased in patients with coronary heart disease (86), and *Cxcr3* KO mice showed a delay in diabetes development compared to their WT counterparts. In humans, in a study assessing diabetes and periodontal disease, CXCR3 gene expression was increased in sites with chronic PD in patients with diabetes and poor glycemic control (87). Considering both diabetes and PD are characterized by a host immunoinflammatory response, it must be noted that there might be genetic overlap in the susceptibility of these conditions. This opens up an exciting avenue for future research where we might be able to translate clinical diagnostic markers across multiple conditions.

Current clinical treatment protocols for PD rely primarily on the removal of dental plaque or the oral microbial biofilm (88, 89). While specific bacterial species are known to be highly associated with PD, including *P. gingivalis*, the oral microbiome is a polymicrobial environment including not only pathogenic bacterial, but healthy microbial species (89, 90). Furthermore, patients can present with the same oral microbial load but with varying disease severities. Indeed, aggressive PD is characterized with a reduced microbial load compared to the amount

of clinical disease destruction (91). Moreover, Loe et al's classic study on tea laborers showed that with no access to oral hygiene, there were varying degrees of disease severity, highlighting the host as a key component in disease manifestation (4). Clinically, the uniform approach to treatment of microbial biofilm removal neglects to consider the host immunoinflammatory response to bacteria and could result in some patients being over-treated and other patients being under-treated. A few groups have explored the use of targeted antibiotics to eliminate pathogenic bacteria in oral cavity; however, this approach can be met with challenges including, antibiotic resistance and the potential for long-term antibiotic usage to maintain the healthy oral microbial population (89). Furthermore, it is understood that while the oral biofilm is necessary to cause periodontitis, it is not sufficient alone and that the exaggerated host immune response is a key factor in disease susceptibility. Taking this into account, several studies have explored the idea of host modulation through the use of nonsteroidal anti-inflammatory drugs (NSAIDs) (92), COX-2 inhibitors (93), and bisphosphonates (94) with each treatment showing mixed results. Furthermore, there can be complications involved with systemic administration of drugs such as increased cardiovascular risks associated with COX-2 inhibitors (93). Nonetheless, modulating the host immunoinflammatory response is a research area that needs to be further explored. In the present study, our GWAS approach and candidate gene validation using animal models, here using a CXCR3 antagonist, allows for clinical translation and targeted treatment options.

In summary, we have identified *Cxcl9* and *Cxcl10,* and their receptor, CXCR3, as associated to PD utilizing a GWAS with the HMDP and a highly reproducible murine model of PD. Furthermore, we have mechanistically interrogated CXCR3's role in PD through the use of knock-out mice and we have begun to explore possible therapeutic modalities to treat PD by using a CXCR3 antagonist (AMG-487) *in vivo*. Our results suggest that modulating the host immune response, and specifically monitoring chemokine expression levels, could aid in our

understanding of PD pathogenesis as well as serve as the foundation for more personalized patient treatment.

Materials and Methods:

Mice

Seven-week old male mice of 104 genetically different strains of the Hybrid Mouse Diversity Panel (HMDP) (n≥6/per strain) (Supplemental Table 2-1) were used according to the guidelines of the Chancellor's Animal Research Committee of the University of California, Los Angeles and the Animal Research: Reporting *In Vivo* Experiments (ARRIVE) protocols for the submission of animal studies were followed (95). Mice were initially purchased from the Jackson Laboratories (Bar Harbor, ME, USA), bred and housed at UCLA for the duration of the study in a temperature and light controlled environment, and fed a standard chow.

Seven-week old female B6.129P2-Cxcr3^{tm1Dgen}/J homozygous chemokine receptor *Cxcr3* knockout (KO) mice were bred and purchased from the Jackson Laboratories (Bar Harbor, ME, USA). Mice were maintained and utilized under the same guidelines and environment as described above.

Induction of Periodontitis

Inflammatory induced bone loss was performed as previously described (14). In brief, mice (n≥3/strain) received 2μL (20μg) of *P. gingivalis*-Lipopolysaccharide (*P.g.*-LPS) (InvivoGen, San Diego, CA, USA) injections in between the first and second maxillary molars on both the right and left sides using a 10μL Hamilton syringe with a 0.33-gauge needle (Hamilton Company, Reno, NV, USA). Mice received injections twice a week for six weeks. Control mice (n≥3/strain) did not receive injections as previously described, because there was no statistical difference in bone levels between non-injected and vehicle injected groups (14). During the

course of injections, mice exhibited no overt clinical signs of soft tissue damage or inflammation. After six weeks of injections, mice were sacrificed, maxillae were harvested, fixed in 10% buffered formalin for 48 hours, and subsequently stored in 70% EtOH for further analysis.

Micro-computed tomography analysis

Maxillae were scanned using a μ-computed tomography (μ-CT) scanner (Skyscan 1172; Skyscan, Aartelaar, Belgium) as previous described (14). In brief, maxillae were scanned at 10μm voxel size and imaged slices were converted to Digital Images and Communication in Medicine (DICOM) format. DICOM files were imported into Dolphin® software (Dolphin Imaging, Chatsworth, CA, USA) for linear bone loss measurements. In Dolphin, maxillae were oriented for each molar, first and second, individually. Molars were oriented with the cementoenamel junction (CEJ) perpendicular to the root in the coronal plane. The root was also aligned parallel in the coronal plane. Each molar was oriented in the area corresponding to the middle of the tooth, aligned by the three roots in the axial plane. The distance from the CEJ to the alveolar bone crest (ABC) was recorded for the first molar distal and second molar mesial. Additional measurements, 0.2mm palatal were recorded for the first molar distal and second molar mesial. Measurements were recorded for the right and left sides independently and averaged to create a mean value for each mouse. All mice utilized for the duration of this study were scanned, oriented, and analyzed using the same parameters. To quantify the amount of bone loss, the averaged CEJ to ABC distance in the control sites was subtracted from the averaged distances in the LPS injected sites. The remaining value represented net bone loss.

Factored Spectrally Transformed-Linear Mixed Modeling

Statistical analysis for the genome-wide association study (GWAS) on LPS-induced periodontal bone loss was performed following previous GWAS studies utilizing the Hybrid Mouse Diversity Panel (HMDP) (96, 97). In brief, genotypes of ~500,000 single nucleotide polymorphisms (SNPs) were obtained from the Mouse Diversity Array. Only SNPs that presented with a minor allele frequency of >5% and missing genotype frequencies <10% were considered in analysis. The following filtering criteria yielded a final set of ~200,000 SNPs that were considered for analysis. In order to perform association testing, Factored Spectrally Transformed-Linear Mixed Modeling (FaST-LMM) (98) was performed. FaST-LMM factors in underlying population structure into statistical analysis and has successfully been employed in other GWAS studies utilizing the HMDP (99-102). FaST-LMM is a linear mixed model method that statistically accounts for population structure in a fast and reproducible manner. In order to improve power, the kinship matrix was constructed using the SNPs from all the other chromosomes when testing all the SNPs on a specific chromosome. Using these parameters, the SNP gets tested in the regression equation only once. The significance level for the GWAS threshold using the HMDP was determined by the family-wise error rate (FWER), which is the probability of detecting one or more false positives across all SNPs/phenotype. These parameters were similar to previous studies utilizing the HMDP (96, 97).

Heritability Calculation

Heritability is defined as the fraction of the variance in a trait is due to genetic factors (103). To estimate heritability in our GWAS, we utilized two approaches: “broad sense” and “narrow sense.” Broad sense heritability estimates total heritability while narrow sense determines heritability due to additive genetic variance. To calculate broad sense heritability, an R statistical

package was utilized and heritability was estimated based on the reproducibility of trait measurements in different animals of each strain as previously described (22). For narrow sense heritability, estimates were based on sharing of genomic regions identical by descent as previously reported (22).

Macrophage Genome-wide expression analysis and correlation to LPS-induced bone loss

A previously performed GWAS on changes in macrophage gene expression in response to *E. coli* LPS utilizing the HMDP was used to correlate SNPs to our LPS-induced PD model (25). In brief, 92 strains (all males) of the HMDP were obtained from the Jackson Laboratories (Bar Harbor, ME) and housed according to NIH guidelines. Primary macrophages were harvested, divided into two groups: control and LPS-stimulated, and gene expression (RNA) was profiled using Affymetrix HT MG-430A arrays for each group (25). GWAS association mapping for macrophage gene expression was performed using Efficient Mixed-Model Association (EMMA). Macrophage expression data was correlated with the LPS-induced bone loss data using the bicorAndPvalue() function from the Weighted Gene Co-expression Network Analysis (WGCNA) R package. Correlations were filtered for a p-value $<10^{-3}$.

RNA Isolation

Seven-week old A/J and C57BL/6J mice were injected with one *P.g.*-LPS-injection (2μL or 20μg of LPS) in between the first and second and second and third molars. Control mice were not injected. After four hours, mice were sacrificed as previously described. Immediately following sacrifice, under the microscope (Leica Microsystems, IL, USA), mice had approximately a

1.00mm X 0.50mm piece of maxillary gingival tissue excised in between the first and second and second and third molars corresponding to the area of LPS injections. Gingival tissues from the right and left sides of two mice were pooled for subsequent RNA isolation. RNA was isolated using a standard TRIzol® (Thermo Scientific, Canoga Park, CA, USA) protocol and RNA quantity and purity was assessed using a NanoDrop 2000 (Thermo Scientific, Canoga Park, CA, USA).

Microarray

RNA samples were prepared for microarray analysis using standard protocols at the UCLA Clinical Genetics Microarray core using the MouseRef-8 v2.0 chip. Gene expression data was analyzed using dChip software (2010.1). Differential gene expression, genes induced by LPS in A/J or C57BL/6J, were filtered using a False Discovery Rate of 50 and a p-value of <0.05.

Histology

Maxillae were decalcified in 15% ethylenediaminetetraacetic acid (EDTA) for four weeks (solution was changed 3x/week). After decalcification, maxillae were paraffin embedded and cut coronally to 5μm thick sections using a microtome (McBain Instruments, Chatsworth, CA, USA). Sections were stained with hematoxylin and eosin (H&E) using standard protocols.

To evaluate immune cell populations and cytokines, immunohistochemistry was performed using the following antibodies: anti-NIMP-R14 (neutrophils) (1:250 ab2557 Abcam, Cambridge, UK), anti-CD3 (T-cells) (1:100 ab5690 Abcam, Cambridge, UK), and anti-Cxcl10 (15μg/mL AF-466-NA R&D Systems, MN, USA). After standard deparafinization protocols, for all antibodies, excluding anti-CD3 and anti-Cxcl10, antigen retrieval was performed using 0.05% trypsin at room temperature for 15 min. Primary antibodies were incubated overnight at 4C in a

humidified chamber. Secondary antibodies (1:200 for all primaries) were incubated for 2hr at room temperature. The immunoreaction was observed using AEC+substrate+chromogen solution (Dako, CA, USA). For anti-CD3 and anti-Cxcl10, antigen retrieval was performed using 10mM sodium citrate pH 6.0 overnight at 60C. Primary and secondary antibodies were incubated as described above. The immunoreaction was observed using DAB peroxidase HRP (Vector Labs, CA, USA). For all stains, slides were digitally imaged using Aperio ImageScope model V11.1.2.752 (Vista, CA, USA). All histological sections used in this study were processed and stained utilizing the same parameters unless otherwise noted.

***Cxcr3* Knockout**

Cxcr3 KO (B6.129P2-Cxcr3^{tm1Dgen}/J homozygous chemokine receptor *Cxcr3* knockout) and matched wild-type (WT) mice were randomly divided into *Cxcr3* KO control (no LPS), *Cxcr3* KO LPS-treated, WT control (no LPS), and WT LPS-treated groups. Mice received LPS-injections as described above for one time point: twelve (six weeks) LPS injections. After LPS treatment, mice were sacrificed and maxillae were harvested for further micro-CT and histological analysis. Quantification of linear bone loss was achieved using the same parameters as described above for the analysis of the HMDP.

Cxcr3 KO and WT histological sections were embedded and processed as described above. Tissues were stained for Tartrate Resistant Acid Phosphatase (TRAP, Sigma Aldrich, MO, USA) to assess osteoclast (OC) counts and anti-Cox-2 (1:250, ab15191 Abcam, Cambridge, UK) to assess general inflammation as described further in Supplemental Methods. Cells that presented with ≥2 nuclei and in were contact with bone were considered OCs (CITE). Osteoclasts were counted on six tissue sections per mouse and all six slides were averaged to create a total OC value for each mouse (n=3 mice/group).

CXCR3 Antagonist

Seven-week old male C57BL/6J mice purchased from the Jackson Laboratories (Bar Harbor, ME, USA) were utilized. (±)-AMG-487 (Tocris, R&D Systems, MN, USA) a CXCR3 antagonist (a small molecular weight peptide), was utilized to block CXCR3 *in vivo*. Mice were divided into three groups: Control (no LPS + vehicle injection), LPS + vehicle injection, and LPS + AMG-487. AMG-487 was reconstituted as described by Walser et al (104). In brief, AMG-487 was initially dissolved in a 50% hydroxypropyl-β-cyclodextrin (Sigma Aldrich, MO, USA) in a sonicating water bath for 2 hours with occasional vortexing. After the AMG-487 powder had completely dissolved, distilled water was added to make a final concentration of 20% hyroxypropyl-β-cyclodextrin solution. Vehicle injections consisted of a 20% hyroxypropyl-β-cyclodextrin solution without AMG-487. At the start of LPS injections, mice received the first injection of AMG-487 at a concentration of 5μg/g twice a day for the whole duration of the experiment (104). *P.g.*-LPS injections were performed as described above. Mice were sacrificed after a total of 12 LPS injections (six weeks). Bone loss measurements, histology, and osteoclast counts (n=5 slides per mouse, n≥5 mice/group) were performed as described above.

Statistics

All statistical analyses were performed using Prism 5 GraphPad (CA, USA). For bone loss analysis, measurements were averaged per mouse and subsequently averaged per group (for all experiments, n≥3) to create a mean bone loss value per group (mean ± standard error of the mean). For quantification of TRAP staining, n≥5 slides per mouse were stained and OC numbers were averaged per mouse. Again, each mouse was averaged to create a mean number of OC's per group (mean ± standard error of the mean). Significance levels were evaluated through either a Student's *t* test or two-way Analysis of Variance (ANOVA) followed

by a Bonferroni post hoc test with a confidence interval of 95%. Significance levels were as follows: $p \leq 0.05^*$, $p \leq 0.01^{**}$, $p \leq 0.001^{***}$.

Study Approval

This study (Animal Research Committee (ARC) protocol number 11-103) followed the guidelines according to the Chancellor's Animal Research Committee of the University of California, Los Angeles and the Animal Research: Reporting *In Vivo* Experiments (ARRIVE) protocols for the submission of animal studies were followed (95).

Acknowledgements:

This work was supported by NIH/NIDCR DE023901-01 and the UCLA Faculty Development grant. SH was supported by NIH/NIDCR T90 DE022734-01. We would like to thank the UCLA Tissue Pathology Core Laboratory for the decalcified histological sections.

Supplemental Methods:

Histology

To evaluate inflammatory cytokines and matrix degradation immunohistochemistry (IHC) was performed using the following antibodies: anti-p65 (NF-κB) (1:200; 600-401-271, Rockland, PA, USA), anti-TNF-α (1:200; ab34674 Abcam, Cambridge, UK), anti-Cox-2 (1:250, ab15191 Abcam, Cambridge, UK), anti-MMP13 (1:200; ab39012 Abcam, Cambridge, UK), and anti-MMP8 (1:100 ab3017 Abcam, Cambridge, UK). IHC was performed as described in materials and methods.

Micro-computed tomography analysis

To evaluate differences in initial bone levels between WT and *Cxcr3* KO mice, 3D volumetric analysis was performed in the mesial femur distal from the growth plate and in the maxillae in between the first and second molars at the injection site.

Femurs were scanned using Skyscan micro-CT (Model 1172; Kontich, Belgium) at 12μm resolution. Using DataViewer (V.1.5.2; Bruker, Billerica, MA), femurs were oriented parallel in the sagittal and coronal planes. Using CTAn (V.1.16; Bruker, Billerica, MA), the axial plane was used for analysis. A region of interest (ROI) was defined starting 10 slices from the end of the growth plate down 200 slices distal from the growth plate. This volume was considered for bone volume/tissue volume (BV/TV) analysis. BV/TV percentage values were recorded for each mouse and averaged to create a mean BV/TV value for each group (n=3/group).

Maxillae were scanned as previously described for linear bone loss measurements. Using DataViewer, maxillae were oriented with the cementoenamel junction (CEJ) of the first and

second molars parallel in the sagittal and coronal planes. In CTAn, an ROI starting from 10 slices down from the CEJ towards the apex of the roots was defined. The ROI was composed of 50 slices total. BV/TV percentages were recorded for each mouse and averaged per group (n=3/group).

Statistics

For BV/TV, statistical significance between groups was assessed using a Student's *t* test. Significance levels were as follows: $p \leq 0.05$*, $p \leq 0.01$**, $p \leq 0.001$***.

Strain:			
BXD24b/TyJ	BXA8/PgnJ	BXA14/PgnJ	KK/HlJ
BXH8/TyJ	CXB1/ByJ	BXD31/TyJ	BXH22/KccJ
BXD34/TyJ	CXB7/ByJ	129X1/SvJ	AXB8/PgnJ
AXB13/PgnJ	C3H/HeJ	CXB11/HiAJ	BXH10/TyJ
BXD69/RwwJ	BXD44/RwwJ	BXH20/KccJ	FVB/NJ
AXB4/PgnJ	BTBRT<+>tf/J	BXD48A/RwwJ	AXB2/PgnJ
BXD28/TyJ	I/LnJ	BXD29/TyJ	MA/MyJ
BXH7/TyJ	BXD12/TyJ	BXD5/TyJ	C58/J
BXH19/TyJ	NZW/LacJ	BXA16/PgnJ	BXD2/TyJ
CXB12/HiAJ	AXB23/PgnJ	NZB/BlNJ	BXD61/RwwJ
BXD45/RwwJ	AXB15/PgnJ	BXD100/RwwJ	BXD75/RwwJ
AXB19a/PgnJ	BXA25/PgnJ	CE/J	BXA4/PgnJ
BXH9/TyJ	CXB9/HiAJ	SM/J	BXA13/PgnJ
AXB10/PgnJ	BXA7/PgnJ	BXD55/RwwJ	NOD/ShiLtJ
BXD63/RwwJ	CXB2/ByJ	BXD71/RwwJ	CBA/J
NOR/LtJ	BXD48/RwwJ	SWR/J	BXD39/TyJ
AXB19b/PgnJ	AXB5/PgnJ	BXA2/PgnJ	BXH2/TyJ
SEA/GnJ	BXH14/TyJ	C57L/J	BALB/cByJ
AXB1/PgnJ	NON/LtJ	RIIIS/J	BXD38/TyJ
BXH6/TyJ	LG/J	BXD11/TyJ	BXD1/TyJ
A/J	BXD40/TyJ	C57BL/6J	C57BLKS/J
AXB24/PgnJ	BALB/cJ	BXD56/RwwJ	SJL/J
BXA12/PgnJ	BXD65/RwwJ	AKR/J	MRL/MpJ
AXB19/PgnJ	DBA/2J	BXD62/RwwJ	BUB/BnJ
BXA1/PgnJ	BXD67/RwwJ	AXB6/PgnJ	BXD60/RwwJ
BXD32/TyJ	PL/J	BXD49/RwwJ	BXD84/RwwJ

Supplemental Table 2-1: Hybrid Mouse Diversity Panel Strains used in LPS-induced bone loss GWAS

Gene Symbol	p Value	Gene Symbol	p Value	Gene Symbol	p Value
0610009D07Rik	5.84E-05	*Psmg3*	0.002838472	*Nr6a1*	0.006161623
Commd2	8.40E-05	*Eif1ax*	0.003000123	*A230050P20Rik*	0.006326493
Rps10	0.000118587	*Arid2*	0.003009682	*Ttc23*	0.006353174
Nup35	0.000146151	*Bean1*	0.003009984	*Oprl1*	0.0063745
Mrpl24	0.000156054	*Pus3*	0.003055869	*Cct5*	0.006381182
Prkx	0.000207815	*Mrpl12*	0.003073584	*Atp13a1*	0.006551226
Cct4	0.000253417	*Rps10*	0.003146496	*Scn3b*	0.006561054
Anapc16	0.000298203	*Atg5*	0.003460048	*Ccnh*	0.006619915
Kdr	0.000354523	*Rpl10a*	0.003473305	*Mrps16*	0.006628675
Trmt10c	0.00064399	*Eif3l*	0.003541534	*Mrps18c*	0.006645203
Eif4ebp1	0.000661064	*Mki67ip*	0.003610504	*Cnot4*	0.006688917
Emg1	0.000682309	*Mcfd2*	0.003639118	*Serpinb6a*	0.006949346
Dhrs7b	0.000831116	*Rpl36al*	0.003654128	*Abhd14a*	0.006974362
Ccdc90b	0.000862342	*Rpl13a*	0.00369796	*Il2rg*	0.007020417
Lsm3	0.000963985	*Glrx3*	0.003732453	*Apaf1*	0.007111279
Fam136a	0.001029201	*Prdx3*	0.003743423	*Rnmt*	0.007143492
Rps10	0.001050644	*Tm2d3*	0.003819081	*Timmdc1*	0.007165735
Rab8b	0.001065865	*Nudt21*	0.003890512	*Med31*	0.007196774
Fopnl	0.00109002	*Slc9a3r2*	0.003902124	*Tlk2*	0.007236991
Pde10a	0.00112583	*S100a5*	0.003931942	*Pik3cd*	0.00728345
Cdc34	0.001136711	*Rpl6*	0.004045841	*Acin1*	0.007306735
Sfrp5	0.001150659	*Wdr12*	0.004266592	*Olfr67*	0.007314483
2810004N23Rik	0.001177513	*Csdc2*	0.004281902	*Stxbp1*	0.007378769
Tmbim1	0.001344347	*H2-T24*	0.004287066	*Eef1d*	0.007401665
Rpl11	0.001348393	*Actn4*	0.004306996	*Cox15*	0.007535107
Degs2	0.001463904	*Magoh*	0.004353762	*Trabd*	0.007619323
Cyp2b10	0.001483993	*Pde6h*	0.004405174	*Pi4k2a*	0.007762646
Rab33a	0.001502455	*1700074P13Rik*	0.004452257	*Usp25*	0.007806236
Jarid2	0.001596535	*Tomm5*	0.004483631	*Mpzl2*	0.007827457
Rps19	0.001631077	*Sfxn2*	0.004562192	*Nfatc2ip*	0.007872592
Eif3i	0.00164701	*Mrpl15*	0.004804508	*Cyth1*	0.007904074
2410016O06Rik	0.001685574	*Asb13*	0.005029013	*Stoml2*	0.00793395
Chd1	0.001713786	*Ift80*	0.005034848	*Eef1g*	0.008136319
Car6	0.001742827	*Tsnax*	0.005075001	*Aldh1b1*	0.008191519
Lipe	0.001750869	*Snrpd2*	0.005196797	*Lipg*	0.008265908
Gsta4	0.001783223	*Uqcrq*	0.005309597	*Pde4dip*	0.008324873
Chml	0.001922438	*Vdac3*	0.005330879	*Dtna*	0.008347501
Ict1	0.002004287	*Cd36*	0.005332134	*Puf60*	0.008357389
Tspan32	0.002046289	*Hnrnph2*	0.005376453	*Dnajc10*	0.008360931
Dnajc10	0.002052228	*Foxa1*	0.005623411	*Nxt1*	0.008376348
Gnb2l1	0.002093453	*Ccdc58*	0.005647556	*Obox2*	0.008386713
Lrp2	0.002355372	*Zfp334*	0.005691464	*Ssr4*	0.008480203
Tceanc2	0.002384423	*Trp73*	0.00569247	*Cwf19l1*	0.00848879
Sec11a	0.002478721	*Cpeb3*	0.005735468	*Cpeb3*	0.008620675
Tusc2	0.002516616	*Ppp1r8*	0.00583799	*Zfp259*	0.00863576
Arpp21	0.002659277	*Lats2*	0.005880437	*Dcp1a*	0.008709569
Ly6g6c	0.002681725	*Arhgap17*	0.00593465	*Naca*	0.008802352
Ssbp1	0.002720235	*Ift46*	0.00607617	*Mtch2*	0.008805066
Grin2a	0.002747356	*Tnfrsf11a*	0.00608382	*Lyplal1*	0.008928973
Rpl18	0.002748924	*Jarid2*	0.006129786	*Oplah*	0.008940633

Supplemental Table 2-2: Genes correlated to macrophage response to LPS and LPS-induced bone loss

Gene Symbol	p Value	Gene Symbol	p Value	Gene Symbol	p Value
Ndst2	0.008944188	*Cntrob*	0.011379305	*Naca*	0.013761834
Thap4	0.009022655	*Zfp111*	0.011576093	*C1qbp*	0.013812458
Ngdn	0.009051458	*Slco1a4*	0.011620618	*Chmp4b*	0.013814064
Wdr75	0.009067986	*Rps10*	0.011642866	*Pou3f1*	0.013883891
Rbx1	0.009109521	*Mtor*	0.011731384	*Ehhadh*	0.013897932
Atp5f1	0.009119528	*Kat2b*	0.011758738	*Pik3r1*	0.01394256
Polr2j	0.009151025	*Krr1*	0.011824472	*Pck1*	0.014053257
Naaa	0.009179006	*Zfyve21*	0.011835751	*Stard5*	0.014155207
Prkce	0.009284539	*Wdr4*	0.011876902	*Pml*	0.014156214
Snrpg	0.009297023	*Pdk4*	0.011967293	*Eng*	0.014216803
Cops5	0.009371503	*Fcna*	0.012019194	*Col20a1*	0.014236102
Ostc	0.009439764	*Phf17*	0.012054359	*Cct7*	0.014260871
Fam174b	0.009496939	*Vwa5a*	0.012167397	*Mad2l1bp*	0.014400541
Znhit3	0.009575728	*Ska1*	0.012213461	*Nsmce1*	0.014448252
Sh3d19	0.009581862	*Cox15*	0.012318955	*Nsun2*	0.014599166
Lrp4	0.009612499	*Tcea2*	0.012421462	*Irf2*	0.014604869
Phb2	0.009710063	*Pias1*	0.012476305	*Banf1*	0.01466258
2610002J02Rik	0.009750912	*Nras*	0.012575531	*Th*	0.014823065
Bpifb2	0.009804674	*Sars*	0.012591431	*Zic5*	0.014825993
Gle1	0.009882414	*Mea1*	0.012598819	*Adam22*	0.014857844
Aimp1	0.00990166	*Efna4*	0.012599856	*Endod1*	0.014920816
Rdm1	0.009905034	*Lrwd1*	0.012634806	*Tapbp*	0.015099648
Opn1mw	0.009915268	*Ccdc166*	0.012689959	*Tmprss2*	0.015108036
Pus1	0.00995546	*Btf3*	0.0127502	*Zfp319*	0.015183174
Cpne3	0.010113068	*Fam105b*	0.012770878	*Iqcc*	0.015203325
Slamf8	0.010116302	*Set*	0.012851027	*2210016F16Rik*	0.015204598
4930441O14Rik	0.010150647	*Trmt112*	0.012862749	*Coro2a*	0.015229719
Mrpl20	0.010225865	*Slc25a20*	0.012885293	*Riok3*	0.015287137
Kcnip2	0.010244863	*Fbxw2*	0.012919157	*Cacnb1*	0.015314675
Slfn3	0.010248742	*Trim27*	0.012928867	*Hoxd4*	0.015368642
Cxcl17	0.010371218	*Riok2*	0.01299446	*Nme6*	0.015374684
Cdkn1c	0.010376821	*Mrpl15*	0.013055541	*0610009D07Rik*	0.015384013
Tomm20	0.010395212	*Amigo1*	0.013057198	*Egln3*	0.015565203
Samp	0.010483479	*Polr1d*	0.01306848	*Tiprl*	0.015631359
Ormdl2	0.010550865	*Atp6v1g2*	0.013092821	*Adprm*	0.015697901
Vti1b	0.010582175	*Nt5c3b*	0.013098732	*Mrpl53*	0.015703078
Xrn1	0.010584487	*Ndufaf5*	0.013105421	*Ankrd17*	0.015927289
Ndufv1	0.010619529	*Tomm40*	0.013125736	*Tbc1d13*	0.015934862
Plekhf2	0.010642538	*Txnl4a*	0.013143417	*Satb2*	0.016017146
Polr2f	0.010666831	*Etfb*	0.013146381	*Tgm2*	0.01602625
Ctdspl	0.010802624	*Hprt*	0.013152363	*Lipf*	0.016046829
Park7	0.010814069	*Arid4b*	0.013208925	*Coq3*	0.016069755
Vsx2	0.01087278	*Mmaa*	0.013307539	*Wdr77*	0.01607356
Nup43	0.010943291	*Polr2h*	0.013405369	*Ndufb9*	0.016174148
Trappc4	0.011064844	*Vwa5a*	0.013560235	*Tbpl1*	0.016183078
Gfra2	0.011069612	*Exoc6*	0.013562551	*Dpyd*	0.016227072
Rrbp1	0.011202877	*Sf3b5*	0.013668438	*Cst7*	0.01626579
Hoxa11os	0.011324408	*Tmem50b*	0.013680863	*Sgcg*	0.016281657
Gstm5	0.01132479	*Erh*	0.013739805	*Rce1*	0.01629652
Clint1	0.011353878	*Theg*	0.013745683	*Mrps33*	0.016327537

Supplemental Table 2-2: Genes correlated to macrophage response to LPS and LPS-induced bone loss

Gene Symbol	p Value	Gene Symbol	p Value	Gene Symbol	p Value
Gab3	0.016331659	*Phb*	0.018564712	*Samhd1*	0.020729898
Aff4	0.01635305	*Blnk*	0.018572219	*Ttc16*	0.020820498
Ncoa2	0.016364502	*2700029M09Rik*	0.018614894	*Sdf4*	0.02085017
*Ppnr**	0.01638302	*Raver1*	0.018632428	*Mogat2*	0.020915851
Pcdh1	0.016391307	*Kat6a*	0.018704557	*Uba7*	0.02099763
Rasgrp1	0.016400058	*Maml2*	0.01878493	*Prkce*	0.021027054
Med1	0.016418188	*Galr3*	0.018788169	*Mmab*	0.021055413
Pcdh20	0.016493448	*Snhg1*	0.018821779	*Psmg2*	0.021094276
Sfrp1	0.016499338	*Mettl22*	0.018967756	*Med1*	0.021100874
Hdac3	0.01653036	*Mtg2*	0.018971825	*Tmem161a*	0.021101842
Inpp1	0.016531107	*Psca*	0.018998123	*Nfkbie*	0.021150521
Nrbp2	0.016540231	*Spcs2*	0.019027763	*Foxk1*	0.021216504
Dqx1	0.016680472	*Prelp*	0.019129889	*Eftud1*	0.021259433
Emc8	0.016687964	*Tfip11*	0.019139269	*Ndufaf4*	0.0213251
Ptges2	0.016713611	*Chchd4*	0.019175379	*Chd4*	0.021376711
Tmcc3	0.016727587	*Psmg2*	0.019217257	*Sema4a*	0.021380304
Rps27l	0.016846562	*Pcbd2*	0.019269668	*Cnot4*	0.021460166
4932438A13Rik	0.016925999	*Endod1*	0.019329371	*Rpl14*	0.021506563
Prps1	0.01693798	*Rpl13a*	0.01941604	*Prmt3*	0.021550105
Psmb3	0.016964923	*Dctpp1*	0.019433571	*Frk*	0.021595739
Rem1	0.017031856	*Cryzl1*	0.019456787	*Bhmt*	0.021642398
Sla	0.017082357	*Mbl1*	0.019462825	*Morc3*	0.02166801
Mrpl17	0.017102395	*Ltf*	0.019478061	*Rcc2*	0.021675985
Mfsd8	0.017160922	*Nt5m*	0.019564381	*Hoxc13*	0.02175563
Ppap2b	0.017175081	*Coro1b*	0.019587949	*Xiap*	0.021916407
Rfk	0.017200507	*Melk*	0.019734374	*Cdc16*	0.021956924
Mrps35	0.017217681	*Gprasp1*	0.019744471	*Ptprc*	0.021966409
Plekhf2	0.017243568	*Ctla2a*	0.019769886	*Eomes*	0.022034698
Tmem208	0.01725639	*Ccng2*	0.019818504	*Mak*	0.022079952
Tomm20	0.017332931	*Otud5*	0.019860495	*1110001J03Rik*	0.022160452
Dnaja4	0.017365883	*Rad51c*	0.019918263	*Bax*	0.022182807
Itgb1bp2	0.017380597	*Mien1*	0.019941738	*Fam118b*	0.022324482
Fjx1	0.017464739	*Kif18a*	0.019953973	*Gata4*	0.022371829
Lce1b	0.017563371	*Rasl12*	0.02002297	*Timm50*	0.022410507
Sox6	0.017639091	*Calu*	0.020061547	*H2afy*	0.022605079
Rpl18	0.017833349	*Rab3ip*	0.020090367	*Tmem184b*	0.022772749
Ube2g2	0.017837031	*Nol12*	0.020101419	*Chad*	0.022780938
Sar1a	0.017841117	*Arf3*	0.020151423	*Mettl1*	0.022797375
Smarca4	0.01789888	*Tor1aip2*	0.020297698	*2810474O19Rik*	0.022830626
Tceb2	0.018043444	*Mrpl48*	0.020359015	*Pvt1*	0.022834255
Bcar3	0.018083498	*Ppat*	0.020361339	*Zbtb21*	0.022834905
Igdcc4	0.018142761	*Ptpn2*	0.020386228	*Sdf2*	0.022877664
Zfpm2	0.018202261	*Asb4*	0.020510828	*Med1*	0.022886942
Rftn2	0.018228586	*Arhgap39*	0.020526349	*Fam92a*	0.022889
Akr1a1	0.018337855	*Comtd1*	0.020533793	*B9d2*	0.022898825
Zfp955a	0.018428159	*Dll1*	0.02055282	*Gm5617*	0.023114053
Cyp27b1	0.018470042	*Arhgef10*	0.020564523	*Tspan6*	0.023274355
Cxcl15	0.018472638	*Cdkl2*	0.02058565	*Ncaph2*	0.023300876
Cd36	0.018494448	*Samhd1*	0.020599799	*Vps36*	0.023303107
Mrpl11	0.01853924	*Kansl1l*	0.020621575	*Serpina1c*	0.023304538

Supplemental Table 2-2: Genes correlated to macrophage response to LPS and LPS-induced bone loss

Gene Symbol	p Value	Gene Symbol	p Value	Gene Symbol	p Value
Uba7	0.023341671	*Egf*	0.025467589	*Zic4*	0.028103212
P2ry14	0.023372203	*Vmn1r15*	0.025521653	*Gata2*	0.028104076
Exosc1	0.023468557	*Snhg1*	0.025594483	*Tmem2*	0.028192431
Arntl2	0.023470236	*Zxdc*	0.025605571	*Orc3*	0.028279916
Pebp1	0.023474732	*Pdlim7*	0.025653302	*Ryk*	0.028311548
Zdhhc6	0.023479052	*Amotl2*	0.025688755	*Epn2*	0.028368132
Ddit4l	0.023488441	*Acvr1c*	0.0256891	*Fam203a*	0.028374675
Zfp94	0.023556047	*Naa15*	0.025789525	*Tmem2*	0.028391525
Ift20	0.023612336	*Atf7*	0.0258337	*Sars*	0.028415711
2700097O09Rik	0.023661039	*Morc3*	0.025870986	*Oas1b*	0.028447731
Mrpl15	0.023753891	*Psmg1*	0.025881194	*Arhgef25*	0.02846353
Twf2	0.023836494	*Ruvbl1*	0.025925673	*Zfand6*	0.028474023
Sema4a	0.023870204	*Parn*	0.025962723	*Syt1*	0.028492286
Gemin8	0.023891305	*Cox7a2*	0.025977747	*Rabggtb*	0.028572379
Nmnat3	0.023915526	*Ptprn2*	0.025992806	*Cox14*	0.028595679
Pvrl4	0.023929628	*Bcl9*	0.026048198	*Prss32*	0.028619272
Esrrg	0.024000928	*Tmx1*	0.02613981	*Marcksl1*	0.028649089
Timm13	0.024124693	*Spcs2*	0.026189141	*Rab10*	0.028675698
Cnbp	0.02419781	*Xpo6*	0.026199401	*Mpg*	0.028761712
Pdlim4	0.024221444	*Cep350*	0.026225668	*Nelfb*	0.028817389
Racgap1	0.024235662	*Polr3k*	0.026374273	*Msh4*	0.028892817
Mnf1	0.024280741	*Polr2e*	0.02640573	*Cct6a*	0.028976156
Mertk	0.024283991	*Slc6a13*	0.026416479	*Ccnc*	0.029014569
Stk17b	0.024291645	*Chst11*	0.026420592	*Tdrd7*	0.029073001
Smad5	0.024337296	*Gucy1a3*	0.026638519	*Eci1*	0.029101532
Ppap2b	0.024368913	*Mafb*	0.026695702	*Map2k6*	0.029106564
Ccr8	0.024386373	*Tiparp*	0.026724268	*Fabp1*	0.029147156
Adhfe1	0.024467552	*Sgol1*	0.026775528	*Rps3*	0.029149445
Serf2	0.0244691	*Tiparp*	0.026856824	*Uqcr10*	0.029232689
Pcdh10	0.024474067	*Polr3f*	0.026937229	*Eya3*	0.029237758
Wap	0.024482973	*Fcrla*	0.02696308	*Kcnq2*	0.029280299
Stxbp1	0.024488095	*Gzmc*	0.026998537	*Gstt3*	0.029404026
Tvp23a	0.024585157	*Jarid2*	0.027039337	*Gykl1*	0.029463769
Igfbp3	0.024609536	*Clic4*	0.027195232	*Arrb2*	0.029467881
Krtcap2	0.024615148	*Grk4*	0.027291304	*Adhfe1*	0.029566982
Ankrd17	0.024651452	*Gimap4*	0.027385386	*D17Wsu104e*	0.029603771
Jmjd6	0.024754784	*Depdc7*	0.027388985	*Il6st*	0.029680597
Eed	0.024768756	*Ndufa12*	0.027455577	*Ift172*	0.029714966
Ruvbl2	0.024798892	*A230046K03Rik*	0.027465112	*Prmt7*	0.029739725
Fxn	0.024809015	*Lin9*	0.027489451	*Slc25a38*	0.029807023
Dusp18	0.024850811	*Nhp2*	0.027544971	*1700011H14Rik*	0.02982188
Btn1a1	0.02491959	*Farsb*	0.027648002	*Gata1*	0.029836045
Trp53inp1	0.025045278	*Parp8*	0.027672838	*Perp*	0.029946025
Gna14	0.025060497	*Serp1*	0.027678319	*Art3*	0.02996591
Pqbp1	0.025155897	*Zfp612*	0.027762188	*Usp29*	0.02999291
Chchd5	0.025160147	*Rbl1*	0.027785648	*Ssna1*	0.030028991
Diexf	0.025164787	*Tmem223*	0.027844203	*Prodh*	0.030091947
Psmg4	0.025267011	*Cbwd1*	0.028025324	*Zp2*	0.030101389
Cnga1	0.025398242	*Tnfrsf17*	0.028070459	*Mat2b*	0.030127349
Lztfl1	0.025428453	*Tmem131*	0.028078548	*Klhl20*	0.030138653

Supplemental Table 2-2: Genes correlated to macrophage response to LPS and LPS-induced bone loss

Gene Symbol	p Value	Gene Symbol	p Value	Gene Symbol	p Value
Ern2	0.03022992	*Ighmbp2*	0.032723424	*Plagl2*	0.035367246
Csn1s2a	0.030314134	*Marcksl1*	0.032732501	*Sobp*	0.035479964
Lgals3bp	0.030314712	*Ccdc34*	0.032931206	*Shank3*	0.035508466
Smpdl3b	0.030380474	*Thtpa*	0.03293936	*Cd2ap*	0.035520389
Dnajb5	0.030466154	*Zscan12*	0.032965032	*AW112010*	0.035635526
Lpin2	0.030489116	*Apbb2*	0.032995596	*Map1b*	0.035645748
Tsga13	0.030520504	*Ddx51*	0.033085188	*Src*	0.03571232
Eef1b2	0.030549658	*Rars2*	0.033093025	*Phf10*	0.035716859
Zfp52	0.030565783	*Eml5*	0.033184773	*Timm9*	0.035722123
Trpc3	0.030708706	*Nub1*	0.033199859	*Cd52*	0.035749967
Prmt1	0.030752095	*A430005L14Rik*	0.033273098	*Socs1*	0.035818106
Wdr61	0.030792646	*Serf1*	0.033278451	*Prim1*	0.035902345
Ikzf2	0.030819684	*Fam118a*	0.033354491	*Mapt*	0.035934646
Sf3b1	0.030842161	*Adcy4*	0.033359029	*Kat2b*	0.035984672
Copg2os2	0.030846748	*Camk1*	0.033372078	*Nap1l1*	0.036046448
Slit2	0.030883785	*Eif2s3x*	0.033398999	*Frrs1*	0.036062924
Ormdl3	0.030946246	*Phyhipl*	0.033476513	*Mphosph8*	0.036188743
Ccr1l1	0.030981648	*Shroom1*	0.033615751	*Ash2l*	0.036230937
Bin1	0.030994632	*Vldlr*	0.033624966	*Rtp4*	0.036276906
Lsm1	0.031021756	*Apaf1*	0.033652595	*Slc25a33*	0.03632589
Timm17b	0.031027744	*Mecom*	0.03368734	*Fam213b*	0.036337887
Scaf4	0.031079113	*Anxa10*	0.033741392	*Ube2b*	0.036382658
Dync1i1	0.031083254	*Cmtr1*	0.033824138	*Surf2*	0.03650694
Nme4	0.031142267	*Nsfl1c*	0.033847412	*Commd4*	0.036521693
Cacna1f	0.031207058	*Jagn1*	0.033887949	*Comt*	0.036569715
Ino80	0.031238657	*Slfn1*	0.034019423	*Rhou*	0.036626396
Trafd1	0.031351775	*Exoc8*	0.034137608	*Ascl1*	0.036665464
*Myg1**	0.031374495	*Mid1*	0.034140811	*Defb8*	0.036756597
Lck	0.031562656	*Gstk1*	0.03417165	*Hyal2*	0.036789958
Rbl1	0.03162505	*Irgm1*	0.034276551	*BC005624*	0.036800849
Tcf4	0.031626447	*Lhcgr*	0.034320369	*Ccr5*	0.036845574
Hspe1	0.0316655	*Elf4*	0.034431719	*Atg5*	0.0369035
Fam104a	0.031675685	*Dnah5*	0.034449608	*Zfp111*	0.036918239
Papd4	0.031833073	*Haus1*	0.034484652	*Stard3*	0.036943675
Dlg2	0.031867679	*Immp1l*	0.034646206	*Ndufb2*	0.03697389
Cbx8	0.031990451	*Akr1a1*	0.03466957	*Phpt1*	0.036983577
Bfar	0.032049384	*Eng*	0.034671907	*Mgat4b*	0.036988105
Lgals8	0.032052028	*A230046K03Rik*	0.034684412	*Bola2*	0.037069748
Exosc4	0.032108152	*Ddx5*	0.034688287	*Trim26*	0.037136069
Amz2	0.032113731	*Nup37*	0.034776836	*Dbr1*	0.037150526
Fbxo42	0.032187622	*Gpn1*	0.034877886	*Tlr3*	0.03715854
Pard6a	0.032191287	*Smpd3*	0.034878942	*Thbs1*	0.037212251
Scyl1	0.032201188	*Rbms1*	0.035034854	*St3gal5*	0.037240238
Tiparp	0.032202034	*Mphosph10*	0.035071219	*Nono*	0.037342414
Pcbp2	0.032234857	*Apoa1bp*	0.035170433	*Wdr5*	0.037357852
2810474O19Rik	0.032395563	*Otud4*	0.035190189	*Ddx60*	0.03736699
Nt5c3b	0.032404029	*Mrgprf*	0.035229427	*Csf2ra*	0.037388829
Ccdc77	0.03264271	*Ptprz1*	0.035247307	*Endod1*	0.037426452
Sin3b	0.032661678	*Tmem42*	0.035309312	*Bhmt2*	0.037521259
Pou3f1	0.032693637	*Nap1l4*	0.035343782	*Slbp*	0.037584715

Supplemental Table 2-2: Genes correlated to macrophage response to LPS and LPS-induced bone loss

Gene Symbol	p Value	Gene Symbol	p Value	Gene Symbol	p Value
Pde2a	0.037676825	*Tsen15*	0.040138081	*Cct2*	0.04250136
Ppp1r16b	0.037711042	*Gemin8*	0.040165745	*Camk1*	0.04255503
Prpsap2	0.037843074	*Pcp4*	0.040316472	*Med28*	0.042739973
Nudt22	0.03795232	*Psmd4*	0.040338525	*Pcbp4*	0.042801739
Serf2	0.038048902	*Polr2m*	0.040352038	*Thoc2*	0.042818192
Marcksl1	0.038092233	*Chmp6*	0.040407051	*Creb3*	0.042819908
Tug1	0.038117351	*Cga*	0.040430864	*Preb*	0.042854314
Dck	0.038138943	*Stk16*	0.040523226	*Mrpl43*	0.042897081
Endod1	0.038144345	*Slc2a1*	0.040559667	*Prmt2*	0.042979751
Rad51c	0.038144556	*Rpl3*	0.040587606	*Hspb1*	0.04303326
Cfb	0.038250452	*Pak1ip1*	0.04059692	*Fcgrt*	0.043105153
Fgf20	0.038308299	*Coa3*	0.040624905	*Micu1*	0.043312706
Rps9	0.038342195	*Gle1*	0.040730697	*Mus81*	0.043334022
Ntmt1	0.038344003	*Atp5e*	0.040752826	*Chmp4b*	0.043352393
Ppan	0.038365091	*Ndufaf4*	0.040758732	*Cox16*	0.043380248
Taf10	0.038388048	*Irg1*	0.04081246	*Cd200*	0.043445867
Aida	0.038388717	*Sec24b*	0.040910048	*Cdk5r1*	0.043490531
D1Ertd622e	0.038440116	*Usf1*	0.040919405	*H13*	0.04349694
Ptn	0.038468276	*Mxd3*	0.041024686	*Eif2ak2*	0.043577809
Lrwd1	0.038625231	*Pole4*	0.04106083	*St3gal5*	0.04369325
Avpi1	0.038693597	*Cd28*	0.041182873	*Krtcap2*	0.043704565
Psmd5	0.038734698	*Arpc1a*	0.041215043	*2810474O19Rik*	0.043747562
Phactr2	0.038766876	*Wasl*	0.041256334	*Slc25a22*	0.043763447
Gbp7	0.038794077	*0610010K14Rik*	0.041262221	*Id3*	0.043771743
Fastkd5	0.038870572	*Tbxa2r*	0.041296644	*Mrps25*	0.043868189
Rcc1	0.038871459	*Cabp5*	0.041388243	*Cd36*	0.043875097
Ndufb11	0.03888295	*Psmb1*	0.041419604	*Ppp1r14b*	0.043877734
Plekhh3	0.038974984	*Mrps12*	0.041457439	*Rfk*	0.044065287
*Sep15**	0.039028083	*Aipl1*	0.041473803	*Arpc3*	0.044070734
Rnf112	0.039114448	*Wipi1*	0.041570253	*Tada1*	0.044103056
Crabp1	0.039157167	*Ppp1r14d*	0.041579969	*Ndrg2*	0.044135021
Slc5a9	0.039363906	*Cox4i1*	0.041851042	*Znrd1*	0.044165501
Senp1	0.039400004	*Thra*	0.04187284	*Phf7*	0.044295927
Cnot4	0.039411481	*Cd247*	0.041930209	*Calm3*	0.044301283
Them4	0.039430503	*Hpcal1*	0.041933545	*Nek8*	0.044319064
Zbp1	0.039470596	*Ccdc86*	0.041982513	*Rps5*	0.044385819
Sdr42e1	0.039483662	*Chd1*	0.04202139	*Clns1a*	0.044397693
Tmem56	0.039689407	*Sdc3*	0.042059173	*1200014J11Rik*	0.044547493
Gins4	0.039710251	*Adra2b*	0.0421641	*Actr10*	0.0445703
Diap3	0.039711096	*Babam1*	0.042213533	*Dph6*	0.044631826
Ndufv1	0.039720937	*Exo1*	0.042222243	*Fank1*	0.044638659
Tmem40	0.039735669	*Fzd6*	0.042231887	*Sass6*	0.04464887
Alyref	0.039830547	*Clpp*	0.042254107	*Hnrnpc*	0.044726957
Prss16	0.03987266	*Stard5*	0.042284816	*Dcps*	0.044737055
Dnajc10	0.039913881	*Serf2*	0.042319725	*Myo1c*	0.04475472
Mrpl23	0.039964772	*Tal1*	0.042343297	*Stat1*	0.044768803
Nudt4	0.04000941	*Zc3h11a*	0.042361963	*Tnfsf10*	0.044783177
Gypc	0.040045064	*Atp5h*	0.042405146	*Ids*	0.044819203
Ing1	0.040133893	*Cpsf2*	0.042434194	*Slc22a17*	0.044823502
Ms4a4c	0.04013509	*Bfar*	0.042500754	*Pdcl3*	0.044841052

Supplemental Table 2-2: Genes correlated to macrophage response to LPS and LPS-induced bone loss

Gene Symbol	p Value	Gene Symbol	p Value	Gene Symbol	p Value
Orc1	0.044844404	*L2hgdh*	0.046850584	*Brd2*	0.048845738
Mov10	0.044847921	*Ndufa8*	0.046853613	*Me1*	0.048869389
Ifi204	0.044854759	*Uty*	0.04691559	*Cdr2*	0.048906765
Tlk2	0.04489882	*Angptl4*	0.04697271	*H2-DMa*	0.048975949
Dhx58	0.044900832	*E2f8*	0.046978051	*Dync1i2*	0.04900221
Srpr	0.04497804	*Gpx4*	0.046999886	*Rab15*	0.04908169
Sec61b	0.044984645	*Cyb5r1*	0.047012707	*Tmco6*	0.049089763
Olfm1	0.04502166	*Mark1*	0.047043352	*Fam98c*	0.049147694
Cfdp1	0.045052112	*Cdc23*	0.047067177	*Sfxn1*	0.049175123
Rragd	0.045082066	*Dgke*	0.047074264	*Irs3*	0.04919168
Fndc3a	0.04519076	*Zdhhc6*	0.047119429	*Erap1*	0.049199439
Fosb	0.04521044	*Brap*	0.04712022	*Zc3h7a*	0.049350721
Rasa4	0.045268655	*Fgf2*	0.047172931	*Pard6g*	0.049446637
Irs4	0.045271383	*Eif2ak2*	0.047181829	*Llgl1*	0.04949715
Rrbp1	0.045359115	*Bbox1*	0.047248602	*Pradc1*	0.049582963
Josd1	0.045426907	*Slc22a5*	0.047249712	*Camsap1*	0.049610503
Tfap2c	0.045433901	*Gabarap*	0.047281298	*Ehd4*	0.049700786
Simc1	0.045515473	*Dtymk*	0.047342587	*Asnsd1*	0.049723129
Cited2	0.045518234	*BC147527*	0.047469161	*Eif2s3x*	0.049811265
Htra3	0.045596446	*Clic1*	0.047495156	*Armc1*	0.04995056
Elf1	0.045644153	*Rap2b*	0.047518549	*Sardh*	0.050011347
Arhgef5	0.045804398	*Eva1a*	0.047525522	*Map7*	0.050058758
Tor1aip1	0.045886818	*Phlpp1*	0.047537239	*Clasp1*	0.050188892
Hras1	0.045902499	*Brk1*	0.047678216	*Epha1*	0.050225589
Pkd2	0.045952093	*Vcan*	0.047723753	*Lama3*	0.050307015
Ednra	0.045973929	*Isy1*	0.047765548	*Cpxm1*	0.050494457
Mnat1	0.045974688	*Cenpn*	0.047772253	*Ttc28*	0.050494746
Clca3	0.045985654	*Hmgb1*	0.047802909	*Hdgf*	0.050511594
Mdp1	0.046019846	*Phb*	0.047828395	*Vdac2*	0.050550734
Siva1	0.046089617	*Ankmy2*	0.047925277	*U2surp*	0.050562492
Nme2	0.046097797	*Gbp7*	0.047929573	*Fmo5*	0.050711973
Sp100	0.046135549	*Snhg5*	0.048046341	*Kif21a*	0.050732309
Ptgr2	0.04615708	*Zcchc6*	0.048138792	*Serf2*	0.050815244
Ndufc1	0.04618582	*Usp12*	0.048171804	*Hopx*	0.050841069
Ccdc6	0.046258358	*Metrnl*	0.048249299	*Med17*	0.050846945
Plekha4	0.046263922	*Mall*	0.048288622	*Dcbld1*	0.05087551
Prkd2	0.046264773	*Rgs11*	0.048315604	*Aldh1a1*	0.050889771
Cited2	0.04636761	*Ryr3*	0.048345872	*Ptprd*	0.050979746
Maf1	0.046385429	*Snx3*	0.048399992	*Kif1b*	0.051107216
Thoc6	0.046418783	*Atg5*	0.048419916	*Plekhb1*	0.051127663
Tmem216	0.046495945	*Trio*	0.048451873	*Taz*	0.051158734
Ddx5	0.046604545	*Vps45*	0.048490876	*Rpl13a*	0.051213235
Galnt7	0.046618146	*Fnbp4*	0.048504509	*Luc7l3*	0.051237339
Prl3a1	0.046625796	*Slc13a2*	0.048506927	*Gid4*	0.051253527
Pomc	0.046654996	*Plekhh1*	0.048508966	*Acat1*	0.051260692
Foxk2	0.04666088	*1700010I14Rik*	0.048523375	*Syt2*	0.051287142
Foxred1	0.046669742	*Riok3*	0.048540692	*Gbp2*	0.051289393
Fkbpl	0.04679434	*Cyp3a11*	0.048625749	*2310011J03Rik*	0.051299167
Ddx5	0.046833364	*Fis1*	0.048651279	*Ankrd17*	0.051353039
Neurl1a	0.046845034	*Dazl*	0.04877002	*Gps1*	0.051354315

Supplemental Table 2-2: Genes correlated to macrophage response to LPS and LPS-induced bone loss

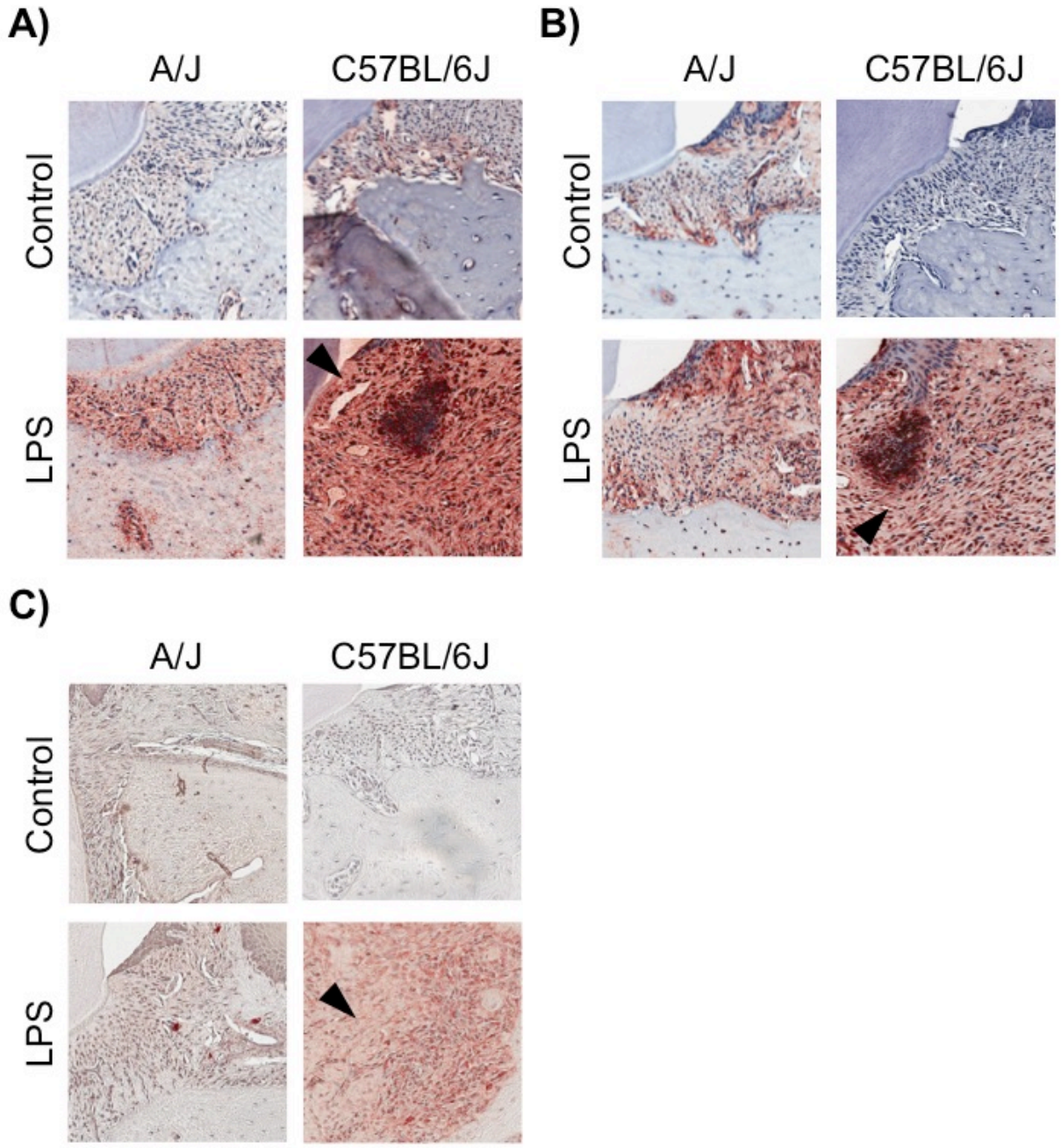

Supplemental Figure 2-1: Histological assessment of pro-inflammatory markers (A) Immunostaining of NF-kB in A/J control, A/J LPS, C57BL6/J control, and C57BL6/J LPS treated mice. Noted the increased staining in C57BL6/J LPS compared to A/J LPS (black arrow). (B) Immunostaining of COX-2 in A/J control, A/J LPS, C57BL6/J control, and C57BL6/J LPS treated mice. Noted the increased staining in C57BL6/J LPS compared to A/J LPS (black arrow). (C) Immunostaining of TNF-A in A/J control, A/J LPS, C57BL6/J control, and C57BL6/J LPS treated mice. Noted the increased staining in C57BL6/J LPS compared to A/J LPS (black arrow). For all images, 20X magnification.

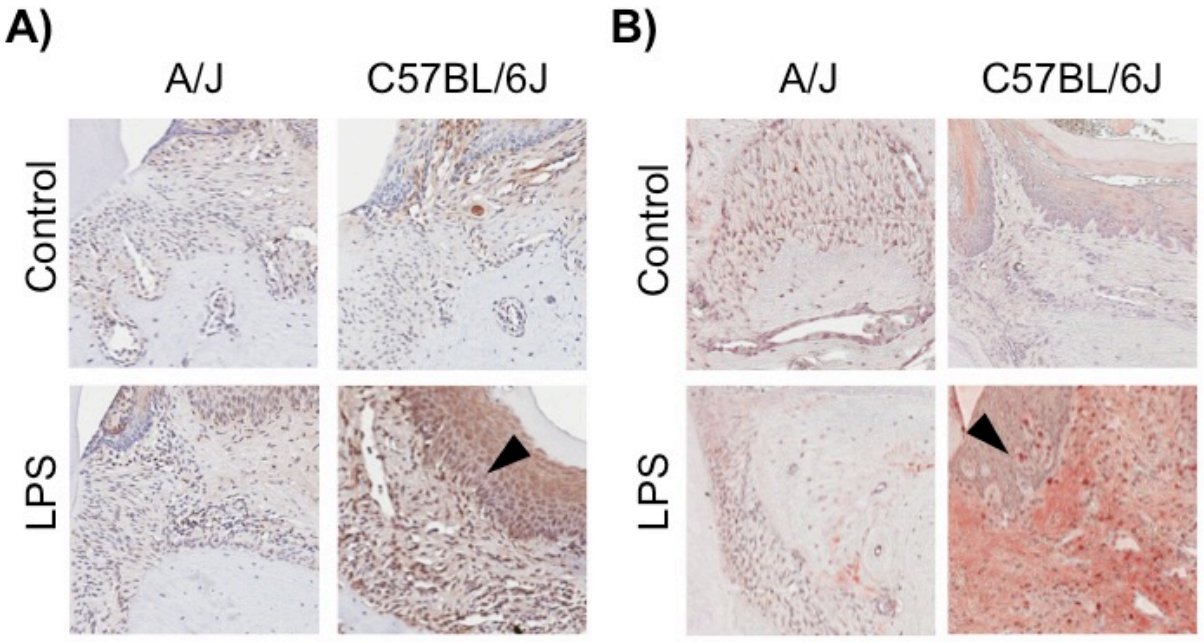

Supplemental Figure 2-2: Histological assessment of matrix degradation (A) Immunostaining of MMP-8 in A/J control, A/J LPS, C57BL6/J control, and C57BL6/J LPS treated mice. Noted the increased staining in C57BL6/J LPS compared to A/J LPS (black arrow). (B) Immunostaining of MMP-13 in A/J control, A/J LPS, C57BL6/J control, and C57BL6/J LPS treated mice. Noted the increased staining in C57BL6/J LPS compared to A/J LPS (black arrow). For all images, 20X magnification.

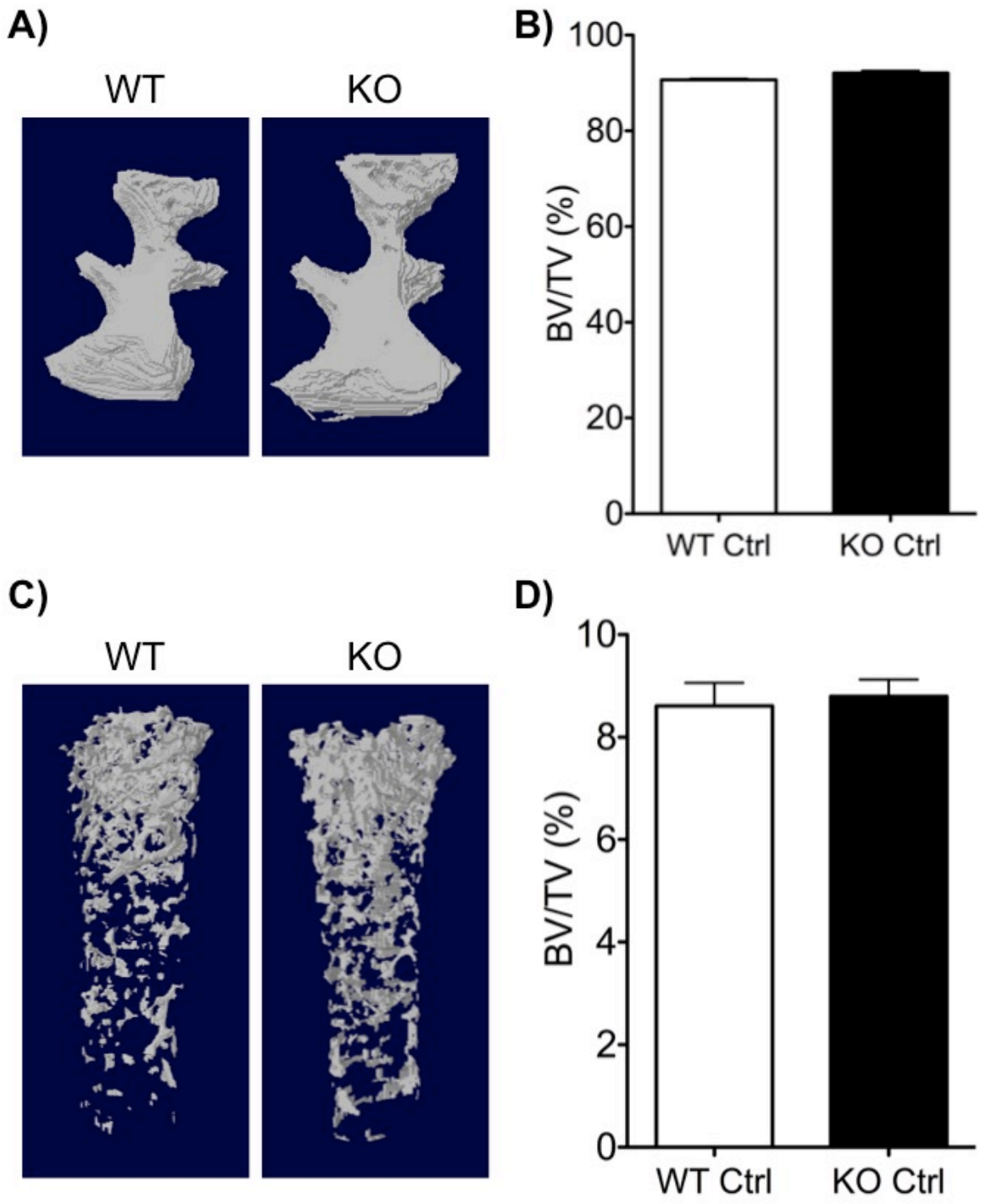

Supplemental Figure 2-3: Radiographic assessment of bone volume/tissue volume (BV/TV) in WT and Cxcr3 KO mice (A) Representative volumetric 3D reconstruction of maxilla in WT and *Cxcr3* KO mice. The area represented is in between the first and second molars. (B) Graph representing % bone volume/tissue volume (BV/TV) in WT control and *Cxcr3* KO mice. (C) Representative volumetric 3D reconstruction of the mesial femur distal from the growth plate of WT and *Cxcr3* KO mice. (D) Graph representing % BV/TV in WT control and *Cxcr3* KO mice. For both graphs (B and D): Significance was compared using a Student's *t* test. n=3 mice/group, p≤0.05*, p≤0.01**, p≤0.001***. Data represented as mean ± standard error of the mean (SEM).

References:

1. Albandar, J.M., Brunelle, J.A., and Kingman, A. 1999. Destructive periodontal disease in adults 30 years of age and older in the United States, 1988-1994. *J Periodontol* 70:13-29.

2. Di Benedetto, A., Gigante, I., Colucci, S., and Grano, M. 2013. Periodontal disease: linking the primary inflammation to bone loss. *Clin Dev Immunol* 2013:503754.

3. Darveau, R.P., Hajishengallis, G., and Curtis, M.A. 2012. Porphyromonas gingivalis as a potential community activist for disease. *J Dent Res* 91:816-820.

4. Loe, H., Anerud, A., Boysen, H., and Morrison, E. 1986. Natural history of periodontal disease in man. Rapid, moderate and no loss of attachment in Sri Lankan laborers 14 to 46 years of age. *J Clin Periodontol* 13:431-445.

5. Michalowicz, B.S. 1994. Genetic and heritable risk factors in periodontal disease. *J Periodontol* 65:479-488.

6. Michalowicz, B.S., Diehl, S.R., Gunsolley, J.C., Sparks, B.S., Brooks, C.N., Koertge, T.E., Califano, J.V., Burmeister, J.A., and Schenkein, H.A. 2000. Evidence of a substantial genetic basis for risk of adult periodontitis. *J Periodontol* 71:1699-1707.

7. Heaton, B., and Dietrich, T. 2012. Causal theory and the etiology of periodontal diseases. *Periodontol 2000* 58:26-36.

8. Loos, B.G., Papantonopoulos, G., Jepsen, S., and Laine, M.L. 2015. What is the Contribution of Genetics to Periodontal Risk? *Dent Clin North Am* 59:761-780.

9. Marian, A.J. 2012. Molecular genetic studies of complex phenotypes. *Transl Res* 159:64-79.

10. Mouse Genome Sequencing, C., Waterston, R.H., Lindblad-Toh, K., Birney, E., Rogers, J., Abril, J.F., Agarwal, P., Agarwala, R., Ainscough, R., Alexandersson, M., et al. 2002. Initial sequencing and comparative analysis of the mouse genome. *Nature* 420:520-562.

11. Rau, C.D., Parks, B., Wang, Y., Eskin, E., Simecek, P., Churchill, G.A., and Lusis, A.J. 2015. High-Density Genotypes of Inbred Mouse Strains: Improved Power and Precision of Association Mapping. *G3 (Bethesda)* 5:2021-2026.

12. Churchill, G.A., Airey, D.C., Allayee, H., Angel, J.M., Attie, A.D., Beatty, J., Beavis, W.D., Belknap, J.K., Bennett, B., Berrettini, W., et al. 2004. The Collaborative Cross, a community resource for the genetic analysis of complex traits. *Nat Genet* 36:1133-1137.

13. Ghazalpour, A., Rau, C.D., Farber, C.R., Bennett, B.J., Orozco, L.D., van Nas, A., Pan, C., Allayee, H., Beaven, S.W., Civelek, M., et al. 2012. Hybrid mouse diversity panel: a panel of inbred mouse strains suitable for analysis of complex genetic traits. *Mamm Genome* 23:680-692.

14. Hiyari, S., Atti, E., Camargo, P.M., Eskin, E., Lusis, A.J., Tetradis, S., and Pirih, F.Q. 2015. Heritability of periodontal bone loss in mice. *J Periodontal Res*.

15. Michalowicz, B.S., Aeppli, D., Virag, J.G., Klump, D.G., Hinrichs, J.E., Segal, N.L., Bouchard, T.J., Jr., and Pihlstrom, B.L. 1991. Periodontal findings in adult twins. *J Periodontol* 62:293-299.

16. Chrzeszczyk, D., Konopka, T., and Zietek, M. 2015. Polymorphisms of Toll-Like Receptor 4 as a Risk Factor for Periodontitis: Meta-Analysis. *Adv Clin Exp Med* 24:1059-1070.

17. Kim, P.D., Xia-Juan, X., Crump, K.E., Abe, T., Hajishengallis, G., and Sahingur, S.E. 2015. Toll-Like Receptor 9-Mediated Inflammation Triggers Alveolar Bone Loss in Experimental Murine Periodontitis. *Infect Immun* 83:2992-3002.

18. Chen, Y.C., Liu, C.M., Jeng, J.H., and Ku, C.C. 2014. Association of pocket epithelial cell proliferation in periodontitis with TLR9 expression and inflammatory response. *J Formos Med Assoc* 113:549-556.

19. Zhan, Y., Zhang, R., Lv, H., Song, X., Xu, X., Chai, L., Lv, W., Shang, Z., Jiang, Y., and Zhang, R. 2014. Prioritization of candidate genes for periodontitis using multiple computational tools. *J Periodontol* 85:1059-1069.

20. Kang, W., Hu, Z., and Ge, S. 2016. Healthy and Inflamed Gingival Fibroblasts Differ in Their Inflammatory Response to Porphyromonas gingivalis Lipopolysaccharide. *Inflammation* 39:1842-1852.

21. Escalona, L.A., Mastromatteo-Alberga, P., and Correnti, M. 2016. Cytokine and metalloproteinases in gingival fluid from patients with chronic periodontitis. *Invest Clin* 57:131-142.

22. Bennett, B.J., Davis, R.C., Civelek, M., Orozco, L., Wu, J., Qi, H., Pan, C., Packard, R.R., Eskin, E., Yan, M., et al. 2015. Genetic Architecture of Atherosclerosis in Mice: A Systems Genetics Analysis of Common Inbred Strains. *PLoS Genet* 11:e1005711.

23. Zhang, P., Fan, Y., Li, Q., Chen, J., Zhou, W., Luo, Y., Zhang, J., Su, L., Xue, X., Zhou, X., et al. 2016. Macrophage activating factor: A potential biomarker of periodontal health status. *Arch Oral Biol* 70:94-99.

24. Silva, N., Abusleme, L., Bravo, D., Dutzan, N., Garcia-Sesnich, J., Vernal, R., Hernandez, M., and Gamonal, J. 2015. Host response mechanisms in periodontal diseases. *J Appl Oral Sci* 23:329-355.

25. Orozco, L.D., Bennett, B.J., Farber, C.R., Ghazalpour, A., Pan, C., Che, N., Wen, P., Qi, H.X., Mutukulu, A., Siemers, N., et al. 2012. Unraveling inflammatory responses using systems genetics and gene-environment interactions in macrophages. *Cell* 151:658-670.

26. Dufour, J.H., Dziejman, M., Liu, M.T., Leung, J.H., Lane, T.E., and Luster, A.D. 2002. IFN-gamma-inducible protein 10 (IP-10; CXCL10)-deficient mice reveal a role for IP-10 in effector T cell generation and trafficking. *J Immunol* 168:3195-3204.

27. Angiolillo, A.L., Sgadari, C., Taub, D.D., Liao, F., Farber, J.M., Maheshwari, S., Kleinman, H.K., Reaman, G.H., and Tosato, G. 1995. Human interferon-inducible protein 10 is a potent inhibitor of angiogenesis in vivo. *J Exp Med* 182:155-162.

28. Luster, A.D., Unkeless, J.C., and Ravetch, J.V. 1985. Gamma-interferon transcriptionally regulates an early-response gene containing homology to platelet proteins. *Nature* 315:672-676.

29. Sochalska, M., and Potempa, J. 2017. Manipulation of Neutrophils by Porphyromonas gingivalis in the Development of Periodontitis. *Front Cell Infect Microbiol* 7:197.

30. Campbell, L., Millhouse, E., Malcolm, J., and Culshaw, S. 2016. T cells, teeth and tissue destruction - what do T cells do in periodontal disease? *Mol Oral Microbiol* 31:445-456.

31. Morton, R.S., and Dongari-Bagtzoglou, A.I. 2001. Cyclooxygenase-2 is upregulated in inflamed gingival tissues. *J Periodontol* 72:461-469.

32. Arabaci, T., Cicek, Y., Canakci, V., Canakci, C.F., Ozgoz, M., Albayrak, M., and Keles, O.N. 2010. Immunohistochemical and Stereologic Analysis of NF-kappaB Activation in Chronic Periodontitis. *Eur J Dent* 4:454-461.

33. Marcaccini, A.M., Meschiari, C.A., Sorgi, C.A., Saraiva, M.C., de Souza, A.M., Faccioli, L.H., Tanus-Santos, J.E., Novaes, A.B., and Gerlach, R.F. 2009. Circulating interleukin-6 and high-sensitivity C-reactive protein decrease after periodontal therapy in otherwise healthy subjects. *J Periodontol* 80:594-602.

34. Romanelli, R., Mancini, S., Laschinger, C., Overall, C.M., Sodek, J., and McCulloch, C.A. 1999. Activation of neutrophil collagenase in periodontitis. *Infect Immun* 67:2319-2326.

35. Hernandez, M., Valenzuela, M.A., Lopez-Otin, C., Alvarez, J., Lopez, J.M., Vernal, R., and Gamonal, J. 2006. Matrix metalloproteinase-13 is highly expressed in destructive periodontal disease activity. *J Periodontol* 77:1863-1870.

36. Zhang, S., Divaris, K., Moss, K., Yu, N., Barros, S., Marchesan, J., Morelli, T., Agler, C., Kim, S.J., Wu, D., et al. 2016. The Novel ASIC2 Locus is Associated with Severe Gingival Inflammation. *JDR Clin Trans Res* 1:163-170.

37. Munz, M., Willenborg, C., Richter, G.M., Jockel-Schneider, Y., Graetz, C., Staufenbiel, I., Wellmann, J., Berger, K., Krone, B., Hoffmann, P., et al. 2017. A genome-wide association study identifies nucleotide variants at SIGLEC5 and DEFA1A3 as risk loci for periodontitis. *Hum Mol Genet* 26:2577-2588.

38. Razzouk, S. 2016. Regulatory elements and genetic variations in periodontal diseases. *Arch Oral Biol* 72:106-115.

39. Nibali, L., Di Iorio, A., Tu, Y.K., and Vieira, A.R. 2017. Host genetics role in the pathogenesis of periodontal disease and caries. *J Clin Periodontol* 44 Suppl 18:S52-S78.

40. Kasbohm, E., Holtfreter, B., Volker, U., Petersmann, A., Samietz, S., Biffar, R., Volzke, H., Meisel, P., Kacprowski, T., Homuth, G., et al. 2017. Exome Variant Analysis of Chronic Periodontitis in 2 Large Cohort Studies. *J Dent Res* 96:73-80.

41. Sanders, A.E., Sofer, T., Wong, Q., Kerr, K.F., Agler, C., Shaffer, J.R., Beck, J.D., Offenbacher, S., Salazar, C.R., North, K.E., et al. 2017. Chronic Periodontitis Genome-

wide Association Study in the Hispanic Community Health Study / Study of Latinos. *J Dent Res* 96:64-72.

42. Offenbacher, S., Divaris, K., Barros, S.P., Moss, K.L., Marchesan, J.T., Morelli, T., Zhang, S., Kim, S., Sun, L., Beck, J.D., et al. 2016. Genome-wide association study of biologically informed periodontal complex traits offers novel insights into the genetic basis of periodontal disease. *Hum Mol Genet* 25:2113-2129.

43. Feng, P., Wang, X., Casado, P.L., Kuchler, E.C., Deeley, K., Noel, J., Kimm, H., Kim, J.H., Haas, A.N., Quinelato, V., et al. 2014. Genome wide association scan for chronic periodontitis implicates novel locus. *BMC Oral Health* 14:84.

44. Schaefer, A.S., Jochens, A., Dommisch, H., Graetz, C., Jockel-Schneider, Y., Harks, I., Staufenbiel, I., Meyle, J., Eickholz, P., Folwaczny, M., et al. 2014. A large candidate-gene association study suggests genetic variants at IRF5 and PRDM1 to be associated with aggressive periodontitis. *J Clin Periodontol* 41:1122-1131.

45. Divaris, K., Monda, K.L., North, K.E., Olshan, A.F., Reynolds, L.M., Hsueh, W.C., Lange, E.M., Moss, K., Barros, S.P., Weyant, R.J., et al. 2013. Exploring the genetic basis of chronic periodontitis: a genome-wide association study. *Hum Mol Genet* 22:2312-2324.

46. Hong, K.W., Shin, M.S., Ahn, Y.B., Lee, H.J., and Kim, H.D. 2015. Genomewide association study on chronic periodontitis in Korean population: results from the Yangpyeong health cohort. *J Clin Periodontol*.

47. El Jilani, M.M., Mohamed, A.A., Zeglam, H.B., Alhudiri, I.M., Ramadan, A.M., Saleh, S.S., Elkabir, M., Amer, I.B., Ashammakhi, N., and Enattah, N.S. 2015. Association between vitamin D receptor gene polymorphisms and chronic periodontitis among Libyans. *Libyan J Med* 10:26771.

48. Shimizu, S., Momozawa, Y., Takahashi, A., Nagasawa, T., Ashikawa, K., Terada, Y., Izumi, Y., Kobayashi, H., Tsuji, M., Kubo, M., et al. 2015. A Genome-wide Association Study of Periodontitis in a Japanese Population. *J Dent Res*.

49. Karimbux, N.Y., Saraiya, V.M., Elangovan, S., Allareddy, V., Kinnunen, T., Kornman, K.S., and Duff, G.W. 2012. Interleukin-1 gene polymorphisms and chronic periodontitis in adult whites: a systematic review and meta-analysis. *J Periodontol* 83:1407-1419.

50. Chen, Y.J., Han, Y., Mao, M., Tan, Y.Q., Leng, W.D., and Zeng, X.T. 2015. Interleukin-1beta rs1143634 polymorphism and aggressive periodontitis susceptibility: a meta-analysis. *Int J Clin Exp Med* 8:2308-2316.

51. Zeng, X.T., Liu, D.Y., Kwong, J.S., Leng, W.D., Xia, L.Y., and Mao, M. 2015. Meta-Analysis of Association Between Interleukin-1beta C-511T Polymorphism and Chronic Periodontitis Susceptibility. *J Periodontol* 86:812-819.

52. Yin, W.T., Pan, Y.P., and Lin, L. 2016. Association between IL-1alpha rs17561 and IL-1beta rs1143634 polymorphisms and periodontitis: a meta-analysis. *Genet Mol Res* 15.

53. Ding, C., Ji, X., Chen, X., Xu, Y., and Zhong, L. 2014. TNF-alpha gene promoter polymorphisms contribute to periodontitis susceptibility: evidence from 46 studies. *J Clin Periodontol* 41:748-759.

54. Song, G.G., Choi, S.J., Ji, J.D., and Lee, Y.H. 2013. Association between tumor necrosis factor-alpha promoter -308 A/G, -238 A/G, interleukin-6 -174 G/C and -572 G/C polymorphisms and periodontal disease: a meta-analysis. *Mol Biol Rep* 40:5191-5203.

55. Xie, C.J., Chen, L., Tong, F.L., Xiao, L.M., and Zhang, J.C. 2012. [Meta analysis of association between TNF-alpha-308 polymorphism and periodontitis in Chinese Han population]. *Shanghai Kou Qiang Yi Xue* 21:447-450.

56. Zheng, J., Hou, T., Gao, L., Wu, C., Wang, P., Wen, Y., and Guo, X. 2013. Association between CD14 gene polymorphism and periodontitis: a meta-analysis. *Crit Rev Eukaryot Gene Expr* 23:115-123.

57. Han, M.X., Ding, C., and Kyung, H.M. 2015. Genetic polymorphisms in pattern recognition receptors and risk of periodontitis: Evidence based on 12,793 subjects. *Hum Immunol* 76:496-504.

58. van Nas, A., Pan, C., Ingram-Drake, L.A., Ghazalpour, A., Drake, T.A., Sobel, E.M., Papp, J.C., and Lusis, A.J. 2013. The systems genetics resource: a web application to mine global data for complex disease traits. *Front Genet* 4:84.

59. Shusterman, A., Durrant, C., Mott, R., Polak, D., Schaefer, A., Weiss, E.I., Iraqi, F.A., and Houri-Haddad, Y. 2013. Host susceptibility to periodontitis: mapping murine genomic regions. *J Dent Res* 92:438-443.

60. Shusterman, A., Munz, M., Richter, G., Jepsen, S., Lieb, W., Krone, B., Hoffman, P., Laudes, M., Wellmann, J., Berger, K., et al. 2017. The PF4/PPBP/CXCL5 Gene Cluster Is Associated with Periodontitis. *J Dent Res* 96:945-952.

61. Marra, F., and Tacke, F. 2014. Roles for chemokines in liver disease. *Gastroenterology* 147:577-594 e571.

62. Antonelli, A., Ferrari, S.M., Giuggioli, D., Ferrannini, E., Ferri, C., and Fallahi, P. 2014. Chemokine (C-X-C motif) ligand (CXCL)10 in autoimmune diseases. *Autoimmun Rev* 13:272-280.

63. van den Borne, P., Quax, P.H., Hoefer, I.E., and Pasterkamp, G. 2014. The multifaceted functions of CXCL10 in cardiovascular disease. *Biomed Res Int* 2014:893106.

64. Maghazachi, A.A. 2010. Role of chemokines in the biology of natural killer cells. *Curr Top Microbiol Immunol* 341:37-58.

65. Shimada, A., Oikawa, Y., Yamada, Y., Okubo, Y., and Narumi, S. 2009. The role of the CXCL10/CXCR3 system in type 1 diabetes. *Rev Diabet Stud* 6:81-84.

66. Lee, E.Y., Lee, Z.H., and Song, Y.W. 2013. The interaction between CXCL10 and cytokines in chronic inflammatory arthritis. *Autoimmun Rev* 12:554-557.

67. Scolletta, S., Colletti, M., Di Luigi, L., and Crescioli, C. 2013. Vitamin D receptor agonists target CXCL10: new therapeutic tools for resolution of inflammation. *Mediators Inflamm* 2013:876319.

68. Antonelli, A., Ferrari, S.M., Corrado, A., Ferrannini, E., and Fallahi, P. 2014. CXCR3, CXCL10 and type 1 diabetes. *Cytokine Growth Factor Rev* 25:57-65.

69. Hofer, M.J., and Campbell, I.L. 2015. Immunoinflammatory diseases of the central nervous system - the tale of two cytokines. *Br J Pharmacol*.

70. Karin, N., and Wildbaum, G. 2015. The role of chemokines in adjusting the balance between CD4+ effector T cell subsets and FOXp3-negative regulatory T cells. *Int Immunopharmacol*.

71. Azad, A.K., Sadee, W., and Schlesinger, L.S. 2012. Innate immune gene polymorphisms in tuberculosis. *Infect Immun* 80:3343-3359.

72. Van Raemdonck, K., Van den Steen, P.E., Liekens, S., Van Damme, J., and Struyf, S. 2015. CXCR3 ligands in disease and therapy. *Cytokine Growth Factor Rev* 26:311-327.

73. Souto, G.R., Queiroz, C.M., Jr., Costa, F.O., and Mesquita, R.A. 2014. Relationship between chemokines and dendritic cells in human chronic periodontitis. *J Periodontol* 85:1416-1423.

74. Amaya, M.P., Criado, L., Blanco, B., Gomez, M., Torres, O., Florez, L., Gonzalez, C.I., and Florez, O. 2013. Polymorphisms of pro-inflammatory cytokine genes and the risk for acute suppurative or chronic nonsuppurative apical periodontitis in a Colombian population. *Int Endod J* 46:71-78.

75. Beikler, T., Peters, U., Prior, K., Eisenacher, M., and Flemmig, T.F. 2008. Gene expression in periodontal tissues following treatment. *BMC Med Genomics* 1:30.

76. Abe, D., Kubota, T., Morozumi, T., Shimizu, T., Nakasone, N., Itagaki, M., and Yoshie, H. 2011. Altered gene expression in leukocyte transendothelial migration and cell communication pathways in periodontitis-affected gingival tissues. *J Periodontal Res* 46:345-353.

77. Schallhorn, R.A., Patel, D.N., Chandrasekar, B., and Mealey, B.L. 2010. Periodontal disease in association with systemic levels of interleukin-18 and CXC ligand 16 in patients undergoing cardiac catheterization. *J Periodontol* 81:1180-1186.

78. Noda, K., Akiyoshi, H., Aoki, M., Shimada, T., and Ohashi, F. 2007. Relationship between transportation stress and polymorphonuclear cell functions of bottlenose dolphins, Tursiops truncatus. *J Vet Med Sci* 69:379-383.

79. Burke, S.J., Karlstad, M.D., Eder, A.E., Regal, K.M., Lu, D., Burk, D.H., and Collier, J.J. 2016. Pancreatic beta-Cell production of CXCR3 ligands precedes diabetes onset. *Biofactors* 42:703-715.

80. Zychowska, M., Rojewska, E., Pilat, D., and Mika, J. 2015. The role of some chemokines from the CXC subfamily in a mouse model of diabetic neuropathy. *J Diabetes Res* 2015:750182.

81. Wu, C., Chen, X., Shu, J., and Lee, C.T. 2017. Whole-genome expression analyses of type 2 diabetes in human skin reveal altered immune function and burden of infection. *Oncotarget* 8:34601-34609.

82. He, J., Lian, C., Fang, Y., Wu, J., Weng, J., Ye, X., and Zhou, H. 2015. Effect of CXCL10 receptor antagonist on islet cell apoptosis in a type I diabetes rat model. *Int J Clin Exp Pathol* 8:14542-14548.

83. Altara, R., Mallat, Z., Booz, G.W., and Zouein, F.A. 2016. The CXCL10/CXCR3 Axis and Cardiac Inflammation: Implications for Immunotherapy to Treat Infectious and Noninfectious Diseases of the Heart. *J Immunol Res* 2016:4396368.

84. Trott, D.W., Lesniewski, L.A., and Donato, A.J. 2017. Selected life-extending interventions reduce arterial CXCL10 and macrophage colony-stimulating factor in aged mouse arteries. *Cytokine* 96:102-106.

85. Corbera-Bellalta, M., Planas-Rigol, E., Lozano, E., Terrades-Garcia, N., Alba, M.A., Prieto-Gonzalez, S., Garcia-Martinez, A., Albero, R., Enjuanes, A., Espigol-Frigole, G., et al. 2016. Blocking interferon gamma reduces expression of chemokines CXCL9, CXCL10 and CXCL11 and decreases macrophage infiltration in ex vivo cultured arteries from patients with giant cell arteritis. *Ann Rheum Dis* 75:1177-1186.

86. Tavakolian Ferdousie, V., Mohammadi, M., Hassanshahi, G., Khorramdelazad, H., Khanamani Falahati-Pour, S., Mirzaei, M., Allah Tavakoli, M., Kamiab, Z., Ahmadi, Z., Vazirinejad, R., et al. 2017. Serum CXCL10 and CXCL12 chemokine levels are associated with the severity of coronary artery disease and coronary artery occlusion. *Int J Cardiol* 233:23-28.

87. Venza, I., Visalli, M., Cucinotta, M., De Grazia, G., Teti, D., and Venza, M. 2010. Proinflammatory gene expression at chronic periodontitis and peri-implantitis sites in patients with or without type 2 diabetes. *J Periodontol* 81:99-108.

88. Dar-Odeh, N.S., Abu-Hammad, O.A., Al-Omiri, M.K., Khraisat, A.S., and Shehabi, A.A. 2010. Antibiotic prescribing practices by dentists: a review. *Ther Clin Risk Manag* 6:301-306.

89. Stone, V.N., and Xu, P. 2017. Targeted antimicrobial therapy in the microbiome era. *Mol Oral Microbiol*.

90. Socransky, S.S., Haffajee, A.D., Cugini, M.A., Smith, C., and Kent, R.L., Jr. 1998. Microbial complexes in subgingival plaque. *J Clin Periodontol* 25:134-144.

91. Diehl, S.R., Wu, T., Michalowicz, B.S., Brooks, C.N., Califano, J.V., Burmeister, J.A., and Schenkein, H.A. 2005. Quantitative measures of aggressive periodontitis show substantial heritability and consistency with traditional diagnoses. *J Periodontol* 76:279-288.

92. Salvi, G.E., and Lang, N.P. 2005. The effects of non-steroidal anti-inflammatory drugs (selective and non-selective) on the treatment of periodontal diseases. *Curr Pharm Des* 11:1757-1769.

93. Yen, C.A., Damoulis, P.D., Stark, P.C., Hibberd, P.L., Singh, M., and Papas, A.S. 2008. The effect of a selective cyclooxygenase-2 inhibitor (celecoxib) on chronic periodontitis. *J Periodontol* 79:104-113.

94. Shinoda, H., Takeyama, S., Suzuki, K., Murakami, S., and Yamada, S. 2008. Pharmacological topics of bone metabolism: a novel bisphosphonate for the treatment of periodontitis. *J Pharmacol Sci* 106:555-558.

95. Kilkenny, C., Browne, W., Cuthill, I.C., Emerson, M., Altman, D.G., and Group, N.C.R.R.G.W. 2010. Animal research: reporting in vivo experiments: the ARRIVE guidelines. *Br J Pharmacol* 160:1577-1579.

96. Crow, A.L., Ohmen, J., Wang, J., Lavinsky, J., Hartiala, J., Li, Q., Li, X., Salehide, P., Eskin, E., Pan, C., et al. 2015. The Genetic Architecture of Hearing Impairment in Mice: Evidence for Frequency-Specific Genetic Determinants. *G3 (Bethesda)* 5:2329-2339.

97. Salehi, P., Myint, A., Kim, Y.J., Ge, M.X., Lavinsky, J., Ho, M.K., Crow, A.L., Cruz, C., Monges-Hernadez, M., Wang, J., et al. 2016. Genome-Wide Association Analysis Identifies Dcc as an Essential Factor in the Innervation of the Peripheral Vestibular System in Inbred Mice. *J Assoc Res Otolaryngol* 17:417-431.

98. Lippert, C., Listgarten, J., Liu, Y., Kadie, C.M., Davidson, R.I., and Heckerman, D. 2011. FaST linear mixed models for genome-wide association studies. *Nat Methods* 8:833-835.

99. Bennett, B.J., Farber, C.R., Orozco, L., Kang, H.M., Ghazalpour, A., Siemers, N., Neubauer, M., Neuhaus, I., Yordanova, R., Guan, B., et al. 2010. A high-resolution association mapping panel for the dissection of complex traits in mice. *Genome Res* 20:281-290.

100. Davis, R.C., van Nas, A., Bennett, B., Orozco, L., Pan, C., Rau, C.D., Eskin, E., and Lusis, A.J. 2013. Genome-wide association mapping of blood cell traits in mice. *Mamm Genome* 24:105-118.

101. Ohmen, J., Kang, E.Y., Li, X., Joo, J.W., Hormozdiari, F., Zheng, Q.Y., Davis, R.C., Lusis, A.J., Eskin, E., and Friedman, R.A. 2014. Genome-wide association study for age-related hearing loss (AHL) in the mouse: a meta-analysis. *J Assoc Res Otolaryngol* 15:335-352.

102. Park, C.C., Gale, G.D., de Jong, S., Ghazalpour, A., Bennett, B.J., Farber, C.R., Langfelder, P., Lin, A., Khan, A.H., Eskin, E., et al. 2011. Gene networks associated with conditional fear in mice identified using a systems genetics approach. *BMC Syst Biol* 5:43.

103. Tenesa, A., and Haley, C.S. 2013. The heritability of human disease: estimation, uses and abuses. *Nat Rev Genet* 14:139-149.

104. Walser, T.C., Rifat, S., Ma, X., Kundu, N., Ward, C., Goloubeva, O., Johnson, M.G., Medina, J.C., Collins, T.L., and Fulton, A.M. 2006. Antagonism of CXCR3 inhibits lung metastasis in a murine model of metastatic breast cancer. *Cancer Res* 66:7701-7707.

CHAPTER THREE

Conclusions and Future Directions

Conclusions and Future Directions:

Microbiome Analysis in Healthy and Periodontitis Conditions

While it's usually overlooked, dental plaque and dental bacteria were some of the first organisms' visualized utilizing microscopy. Indeed, dental plaque, which is composed of a community of microorganisms collectively called a "biofilm," contains bacteria that were some of the first studied in the field of microbiology.

Antonie van Leeuwenhoek, a Dutch scientist performed some of his initial microscopy experiments by scraping plaque from his teeth and observing the "moving animalcules" under a microscope, incidentally establishing foundations for modern microbiology (1). At the time, van Leeuwenhoek only had the aid of a simple microscope, however some of the bacteria he observed and described, though unknown at the time, were some of the most abundant microorganisms that reside in the oral cavity (1).

Following van Leeuwenhoek, several scientists and dentists after him begun to better characterize and understand the bacterial communities that reside in the oral cavity. W.D. Miller, a dental practitioner in the 1890's wrote a book titled "Microorganisms of the Human Mouth," which outlined his analysis of oral bacteria (2). Through his work, he concluded that oral microorganisms were not individual bacteria, but a collective of different bacterial species working together to create a bacterial community (2). Today, the "biofilm" concept of oral bacteria is known to be the cause of dental caries, as well as, periodontal disease.

Currently, due to pioneers like Socransky (3), who characterized specific bacterial species, or keystone species, such as *Porphyromonas gingivalis* (*P.g.*), involved in periodontal disease, our

understanding of the oral microbial community, or oral “microbiome” has greatly expanded. However, how the oral microbiome interacts with the host immune response and how shifts in the oral microbiome during health and disease effect clinical outcomes are areas that need to be further explored.

The genome-wide association approach (GWAS) using the Hybrid Mouse Diversity Panel, such as we have employed with a murine model of *P. gingivalis* (*P.g.*)-Lipopolysaccharide (LPS)-induced bone loss, could easily be applied in a microbiological study of periodontitis. For example, oral microbiome samples could be collected from the HMDP and with the advancements of high-throughput 16S RNA bacterial sequencing, unique microbiome profiles for each strain of the HMDP under healthy and disease conditions could be obtained. Furthermore, microbiome profiles could be associated with our GWAS of *P.g.* LPS-induced bone loss in order to define which bacterial species specifically promote periodontitis susceptibility or which bacterial species in abundance create a high bone loss phenotype. Indeed, the interplay between the resident oral microbome and the host genetic framework is an area that needs to be further explored and a detailed understanding would greatly aid in patient treatment and management.

Gene Expression Changes in Healthy and Periodontitis Conditions

Another avenue of research that would greatly aid in understanding periodontitis susceptibility is detailed characterization of gene expression changes during health and disease, and the overall network of how specific genes work together to increase disease risk.

As discussed previously, several study designs have been employed to begin to understand the genetic framework of PD, including Genome-wide Association Studies (GWAS), assessing patient samples for differences in gene and cytokine expression, and dissecting animal models of periodontitis, which have all generated meaningful data. However, detailed gene expression profiles of periodontitis in health and disease have currently not been defined.

Allele Specific Expression (ASE) is the unequal expression of multiple alleles of a gene in a given organism (4, 5). For example, heterozygous Single Nucleotide Polymorphisms (SNPs), or two different alleles in the same position of DNA, may be transcribed into mRNA in an unequal fashion (4-6). An example of this is X chromosome inactivation in females and parental imprinting of alleles that are expressed in a sex-specific manner (4-6). Furthermore, gene expression that is affected by genetic variation has been shown to be fairly common in natural populations and specifically common for complex traits, of which periodontitis is classified. A complex trait is the result of many genes and environmental factors acting in concert to create the trait phenotype, which is in contrast to monogenic traits, where one gene is responsible for the majority of the trait phenotype. The genetic loci that contribute to gene expression levels are classified as expression quantitative trait loci (eQTLs) (6). eQTLs that act on the same DNA molecule are further termed *cis*-eQTLs, and these act in an allele specific manner. For example, a *cis*-eQTL could result from sequence differences in a promoter or an enhancer of the gene or sequences important for the stability of the RNA so that its turnover rate is affected (5). ASE analysis can identify *cis*-eQTL in an allele specific manner and this type of expression analysis has become achievable for multiple reasons including: the advancement of gene expression analysis (microarrays and deep RNA-sequencing platforms) and genome-wide association studies in humans and animal models where the entire genome can be assessed with fine mapping resolution.

The development of high-throughput RNA-sequencing (RNA-Seq) methods has ushered in a novel approach to expression analysis and in particular genome-wide expression analysis. RNA-Seq has many advantages to the classic microarray in that RNA-Seq allows for quantification of transcript levels and when RNA products contain sequence differences, sequencing can distinguish alleles of the genes. Furthermore, RNA-Seq can be applied to a large number of samples in a high-through put fashion. RNA-Seq can be particularly useful in assessing ASE and when utilizing inbred mice. For example, when inbred mice, and mice that present with apposing phenotypes for a particular trait, are bred to create F_1 heterozygous mice, RNA-Seq can be employed to identify ASE as well as imprinted genes. While a few studies have employed this method to study gene expression in murine brain, liver, and adipose tissue, even fewer have employed this approach in the study of periodontitis (7-9).

One study in particular, Shusterman, et al, used F_2 crosses of two mice strains, one resistant to oral infection-induced periodontitis and one susceptible to oral infection-induced periodontitis, as well as, combined murine data with human GWAS to identify eQTL's associated with periodontitis (10). As discussed previously, Shusterman et al's, study identified *Cxcl* family members as associated with periodontitis, which parallels our GWAS findings (10).

Using the data we generated from our GWAS study could serve as a foundation for future genetic murine study designs. Indeed, the extreme phenotypes in A/J and C57BL/6J provide the tools to identify genes involved in LPS-induced bone loss utilizing mouse genetic approaches. In order to exploit the observed opposing bone loss phenotypes, RNA-Seq could be employed to assess ASE on F_1 mice generated from reciprocal crosses of A/J and C57BL/6J. RNA-seq would not only allow for the quantification of gene expression in periodontitis, but also for quantification of ASE if the expressed sequences of the two alleles differ by at least one base, by directly counting the reads of each allele in the heterozygous samples (4). By

sequencing whole gene expression transcripts between A/J and C57BL/6J F_1 control and LPS treated mice, a novel, unbiased, "big picture" approach would allow the identification of transcript variants that are responsible for resistance and susceptibility to *P. gingivalis* Lipopolysaccharide (LPS)-induced bone loss (4, 5). Furthermore, these expression data could be combined with ongoing Genome-Wide Association Studies (GWAS) exploring the genetic basis of periodontal bone loss to identify overlapping genes and inform candidate gene selection (11).

Therapeutic Modalities – Translating Basic Science to Clinical Protocols

Taken together, understanding shifts in the oral microbial community, as well as, genes and changes in gene expression that promote resistance or susceptibility to disease, helps achieve the ultimate goal of providing clinically reliable personalized treatment options for patients. Several groups have used antibiotics, nonsteroidal anti-inflammatory drugs (NSAIDs), bisphosphonates, and small molecule inhibitors systemically and locally as treatment for periodontitis (12-15). In our study, we identified CXCR3 as partially responsible for *P.g.*-LPS induced bone loss. Additionally, we explored the therapeutic potential of blocking CXCR3 *in vivo* with the use of a CXCR3 antagonist systemically. While systemic treatment showed an improvement in periodontal bone loss, the ideal goal would be to apply treatment methods locally.

New small molecule nanotechnology or nanoparticles offer many advantages for local delivery of drugs. Nanoparticles are small molecule particles that can be formulated from artificial polymers or lipids. As drug carriers, nanoparticles offer high stability, high carrier capacity, the ability to incorporate both hydrophilic and hydrophobic drug compounds, controlled or sustained

release of the drug over time, and various routes of administration (16-19). Using this approach, we have performed preliminary studies using the CXCR3 antagonist incorporated into nanoparticles as a local delivery system and our *P.g.*-LPS injection model of periodontitis. Through this, we observed a reduction in bone loss after local delivery of CXCR3 antagonist nanoparticles at two different doses (Figure 3-1). While these studies are preliminary, after candidate gene identification and validation, small molecule antagonists are an attractive option for local therapeutic treatment and further work is needed to validate potential targets to treat periodontitis.

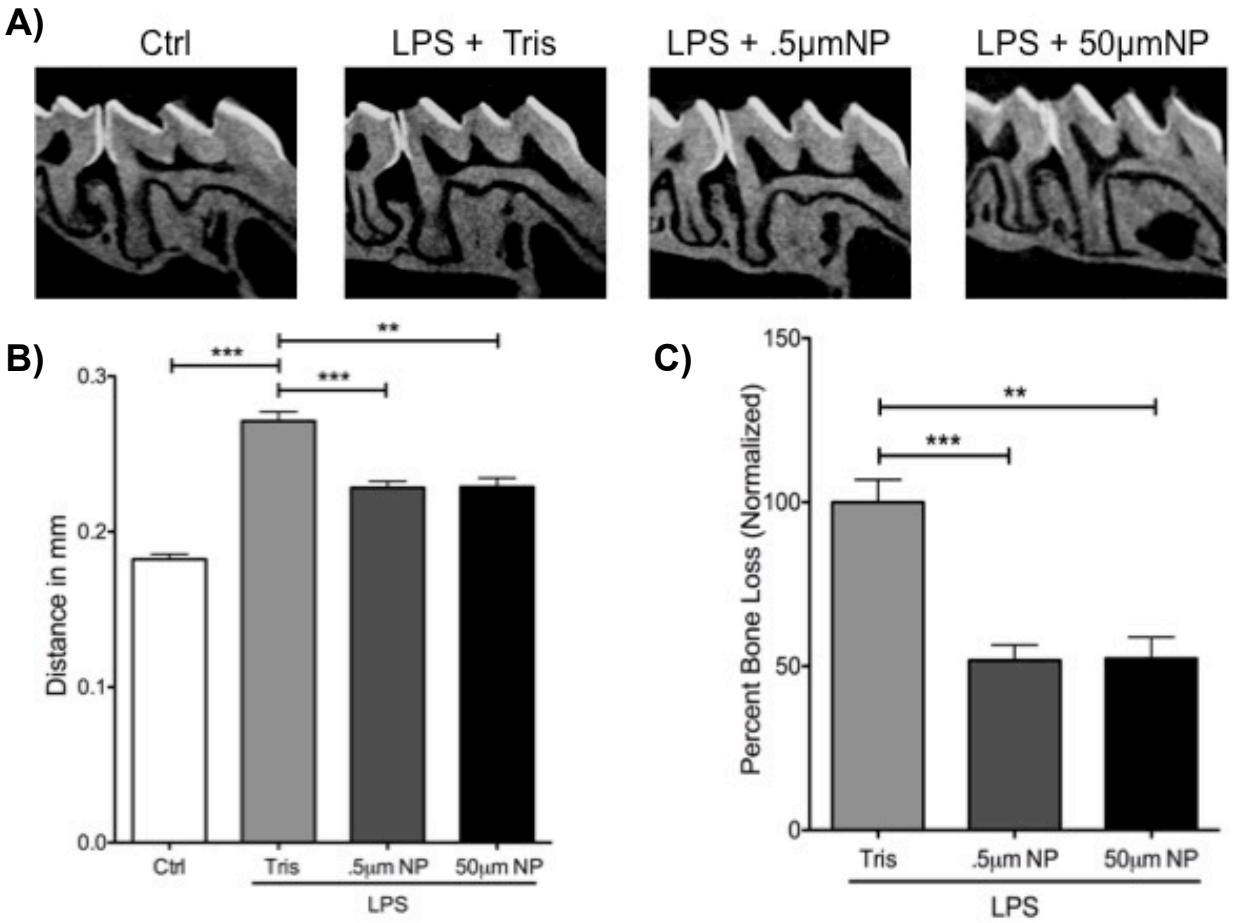

Figure 3-1: Local delivery of CXCR3 antagonist, AMG-487, reduces alveolar bone loss. (A) Representative radiographic images of control (Ctrl), LPS + Tris, LPS + .5µm AMG-487 nanoparticles (NP), and LPS + 50µm NP. (B) Graph representing bone levels in control (Ctrl), LPS + Tris, LPS + .5µm AMG-487 nanoparticles (NP), and LPS + 50µm NP. (C) Graph representing the normalized percent bone loss (ctrl subtracted) in LPS + Tris, LPS + .5µm AMG-487 nanoparticles (NP), and LPS + 50µm NP. For both graphs (B and C) data is represented as mean ± standard error of the mean. For all groups n≥5.

Conclusions

In conclusion, current clinical treatment protocols for periodontitis generally rely on clinical and radiographic assessment of disease presentation as well as potential environmental confounding factors including diabetes or smoking status. General clinical protocols rely on biofilm maintenance even though, while biofilm presence is necessary, it is not sufficient alone to cause disease. In most cases this treatment paradigm is effective, however, on occasion, this results in the over treatment of some patients and the under treatment of others. In order to guide in a new era of periodontal treatment and management, the ideal scenario would be to not only include, clinical, radiographic, biofilm status, and environmental factors, but to consider the oral microbiome, and specifically the host genetic immunoinflammatory response. Collectively, clinical, radiographic, biofilm status, environmental factors, microbial flora, and the host genetic framework all play integral roles in periodontitis susceptibility and a detailed understanding of each piece of the puzzle would facilitate a new age of truly personalized periodontal treatment.

References:

1. Gest, H. 2004. The discovery of microorganisms by Robert Hooke and Antoni Van Leeuwenhoek, fellows of the Royal Society. *Notes Rec R Soc Lond* 58:187-201.

2. Miller, W.D. 1891. *The Micro-organisms of the Human Mouth*. American Journal of Medical Science.

3. Socransky, S.S., Haffajee, A.D., Cugini, M.A., Smith, C., and Kent, R.L., Jr. 1998. Microbial complexes in subgingival plaque. *J Clin Periodontol* 25:134-144.

4. Hasin-Brumshtein, Y., Hormozdiari, F., Martin, L., van Nas, A., Eskin, E., Lusis, A.J., and Drake, T.A. 2014. Allele-specific expression and eQTL analysis in mouse adipose tissue. *BMC Genomics* 15:471.

5. Lagarrigue, S., Martin, L., Hormozdiari, F., Roux, P.F., Pan, C., van Nas, A., Demeure, O., Cantor, R., Ghazalpour, A., Eskin, E., et al. 2013. Analysis of allele-specific expression in mouse liver by RNA-Seq: a comparison with Cis-eQTL identified using genetic linkage. *Genetics* 195:1157-1166.

6. Pastinen, T. 2010. Genome-wide allele-specific analysis: insights into regulatory variation. *Nat Rev Genet* 11:533-538.

7. Gregg, C., Zhang, J., Butler, J.E., Haig, D., and Dulac, C. 2010. Sex-specific parent-of-origin allelic expression in the mouse brain. *Science* 329:682-685.

8. Gregg, C., Zhang, J., Weissbourd, B., Luo, S., Schroth, G.P., Haig, D., and Dulac, C. 2010. High-resolution analysis of parent-of-origin allelic expression in the mouse brain. *Science* 329:643-648.

9. Wang, X., Soloway, P.D., and Clark, A.G. 2011. A survey for novel imprinted genes in the mouse placenta by mRNA-seq. *Genetics* 189:109-122.

10. Shusterman, A., Munz, M., Richter, G., Jepsen, S., Lieb, W., Krone, B., Hoffman, P., Laudes, M., Wellmann, J., Berger, K., et al. 2017. The PF4/PPBP/CXCL5 Gene Cluster Is Associated with Periodontitis. *J Dent Res* 96:945-952.

11. Hiyari, S., Atti, E., Camargo, P.M., Eskin, E., Lusis, A.J., Tetradis, S., and Pirih, F.Q. 2015. Heritability of periodontal bone loss in mice. *J Periodontal Res*.

12. Salvi, G.E., and Lang, N.P. 2005. The effects of non-steroidal anti-inflammatory drugs (selective and non-selective) on the treatment of periodontal diseases. *Curr Pharm Des* 11:1757-1769.

13. Yen, C.A., Damoulis, P.D., Stark, P.C., Hibberd, P.L., Singh, M., and Papas, A.S. 2008. The effect of a selective cyclooxygenase-2 inhibitor (celecoxib) on chronic periodontitis. *J Periodontol* 79:104-113.

14. Shinoda, H., Takeyama, S., Suzuki, K., Murakami, S., and Yamada, S. 2008. Pharmacological topics of bone metabolism: a novel bisphosphonate for the treatment of periodontitis. *J Pharmacol Sci* 106:555-558.

15. Stone, V.N., and Xu, P. 2017. Targeted antimicrobial therapy in the microbiome era. *Mol Oral Microbiol*.

16. Mudshinge, S.R., Deore, A.B., Patil, S., and Bhalgat, C.M. 2011. Nanoparticles: Emerging carriers for drug delivery. *Saudi Pharm J* 19:129-141.

17. Kumar, A.J., Anumala, N., and Avula, H. 2012. Novel and often bizarre strategies in the treatment of periodontal disease. *J Indian Soc Periodontol* 16:4-10.

18. Cui, Z.K., Sun, J.A., Baljon, J.J., Fan, J., Kim, S., Wu, B.M., Aghaloo, T., and Lee, M. 2017. Simultaneous delivery of hydrophobic small molecules and siRNA using Sterosomes to direct mesenchymal stem cell differentiation for bone repair. *Acta Biomater* 58:214-224.

19. Bastiat, G., and Lafleur, M. 2007. Phase behavior of palmitic acid/cholesterol/cholesterol sulfate mixtures and properties of the derived liposomes. *J Phys Chem B* 111:10929-10937.